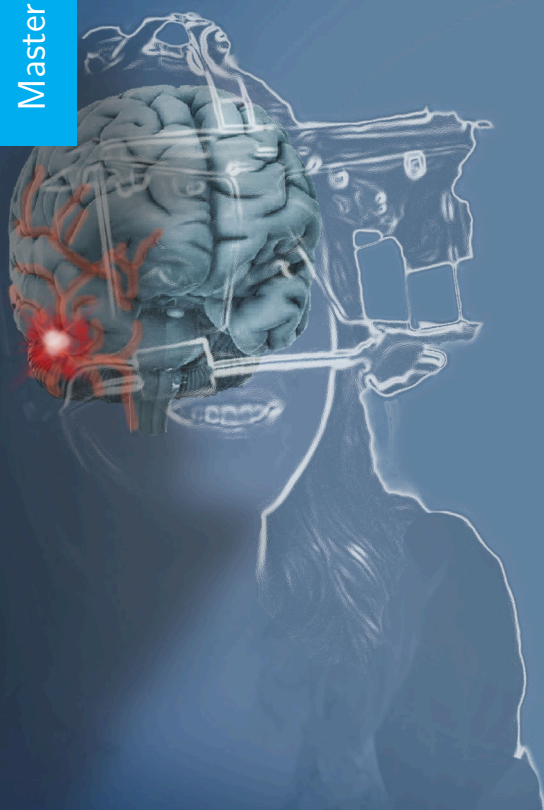


Quantifying loss of motor skills after cerebellar stroke

Control behavior of cerebellar patients in a preview tracking task

Yvonne Haartsen

Master Thesis



Quantifying loss of motor skills after cerebellar stroke

Control behavior of cerebellar patients in a preview tracking task

MASTER OF SCIENCE THESIS

For the degree of Master of Science in Aerospace Engineering at Delft
University of Technology

Yvonne Haartsen

November 9, 2017



Copyright © Y. Haartsen
All rights reserved.

DELFT UNIVERSITY OF TECHNOLOGY
DEPARTMENT OF
CONTROL AND SIMULATION

The undersigned hereby certify that they have read and recommend to the Faculty of
Aerospace Engineering for acceptance a thesis entitled

QUANTIFYING LOSS OF MOTOR SKILLS AFTER CEREBELLAR STROKE

by

YVONNE HAARTSEN

in partial fulfillment of the requirements for the degree of

MASTER OF SCIENCE AEROSPACE ENGINEERING

Dated: November 9,2017

Reader(s):

Dr.ir. D.M. Pool

Dr.ir. J.J.M. Pel

Prof.dr.ir. M. Mulder

Dr.ir. M.M. van Paassen

Dr.ir. M. Voskuijl

Table of Contents

Acronyms	v
1 Introduction	1
I Scientific Paper	3
II Preliminary report	17
2 The cerebellum and its functions	19
2-1 Cerebellar anatomy and pathways	19
2-2 Vestibular ocular reflex	20
2-3 Motor control in the cerebellum	21
2-3-1 The forward model	22
2-3-2 The inverse model	22
2-4 Consequences of lesions in the cerebellum for eye and hand movements	23
2-5 Relation to basal ganglia	25
2-6 Assessment of cerebellar dysfunction	25
2-6-1 Montreal Cognitive Assessment (MoCa)	26
2-6-2 International Cooperative Ataxia Rating Scale	26
3 Manual tracking tasks	27
3-1 The human controller	27
3-2 Tracking behaviour in pursuit and preview tasks	27
3-3 Forcing functions	28
3-4 System identification	29
3-5 Pilot models	30
3-6 Model fitting and parameter estimation	31

4	Measuring visuomotor deficits	33
4-1	Tapping tasks	33
4-2	Pursuit tracking	34
4-3	Preview tracking	35
5	Preliminary Experiment 1: Comparison between joystick tracking task and touch screen tracking task	37
5-1	Introduction	37
5-2	Method	38
5-2-1	Subjects	38
5-2-2	Apparatus	38
5-2-3	Experiment	38
5-3	Results	39
5-3-1	Questionnaire	40
5-3-2	Results in the time domain	40
5-3-3	Tracking performance and control activity	40
5-3-4	Model fitting	41
5-3-5	Parameter Estimation	43
5-4	Conclusion	43
6	Preliminary experiment 2: Simulation to investigate influence of lost data	45
6-1	Introduction	45
6-2	Method	45
6-2-1	Remnant	46
6-2-2	HC describing models	46
6-2-3	LOC scenarios	46
6-3	Results	47
6-3-1	Single integrator dynamics	47
6-3-2	Gain dynamics	51
6-4	Conclusion	54
7	Preliminary experiment 3: Effect of disturbance signal on human tracking behaviour in a preview tracking task	55
7-1	Introduction	55
7-2	Method	55
7-2-1	Subjects	55
7-2-2	Apparatus	56
7-2-3	Experiment	56
7-2-4	Preview time	57
7-3	Results	57
7-3-1	Performance and control activity	58
7-3-2	System Identification	59
7-3-3	Model fitting and parameter estimation	62
7-4	Gaze data	63
7-5	Conclusion	63

8	Project plan	65
8-1	Conclusions leading to the final experiment	65
8-2	Research questions and hypotheses	65
8-2-1	Tracking	66
8-2-2	Gaze	66
8-3	Subjects	67
8-4	Apparatus	67
8-5	Experiment	67
9	Influence of left and right hand on control behaviour	69
9-1	Introduction	69
9-2	Method	69
9-2-1	Subjects	69
9-2-2	Apparatus	69
9-2-3	Experiment	70
9-3	Results	70
9-4	Discussion	71
9-4-1	Social influence	72
9-4-2	Brain lateralization	72
9-5	Conclusion	72
III	Appendices	73
A	Latin square design	75
B	Touchscreen vs Joystick operator describing functions	77
B-1	Gain-Touchscreen	78
B-2	Gain-Joystick	79
B-3	Single integrator-Touchscreen	80
B-4	Single integrator-Joystick	81
C	Loss of contact	83
C-1	LOC scenarios	83
C-2	PSD error signal for all LOC scenarios	84
D	Preview test operator describing functions	85
E	Individual variance contributions	95
F	Left vs. right hand experiment operator describing functions	97
F-1	Lefthanded subjects	98
F-2	Righthanded subjects	101

IV Paper Appendices	105
G Individual operator describing functions	107
G-1 Patients affected	108
G-2 Patients unaffected	110
G-3 Control subjects	112
G-4 Young adults	114
H Experiment information and consent forms	127
Bibliography	139

Acronyms

CODECS	Cognitive DEficits in Cerebellar Stroke
EMC	Erasmus Medical Center
FCM	Fourier Coefficient Method
HC	Human controller
ICARS	International Cooperative Ataxia Rating Scale
LOC	Loss Of Contact
MMSE	Mini-Mental State Exam
MoCa	Montreal Cognitive Assessment
PD	Parkinson's disease
PSD	Power Spectral Density
VAF	Variance Accounted For
VOR	Vestibular-Ocular Reflex

Chapter 1

Introduction

We are able to perform complex tasks without thinking about precise planning and coordination. During childhood we learned to walk, grab and point. Later activities became more complex as we learned to write, text or draw. In the human body, fine motor control is partly regulated by a part of the brain called the cerebellum. It controls involuntary movements such as balance and posture, but is also involved in conducting smooth, accurate voluntary movements. The cerebellum receives vestibular and visual inputs for guided movement and uses internal models for accurate execution.

Damages to the cerebellum may lead to motor deficits. Movements of patients with cerebellar stroke become uncoordinated with errors in speed and accuracy. This holds for eye movements as well as for limb movements. The symptoms depend highly on the location of the lesion. Examples are intention tremor, unsteady gait, nystagamus, balance problems and dysmetria. Vercher and Gauthier [1] showed that the cerebellum is involved in coordinating eye-hand combined movement.

Consequences and treatment of cerebellar dysfunction are not straightforward. Every case has to be assessed differently. For most cases, the revalidation phase lasts approximately six months. Every three months the patient is tested by a medical specialist. At the Erasmus University Medical Center (EMC) the International Cooperative Ataxia Rating Scale [2] is used to quickly scan for cerebellar ataxia. In the end, a final score indicates whether the patient functions normally. Nevertheless, in some cases patients still experience difficulties with smooth movement. The testing methods cannot assess fine motor skills in detail. A test that can objectively analyse motor impairment would give better insight in the condition of a patient after a cerebellar stroke. It could also monitor long-term improvement.

A more refined method to quantify fine motor skill, is by using a tracking task, where precise coordination of hand- and eyemovement is important. A tracking test to measure motor skill degradation in patients with neurodegeneration, such as Parkinson's Disease (PD) and

Alzheimer disease, has been developed previously in a collaborative study between the dept. of Control and Simulation of the TU Delft and the dept. of Neuroscience at the EMC [3, 4]. The results of the study showed that PD patients have a lower control gain, lower performance and higher damping ratio when compared to the control group.

One interesting subject, that was out of the scope of the Parkinson's project, is preview tracking. In 1989 Jones and Donaldson [5] investigated predictive motor planning in PD patients. They found that PD patients had difficulties with integrating explicit preview information in a motor response strategy.

From an engineering perspective human behavior in preview tasks has already been investigated [6–8]. At the TU Delft a model of the human controller (HC) in preview tasks, that can be used for quantifying preview control skill, has been developed by Van der El et al. [9].

The population of PD patients available for testing is small at the EMC. Since cerebellar patients show a degradation of fine motor skill, the tracking task developed by the dept. of Neuroscience, can also be applied to this group. Therefore, cerebellar patients will be considered for the current project, instead of PD patients.

The aim of the current project is to develop a preview tracking task, that will be used to investigate control behaviour of cerebellar patients. The objective of this project is:

To develop a preview tracking task that may be used as an additional tool for the detection of degraded eye-hand coordination after a cerebellar stroke using system identification methods.

This report is divided in four parts. In Part I the graduation paper can be found that describes the final experiment. Part II describes literature and experiments that led to the design of the final experiment. Next, Part III presents appendices related to Part II. Finally, Part IV shows appendices related to Part I. Chapters 2 to 8 and A to E have been graded as part of AE4020. Part I, Chapters 9, F and Part IV hold new material.

Part I

Scientific Paper

Quantifying Visuo-motor Impairment after a Cerebellar Stroke using a Preview Task and System Identification Techniques

Yvonne Haartsen*, Supervisors: Daan M. Pool*, Johan J. M. Pel**, Max Mulder*

Abstract—A cerebellar stroke causes motor deficits and may complicate daily activities of patients. Their movements become uncoordinated with errors in speed and accuracy. To quantify the level of impairment, this paper proposes a preview tracking task. Such a task assesses and quantifies eye-hand coordination skills. A preview experiment on a touch-screen has been conducted with four cerebellar patients, four age-matched healthy control subjects, and a group of 26 young adults. Age-matched control subjects and young adults performed eight runs of the preview task, with the dominant hand only. Patients performed eight runs with each hand to make a distinction between the hand affected by the lesion and the unaffected hand. During the experiment, both eye- and hand movements were recorded. Results were obtained with system identification techniques. A model of the human controller in preview tasks was fitted to the estimated frequency response of the subject. The resulting control parameters revealed the tracking behaviour of the subjects. Patients show significantly higher visual time delays, neuromuscular damping ratios and lead time constants than age-matched control subjects. Consequently, patients engage in a more cautious control strategy than age-matched control subjects. Overall, the proposed task is found to be capable of detecting visuo-motor impairment in cerebellar patients. It could be used to quantify impairment as a result of neurological disorders, and monitor improvement during the revalidation phase and afterwards.

I. INTRODUCTION

AFTER a cerebellar stroke, patients can experience problems with many daily activities [1]. Symptoms highly depend on the location of the lesion and the severity of the stroke. The cerebellum can be divided into three functional regions that maintain posture, balance and coordinate voluntary movement [2]. It plays an important role in correcting ongoing movements to increase accuracy and efficiency. To initiate movement, the motor cortex generates a command and sends it to the actuator (muscle). The final outcome of the command is fed back to the motor cortex by sensory systems such as the visual system, proprioceptive system and vestibular system. Sensory feedback is slow and only relying on this feedback loop would lead to high delays. Therefore, the cerebellum uses an internal model [3]–[5] to predict the final outcome of the command. It directly sends internal feedback to the motor cortex, omitting the slow sensory feedback loop. The fast flow of corrective commands from the cerebellum leads to smooth

execution of the movement. After a stroke, the corrective response of the cerebellum is disrupted. The main symptom attributed to cerebellar dysfunction, is *ataxia* [6]. Movement of patients becomes uncoordinated, with errors in speed and accuracy. They display overshoot and undershoot in their movements as a sign of *dysmetria*. During a target-reaching task this may result in intention tremor [2]. Another aspect of cerebellar ataxia is *hypotonia*. This indicates decreased muscle tone, causing undamped limb movements.

To assess the level of impairment after a stroke, the qualitative International Cooperative Rating Scale test [7] can be performed, where impairment is rated by a score of 0 to 100. The downside of such a test is that it is semi-subjective, has a low resolution and does not assess and quantify the fine motor skills, such as eye-hand coordination, in detail.

A test that could objectively analyse motor impairment, is a manual tracking task [8]. During such a task, the subject has to minimize the error between an element he controls and a target, that follows a seemingly random path.

Tracking tasks have been applied previously to patients with impaired motor planning and execution [9]–[21]. The tracking parameters, such as tracking error, velocity and time lag, can be calculated from a time trace of the task.

In 1994 Donkelaar and Van Lee [17] found increased response times and increased error and/or variability of hand movements of cerebellar patients in a tracking task. Vercher and Gauthier [15] and Miall et al. [22] investigated the role of the cerebellum in visuo-oculo-manual tracking tasks. They found that, after cerebellar lesioning, monkeys showed increased delay between eye- and hand movements, decreased accuracy and high peak velocity of corrective movements. The consequences of *hypotonia* were studied by Morrice et al. [16]. They added a mechanical load to increase limb stiffness. After adding a viscous load to the input device, the tracking performance of cerebellar patients improved.

A more sensitive method to determine tracking behaviour of Parkinson's disease (PD) patients, was proposed by Oishi et al. [23] and De Vries [24]. Oishi et al. used system identification techniques and a second-order linear model to find the neuromuscular damping ratio and natural frequency. They found a higher damping for PD patients. The same was concluded by de Vries, who used a pursuit tracking task and the Fourier Coefficient method to identify tracking behaviour of PD patients. Besides a higher damping, PD patients also showed a lower control gain.

For the cerebellar patients, a preview task [25]–[31] could

*Department of Control and Simulation, Faculty of Aerospace Engineering, TU Delft, The Netherlands

**Department of Neuroscience, Erasmus MC, Rotterdam, The Netherlands

give more insight in the visuo-motor system. In a preview task, a section of the future path is shown to the subject. The task addresses the eye-hand coordination skills of the subject, which strongly depend on the cerebellum [32]. Also, the preview task more closely resembles everyday tasks, such as driving a car. Preview tracking has been implemented in a few studies on motor functions in patients with neurological disorders [12], [14], [33], [34]. In 1989 Jones and Donaldson [33] conducted a manual tracking test with PD patients. They found that predictive planning was impaired for PD patients, when preview was involved.

So far, preview tracking in combination with system identification techniques has not been conducted with patients that suffer from a neurological dysfunction.

The goal of this paper is to develop a preview tracking task that may be used as an additional tool for the detection of degraded eye-hand coordination after a cerebellar stroke using system identification methods. A preview experiment will be conducted with patients suffering from a cerebellar stroke and health control subjects. During the experiment, gaze data and the subjects' manual input are recorded to determine the frequency response. Control parameters will then be estimated using a model of the human controller in preview tasks. The results of the patients and control subjects will be compared to identify consequences of cerebellar dysfunction in steering behaviour.

The paper is structured as follows. Section II describes the control task. In Section III will be explained how data were recorded. Also, the medical status of the patients will be presented and some predictions will be made in the hypotheses. Section IV describes the data analysis, including applied system identification methods. Next, Section V shows the results of the experiment, followed by a discussion in Section VI. The recommendations for further research will be given in Section VII. Finally, conclusions will be drawn in Section VIII.

II. CONTROL TASK

The manual tracking task presented to the patients is a preview tracking task [26], [27], [29]. By presenting a part of the intended path of the target, the subject has the opportunity to anticipate for his own time-delay and improve performance [27]. Hereby, the subjects' ability to convert visual information to a motor plan, can be studied. A block diagram of a preview task as proposed by [31] can be found in Figure 1.

The H_{o_n} and H_{o_f} blocks describe the HC's response to the target function at the near- and far-view point, respectively. To track the low frequencies, the Human Controller (HC) reacts to the future target function at a far-view point, $(t + \tau_f)$. High frequencies of the target function are tracked at the near-view point, $(t + \tau_n)$.

$H_{o_{e^*}}$ describes the internal error between the controlled element and the target at the filtered far-view point, $e^*(t) = f_{t,f}^*(t) - y(t)$. During the task, the HC tries to minimize the internal error, $e^*(t)$.

The neuromuscular system represents the physical limits of the subject's arm at high frequencies. It is described by the H_{nms}

block. The $e^{-\tau_v j\omega}$ -term indicates the visual time delay of the HC. To compensate for non-linear behaviour of the HC, the remnant term, $n(t)$ is added to the HC output [8]. The resulting signal $u(t)$, is fed into the system, H_{ce} and perturbed by the disturbance function, $f_d(t)$.

A. Display

The display presented to the subjects is shown in Figure 2. The target marker (blue ring) moved horizontally according to the forcing function (blue line). Subjects were instructed to keep the red circle (controlled element output $y(t)$) within the blue, target marker by moving it left and right. The controlled element and target marker were shifted downwards by -8 degrees, relative to the center of the screen. This motivated subjects to look at the preview line.

B. Forcing functions

For the preview tracking task, two independent quasi-random, multi-sine signals excite the system. Both are needed to separate the responses of the HC to the target and the controlled element. The target signal (f_t) controls the horizontal position of the target, and the disturbance signal (f_d) perturbs the controlled element. Both signals have been constructed as a sum-of-sines signal, using the magnitude response of a low-pass filter as magnitude for the sine components, as proposed by Zaal et al. [35]. The disturbance signal should not be too strong, to prevent the task from becoming a disturbance-rejection task. Therefore the amplitudes were scaled such that for f_t , the variance was 1 deg^2 and for f_d , the variance was 0.25 deg^2 . The characteristics of the signals can be found in Table I.

TABLE I
FORCING FUNCTION SIGNAL PROPERTIES

Target f_t				Disturbance f_d			
n_t , -	ω_t , rad/s	A_t , deg	ϕ_t , rad	n_d , -	ω_d , rad/s	A_d , deg	ϕ_d , rad
4	0.614	1.079	7.239	3	8.948	0.507	8.948
7	1.074	0.776	0.506	5	0.030	0.420	0.030
11	1.994	0.391	7.860	11	0.773	0.210	0.773
17	2.915	0.225	8.184	17	4.199	0.115	4.199
23	4.449	0.117	9.012	23	3.680	0.072	3.680
29	5.676	0.082	6.141	31	1.705	0.046	1.705
37	6.596	0.066	6.776	41	1.585	0.031	1.585
53	8.130	0.051	6.265	59	5.650	0.020	5.650
79	12.118	0.035	4.432	83	7.711	0.014	7.711
109	16.720	0.028	2.672	107	8.125	0.012	8.125
157	24.084	0.024	8.009	151	9.458	0.011	9.458

C. Preview time

The preview time is the length of the visible future part of the target function (blue line in Figure 2). The performance of the HC improves as preview time increases, until an optimal preview time is reached [27]. After this time, the performance stabilizes. Jones and Donaldson [33] used 8 seconds of preview time for Parkinson's disease patients. Hiramatsu and Uno [25] suggested 0.5 to 2.0 seconds of preview time

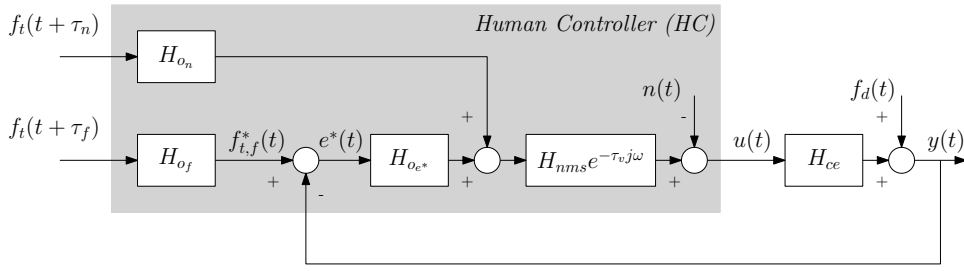


Fig. 1. Block diagram of HC behavior preview tracking task developed by Van der El et al. [31]

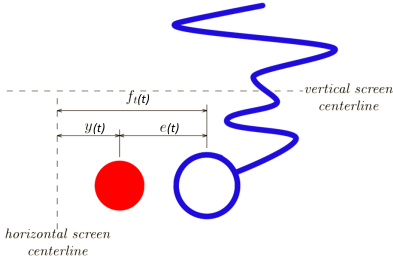


Fig. 2. Preview tracking task display, adapted from [24]

where the 2.0 seconds is considered appropriate for elderly subjects. Van der El et al. [36] showed that the critical preview for the current preview tracking task is likely between 0.5 and 0.75 seconds. Meaning that a subjects' performance does not improve any further when the preview time exceeds 0.75 seconds. Patients 1 and 2 were tested with 1.0 seconds of preview time, compliant with the preview times suggested for old, sick subjects by [25] and [33]. However, the complexity of the forcing function and limited height of the screen lead to a great amount of visual information and high workload for the subjects. Therefore, the preview time was changed to 0.5 seconds, in compliance with findings from Van der El et al. [36]. The remaining patients, age-matched control subjects and all young adults were shown 0.5 seconds of the future path of the target.

III. METHOD

A. Subjects

The manual tracking task has been conducted with three groups of subjects. Besides a patient group and healthy age-matched control group, a group of experienced and inexperienced young adults will be tested. So far, this specific preview test has been conducted with subjects who have had experience with manual tracking tasks [31], [36], [37]. Consequently, their performance quickly stabilized and subjects could easily cope with the difficulty of the test and large amount visual information. The test data from the young adult group will provide a basis of reference results for this preview task.

1) *Young adults*: The test was performed by 26 young adults aged 17-34 years ($\mu = 23.5$ years, $\sigma = 3.9$ years). Five of these subjects had experience with manual tracking tasks. Others had little or no experience. Ten subjects were left-handed, others were right-handed. All subjects performed the task with the dominant hand.

2) *Patients*: Four patients participated in the experiment, age ranged from 46-75 years ($\mu = 56.3$ years, $\sigma = 12.9$ years) and all patients were right-handed. Personal profiles can be found in Table II. In case of a unilateral stroke, the ipsilateral (same) side of the body is affected [6]. Thus the side of the lesion in Table II, corresponds to the affected hand. The patients were recruited at the dept. of Neurology at the EMC from the COgnitive DEficits in Cerebellar Stroke project (CODECS). During this project, patients are clinically tested on cognitive impairment after three and six months of revalidation. The level of motor impairment was determined using the International Cooperative Ataxia Rating Scale (ICARS) [7]. It semi-quantifies cerebellar ataxia symptoms in four domains: postural and stance disturbances; limb movements disturbances; speech disorders; and oculomotor disorders. The patient carries out several tests and the examiner assigns a score where 0 points indicates no signs of ataxia. The Mini Mental State Examination (MMSE) [38] was performed to test the cognitive status of the subjects. They are tested on registration, orientation, attention, calculation, recall and language. A maximum of 30 points can be scored, based on the performance of the subject. The current experiment was conducted at least six months after the stroke.

3) *Age-matched healthy control subjects*: A group of age-matched, healthy control subjects, ($\mu = 57.3$ years, $\sigma = 7.9$ years), was tested to compare to the patient data. The details of the control group can also be found in Table II.

B. Apparatus

The experiment setup is shown in Figure 3. The setup used in the current study is similar to that used by De Vries [24]. The infrared eye-tracking system (Chronos Vision, Berlin, DE [39]) measures the location of the gaze for each eye individually. It consists of a helmet that can be adjusted to headsize and interpupillary distance of the subject. The eyes are recorded individually by two cameras through a dichroic mirror. The measurement resolution is better than 0.05 deg. To ensure a fixed distance to the screen, subjects place their head on a chinrest. A 32 inch touch screen (ELO Touch Solutions, Milpitas, CA) displays the task and accurately measures finger position. To avoid data-loss due to friction between fingertip and screen, patients wear a glove (Vicon Motion Systems, Oxford, UK). All systems are synchronised using a trigger controlled by MATLAB.

TABLE II
CLINICAL INFORMATION OF PATIENTS

ID	Age	Sex	Handedness	MMSE	Diagnosis (affected side)	Days since event	ICARS
1	50	M	Right	30	Hemorrhage (right)	315	n.a.
2	46	M	Right	25	PICA infarct (left)	289	7
3	75	M	Right	23	Infarct (right)	274	2
4	54	F	Right	30	Infarct (right)	245	0
1	49	F	Right	30	-	-	-
2	52	F	Right	29	-	-	-
3	64	M	Right	30	-	-	-
4	64	F	Right	30	-	-	-



Fig. 3. The setup at the EMC used for measuring loss of eye-hand coordination and cognitive skills. (1) touch screen, (2) infrared eye-tracking system, (3) infrared motion detection system [40]

C. Experiment procedure

Prior to the experiment, the patients and age-matched control subjects filled in a questionnaire on daily activities, followed by the MMSE to scan for cognitive dysfunction. The first part of the main experiment involved eye and eye-hand coordination tests where accuracy and reaction time were measured. The same tests have been used at the EMC to investigate the effect of neurodegenerative diseases on eye-hand coordination and cognitive skills [40]–[42]. In the second part of the experiment, the subjects performed the manual tracking task. For patients, 16 runs were recorded, eight with the dominant hand and eight with the non-dominant hand. Thereby, the affected limb and unaffected limb can be compared. Control subjects performed eight runs with the dominant hand.

D. Hypotheses

The following hypotheses are proposed based on literature:

I The first hypothesis is that, due to ataxia, the performance of patients is worse than that of control subjects. For the same reason, control activity might be lower too. The same result followed from [17] and [22] who detected more tracking errors in case of cerebellar dysfunction.

II For the second hypothesis we expect that patients make limited use of the preview information. Jones and Donaldson [33] concluded that PD patients "...might be less able to integrate explicit preview information into an optimal motor response plan.". Since the visuo-motor system of cerebellar patients is affected, the same might hold for this group.

Another reason why patients are expected to not use the preview, is because they are inexperienced controllers. It might take some practice to efficiently process preview information.

III Due to ataxia, we expect that cerebellar patients show lower gains and higher time delays. Vercher and Gauthier [15] also found high delays after cerebellar lesioning. The neuromuscular damping ratio will be lower due to hypotonia [16].

IV. DATA ANALYSIS

A. Loss of contact

An important drawback of a touch-screen interface, is risk of Loss Of Contact (LOC) with the screen. The subject could get tired, causing him to relax the arm and loose contact. Also, the friction with the screen might lead to short instances of loss of contact. During such an incident, no data are recorded, leading to gaps in the user input $u(t)$. For analysis, a continuous signal is desirable. Therefore, the disrupted input will be reconstructed by interpolating the signal with splines. In case of $>8\%$ data loss or if data has a low quality, the trial has to be excluded [43]. Figure 4 gives an overview of the LOC incidents and the included trials.

B. HC response

To investigate control behaviour of the subjects, the HC response will be estimated using the Fourier Coefficient Method (FCM). This black-box identification method gives an estimation of the response in the frequency domain. This method will be applied to both the manual tracking data and the gaze data.

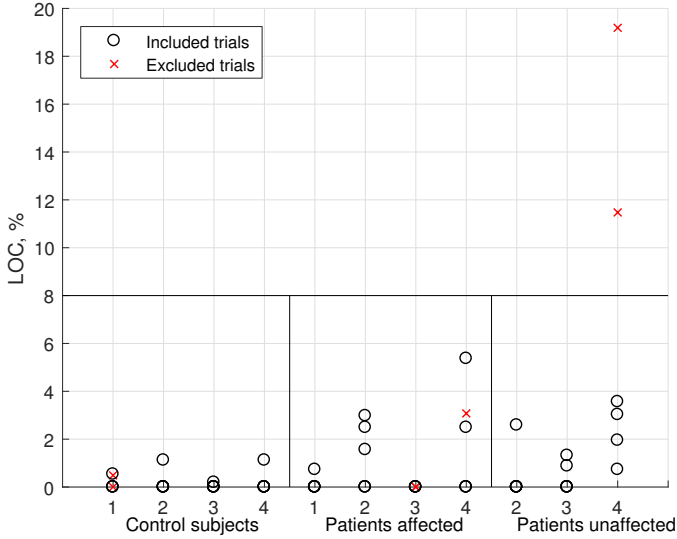


Fig. 4. Loss of contact in % per trial and excluded trials

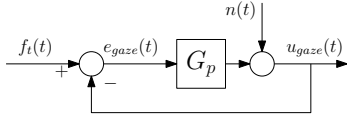


Fig. 5. Simple block diagram of smooth pursuit during a preview task

1) *Tracking response*: The HC reacts to multiple inputs in Figure 1. Therefore, the task is a multi-loop tracking task [44] and both loops will be identified simultaneously. After Fourier transforming the inputs and outputs of the closed-loop system of Figure 1, Equation (1) can be derived:

$$U(j\omega) = H_{o_t}(j\omega)F_t(j\omega) + H_{o_x}(j\omega)X(j\omega) + N(j\omega) \quad (1)$$

The remnant $N(j\omega)$ accounts for non-linear behaviour. The HC responds to a multi-sine signal with a significant amount of power at the frequencies of the input sines. At these frequencies the contribution of the remnant in the HC response is small. Therefore, at the input frequencies, the remnant can be neglected and the HC response can be estimated. The same method can be applied to estimate the response at the disturbance frequencies ω_d . Equation (2) shows the estimation of the HC response to the target function (\hat{H}_{o_t}) and the disturbance function (\hat{H}_{o_x}) at the target frequencies.

$$\begin{aligned} \hat{H}_{o_t}(j\omega_t) &= \frac{\tilde{U}(j\omega_t)X(j\omega_t) - U(j\omega_t)\tilde{X}(j\omega_t)}{\tilde{F}_t(j\omega_t)X(j\omega_t) - F_t(j\omega_t)\tilde{X}(j\omega_t)} \\ \hat{H}_{o_x}(j\omega_t) &= \frac{\tilde{U}(j\omega_t)F_t(j\omega_t) - U(j\omega_t)\tilde{F}_t(j\omega_t)}{\tilde{F}_t(j\omega_t)X(j\omega_t) - F_t(j\omega_t)\tilde{X}(j\omega_t)} \end{aligned} \quad (2)$$

2) *Gaze response*: During the tracking task, the subject's gaze fixates on the the moving target, causing continuous eye movements. This type of eye movement is called *smooth pursuit* [45]. A simple, schematic overview of the visual response to the target, is depicted in Figure 5. The HC is expected to focus his gaze mostly on the target, therefore, the gaze response will be estimated at the target frequencies. Since there is one input ($f_t(t)$), the system can be considered as a

pursuit task and a single-loop identification procedure will be used [46]. Equation (3) describes the gaze response, $G_p(j\omega_t)$, of the HC to the target function.

$$\hat{G}_p(j\omega_t) = \frac{U_{gaze}(j\omega_t)}{E_{gaze}(j\omega_t)} \quad (3)$$

C. HC model

As shown in Figure 1, the HC can be represented by a quasi-linear describing function [8]. Equations (5) to (9) show the HC model used for the current project. The HC describing parameters are depicted in blue. The model was adapted from Van der El [31] for a HC in the preview tracking task with gain dynamics. The HC equalization in the internal error $H_{o_{e^*}}(j\omega)$, is chosen to be $\frac{1+T_{L,e}j\omega}{j\omega}$ (see Equation (6)). In the results section, in Figure 10, it will be shown that at low frequencies, the estimated frequency response of the subjects resembles a single integrator. This part of the response is approached with the $\frac{1}{j\omega}$ -term. To ease the tracking of high frequencies, a first order low-pass filter has been added to the controlled element, with a cut-off frequency of 10 rad/s. The CE dynamics can be found in Equation (4). To compensate for the filter, subjects generate lead. The $(1 + T_{L,e}j\omega)$ -term estimates the lead.

$$H_{ce} = K \frac{1}{(1 + \frac{1}{10}s)} \quad (4)$$

$H_{o_f}(j\omega)$ in Equation (7), describes the HC's response to the far-viewpoint. $H_{o_n}(j\omega)$ in Figure 1, indicates the response of the HC to high frequencies. The HC model will not include the near-viewpoint since it is not expected that inexperienced patients track the target at high frequencies.

$$H_{nms}(j\omega) = \frac{(j\omega)^2}{(j\omega)^2 + 2\zeta_{nms}\omega_{nms}j\omega + \omega_{nms}^2} \quad (5)$$

$$H_{o_{e^*}}(j\omega) = K_e \frac{1 + T_{L,e}j\omega}{j\omega} \quad (6)$$

$$H_{o_f}(j\omega) = K_f \frac{1}{1 + T_{L,f}j\omega} \quad (7)$$

$$H_{o_t}(j\omega) = H_{o_f}(j\omega)e^{j\omega\tau_{pf}}H_{o_{e^*}}(j\omega)H_{nms}(j\omega)e^{j\omega(-\tau_v)} \quad (8)$$

$$H_{o_x}(j\omega) = H_{o_{e^*}}(j\omega)H_{nms}(j\omega)e^{j\omega(-\tau_v)} \quad (9)$$

D. Parameter estimation

Through combination of the HC response and HC model, the HC describing parameters can be estimated. The estimation procedure consists of two steps. The cost function from step 1 in Figure 6, fits the H_{o_x} model to the \hat{H}_{o_x} response with parameters $(K_e, \tau_v, \omega_{nms}, \zeta_{nms}, T_{L,e})$. It minimizes the difference between the response and model by constantly changing the HC describing parameters, until a minimum difference of J_x is found. To ensure that the final result is a global minimum, the process will be repeated 50 times. The weighting factor puts emphasis on high frequencies and excludes inaccurate points by $W_1 = \begin{bmatrix} 0 & \frac{1}{|\hat{H}_{o_x}(j\omega_i)|} & 0 \end{bmatrix}$. Once the error parameters are found, they are fixed and

passed to the cost function of step 2 in Figure 6. Next, the remaining preview parameters are estimated, using the target response \hat{H}_{o_t} , and model H_{o_t} . W_2 is the weight factor for the second cost function. Splitting the fitting procedure increases computation time and accuracy. The resulting eight parameters reveal the control behaviour of the HC.

E. Statistical tests

The normality of the data was confirmed with the Shapiro-Wilk test. Despite the small subject groups, the significance of the parameters was determined using the independent t-test. From the data, 5 groups were distinguished. The young adults group holds a small subgroup of experienced subjects. Furthermore, the patient data can be split into the affected hand and the unaffected hand.

V. RESULTS

A. Performance and control activity

The performance and control activity of the different subject groups are depicted in Figures 7a and 7b. The marker indicates the median of the data and the edges of the boxes represent the 25th and 75th percentiles. Performance is expressed as the variance of the error signal and control activity as the variance of the control input. There is no significant difference between the performance and control activity of the control subjects and the patients. There are, however, two patients whose results stand out. Patient 3 shows a large decrease in performance for the unaffected hand. Supposedly, this is a consequence of the patient's handedness. For patient 3, the unaffected hand was the non-dominant left hand and he may not be used to performing fine motor skill tasks with this hand. Another remarkable result is the excellent performance of patient 1 compared to other groups. To put patient 1 in perspective, the performance of the subgroup of experienced young adults has been plotted separately in red. The performance of patient 1 is on point with this group.

B. Use of preview

It is not straightforward that every subject deploys a true preview control strategy. Through instructions and placement of the target and preview line on the display, the subject is motivated to use the preview information. Nevertheless, many subjects prefer the pursuit strategy, where they ignore the preview and correct the instantaneous error $e(t)$. There are several indications of a preview strategy that can be derived from manual tracking data and recorded gaze data. In this section three cases will be compared with data from one subject from each group. The subjects were chosen based on the quality of the gaze data.

1) *Gaze data:* The gaze target response can be determined by applying the Fourier Coefficient method to the horizontal gaze data, as explained in Section IV-B2. Figures 8a, 8b and 8c show the estimated response of the horizontal gaze data. Both the patient and the control subject show a decreasing phase, corresponding to a positive delay. The young adult on the other hand, shows a positive phase and thus a negative

delay. This indicates that the gaze of the young adult is ahead of the current target position.

Another, rather crude, method to determine if the subject uses the preview line, is by analysing the vertical gaze data. Figures 9a, 9b and 9c show the corresponding vertical gaze data, its average and the median of the average signal. The y-axis represents the preview line on the screen, thus the bottom of the graphs corresponds to the location of the target marker (blue ring). The figures show on which part of the preview line the subject is focusing his gaze. The patient and control subject focus their gaze close to the target, while the young adult tends to focus on the center of the display.

2) *Tracking data:* Figure 10 shows manual tracking data from each case. The young adult and patient show a negative time delay for the target response. This indicates that they anticipate the future path of the target by increasing their look-ahead time. Some subjects tend to perceive the preview line in their peripheral vision [37]. This might explain why the patient shows a negative delay in Figure 10c, but a positive delay in Figure 8a. He is reacting to the preview line without directly looking at it. The age-matched control subject on the other hand, does not react to the future target. Therefore, at high frequencies, his phase lag in H_{o_t} , Figure 10c, increases.

C. HC Parameters

The HC parameters, depicted in Figure 11, describe the control behaviour of the subjects. The boxes represent each subject group with the marker as the median. The edges of the boxes represent the 25th and 75th percentiles of the data. Next to the boxes, the data of the individual patients are plotted for both hands. For patient 1, the unaffected hand was not measured.

The first parameter, K_e , is the gain, related to performance (see Figure 11a). It describes how strongly the subject reacts to the input signals. Again, subject 1 shows a gain similar to that of experienced young adults. The other patients show low gains when compared to the control subjects and young adults, although this is not significant. The median of age-matched control subjects and young adults lies at 1.8 while that of patients lies at 1.5.

Another parameter that does show tracking impairments of cerebellar patients, is the visual time delay, τ_v , depicted in Figure 11b. The time delay of patients is significantly higher than that of control subjects ($t(6) = 2.60, p < 0.05$). On average, the time delay of patients is 22% higher than that of age matched control subjects. Also compared to young adults, the patients show large delays, on average 39% higher. The low performance of the unaffected hand of patient 3 is apparent in both a lower gain and an increased delay. For patients 2 and 4, the time delay slightly decreases for the unaffected hand.

The neuromuscular dynamics represent the physical limits of the subject's arm movements. The natural frequency, depicted in Figure 11c, does not reveal any impairments in the tracking behaviour of patients. The damping ratio on the other hand, is significantly higher for patients than for control subjects ($t(6) = 3.44, p < 0.05$), see Figure 11d. On average, the

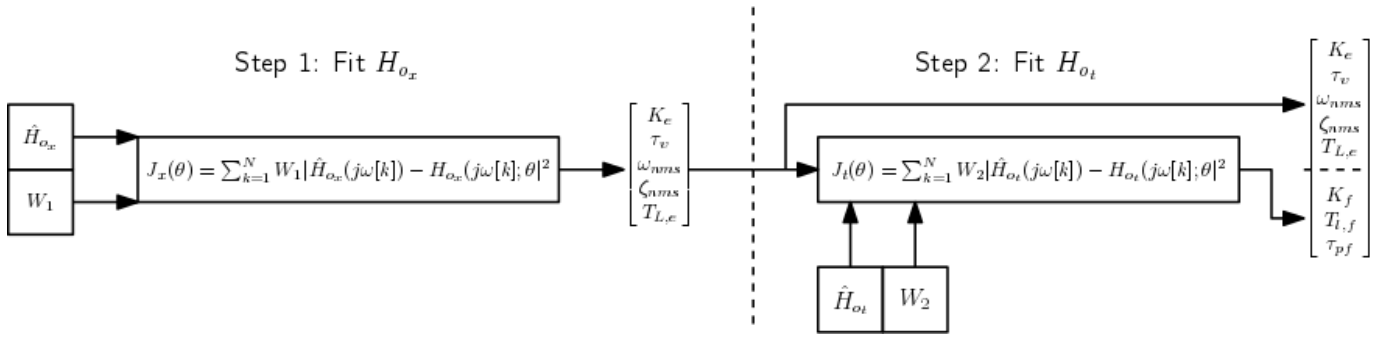


Fig. 6. Schematic overview of parameter estimation procedure

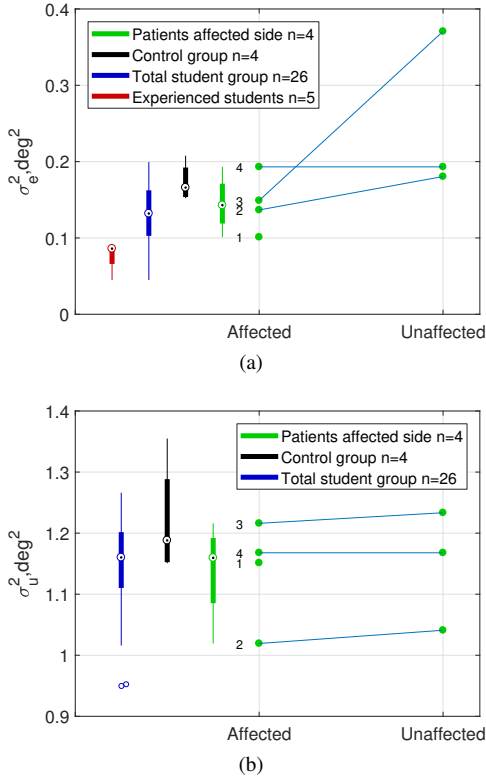


Fig. 7. Performance (7a) and control activity (7b)

damping ratio of patients is 230% higher than that of age-matched control subjects and twice the damping ratio of young adults. Also, when comparing the affected hand to the unaffected hand, for all patients ζ_{nms} increases by 84% when steering with the affected hand.

The lead constant is significantly higher for patients than for control subjects ($t(6) = 2.59$, $p < 0.05$). According to McRuer and Jex [8], an HC adapts his steering behaviour to obtain a -20 dB decade slope for $|H_{ce}H_p|$ in the crossover region. The controlled element, H_{ce} , consists of a low-pass filter with cut-off frequency 10 rad/s. To compensate for the controlled element lag, subjects are expected to generate lead at 10 rad/s, corresponding to a lead time constant of $T_{L,e} = 0.1$ s. For the control subjects, the average lead constant is 0.11s, for young adults $T_{L,e} = 0.14$ s. Patients, however, on average start to generate lead at 3.8 rad/s, corresponding to a

lead time constant of 0.26s.

As mentioned before, not every subject uses the preview information to anticipate and counter their time delay. This is apparent from the large spread of look-ahead times, τ_{pf} . Patients 2 and 3 have a look-ahead time close to 0.6 while 1 and 4 do not seem to look ahead at all. From the preview parameters, there appears to be no correlation between using preview and suffering from cerebellar dysfunction.

D. Crossover frequency and Phase margin

The crossover frequency and phase margin describe performance and stability, they are depicted in Figure 12. With one exception, all patients have a higher crossover frequency than the control subjects. The phase margin shows a large spread for patients. These results are likely to be related to the HC parameter $T_{L,e}$. To verify this, patient data with a corrected $T_{L,e}$ is added to Figure 12. If the $T_{L,e}$ of patients is changed to $T_{L,e} = 0.1$ s (as found for the control subjects), the crossover frequency and phase margin decrease. The patients thus generate lead to increase their phase margin and achieve added stability. Since the lead is generated at a frequency lower than ω_c , the crossover frequency increases too.

VI. DISCUSSION

In this paper, the preview experiment is proposed as an additional tool for the detection of degraded eye-hand coordination after a cerebellar stroke. It is important to determine whether this experiment is able to detect the consequences of cerebellar impairment and whether the task is suitable for a vulnerable subject group.

A. Clinical importance of the task

First, the clinical importance of the proposed tracking task must be addressed. Currently, there are no functional bedside tests to monitor the recovery of patients after a cerebellar stroke. After the acute phase of the stroke (1-2 weeks), the patient is transferred to the revalidation phase (6 months). Based on the patient's symptoms, the occupational therapist and physical therapist set-up a plan to resume daily activities and improve motor skills [1]. Semi-objective questionnaires and small motor function tests [7] are used to judge whether the patient can be discharged. The proposed experiment could

objectively monitor improvement during recovery and afterwards. For other neurological disorders, it could also assist in determining the appropriate dose of medicinal treatment.

B. Sensitivity of the task

Hypothesis I predicted worse performance and lower control activity for patients. These predictions were not confirmed. There was no significant difference in performance or control activity between patients and age-matched control subjects. Hypothesis II predicted that patients would not use preview information due to a lack of experience and inability to process explicit visual information. The results show a more complex outcome. Some patients show clear signs of preview use (e.g., a negative delay), while others do not. The same holds for the age-matched control subjects and the young adults. Whether or not the preview information is

used, is therefore not related to cerebellar dysfunction, but rather to a personal ability to cope with a large amount of information. This ability might be improved through practice, but experience is not a condition for preview tracking.

The tracking task in general, by facilitating human control identification and modelling, is capable of identifying impairment based on several control parameters. Although not significant, the difference in gain between patients and other subjects is worth mentioning. Hypothesis III predicted the lower gain and higher delay for patients. The significantly higher delay could be the result of the slow, inner transport loops, associated with cerebellar dysfunction [3], [4], [32].

The significantly higher damping ratio for patients was not expected. Ataxia is generally associated with dysmetria; loose, uncoordinated movements. The high damping ratio on the other hand, indicates stiff movements. A high damping

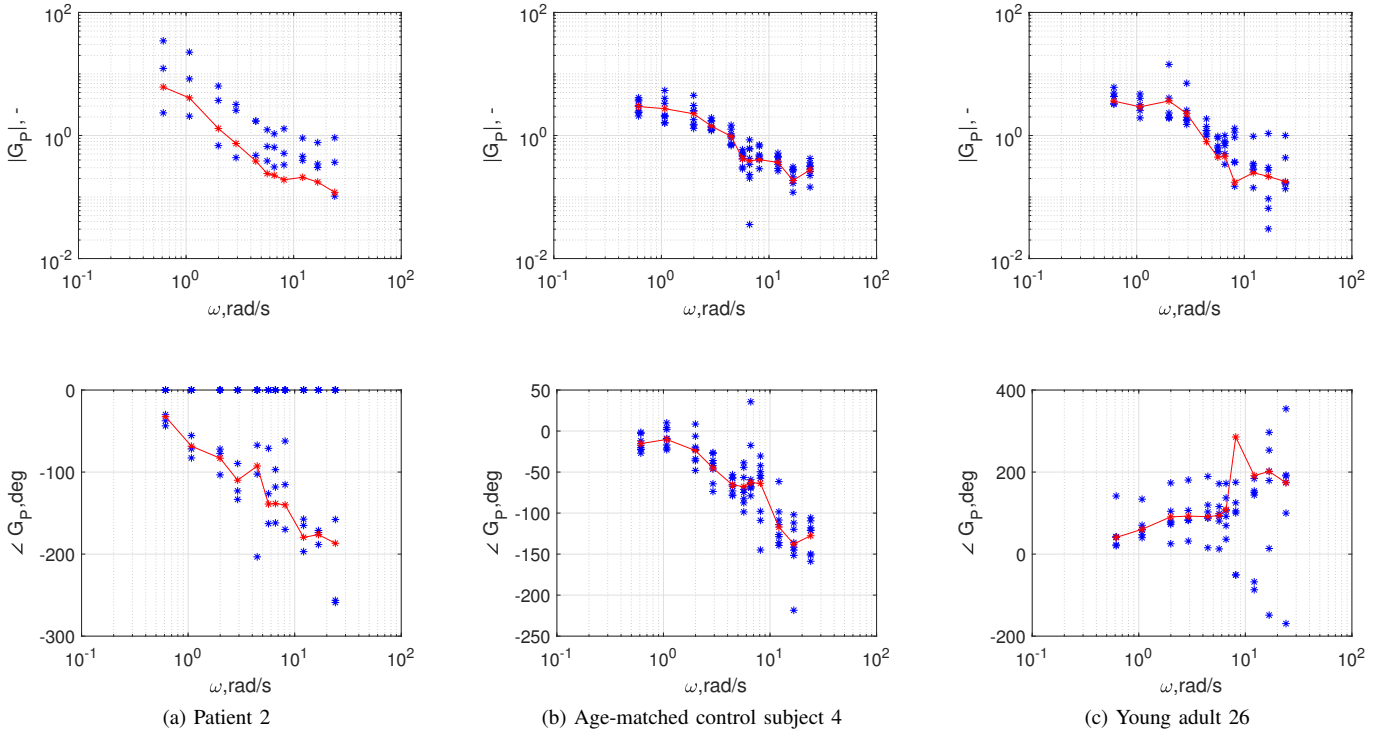


Fig. 8. Horizontal gaze data

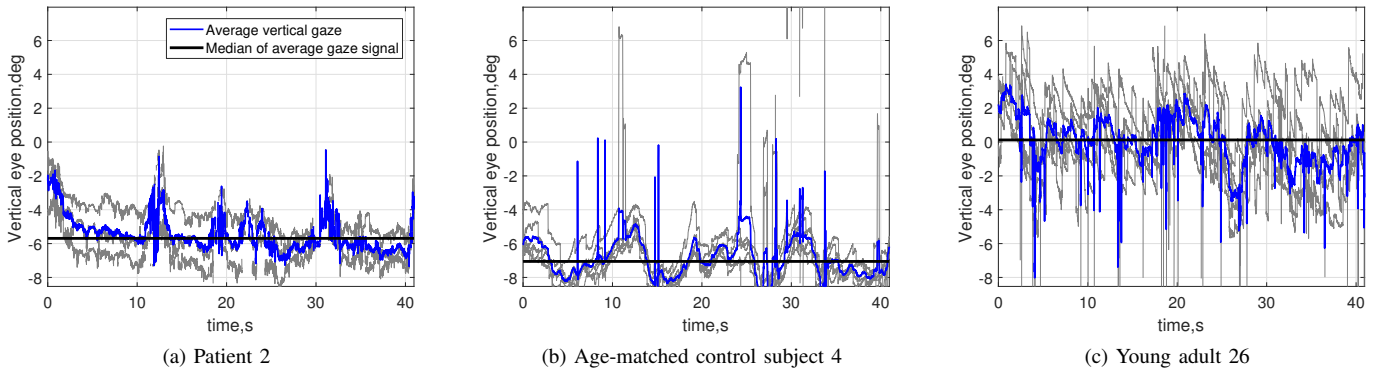


Fig. 9. Vertical gaze data

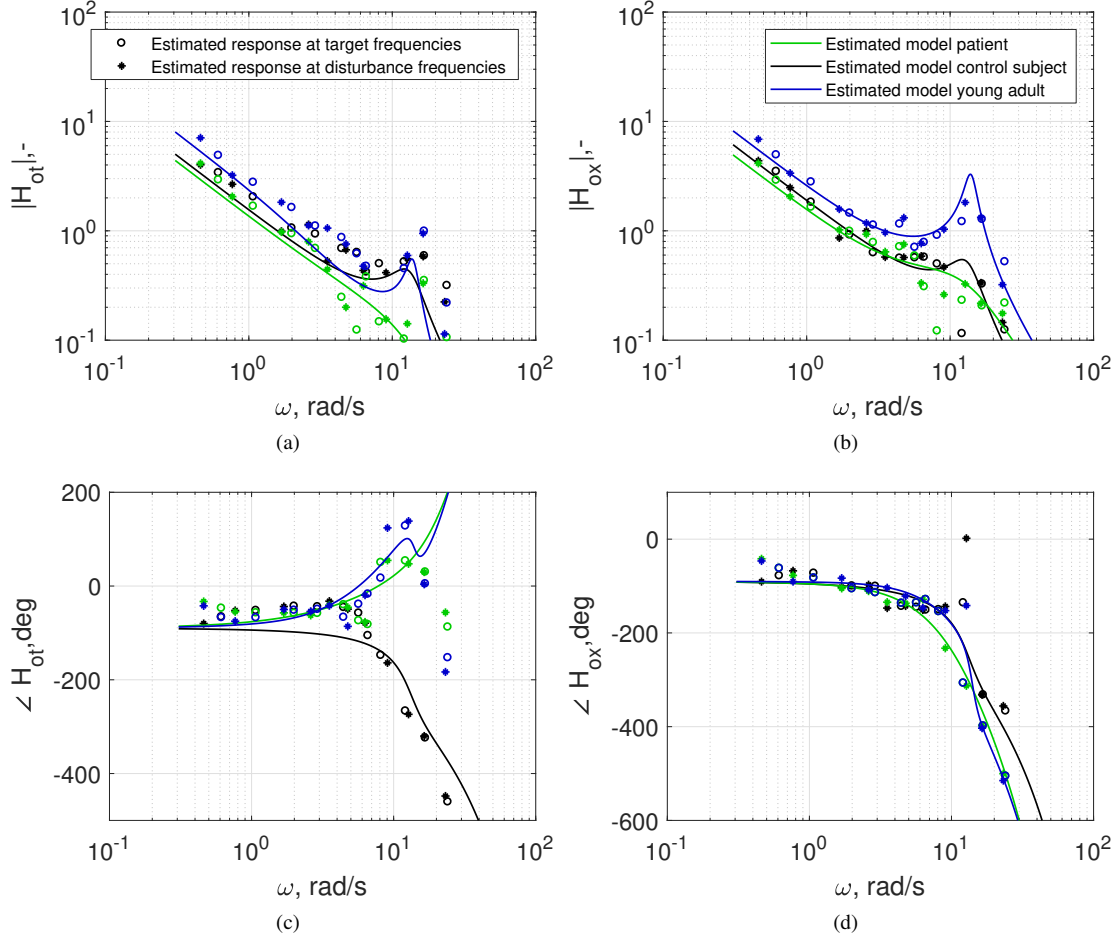


Fig. 10. Estimated response and estimated model from patient, control subject and young adult

might be a sign of physical impairment due to neurological dysfunction in general. Pool et al. [24] also found a higher damping for Parkinson's patients.

For the current control task, the lead time constant was not expected to be a key control parameter. Patients try to reduce tracking errors in the crossover region. To obtain the same $|K_e T_{L,e}|$ as control subjects, they must generate additional lead at low frequencies to compensate for their low gain. Thereby, the phase margin is increased, leading to more stability. An example of this strategy can be found in the estimated model for H_{ox} for patient 4 and age-matched control subject 2 in Figure 13. The patients seem to deploy a strategy where they are more cautious and less active than control subjects.

Another topic of discussion is the quality of the results of the current experiment, considering the small sample size. Only four patients were available for testing. Although some results are significant, with this sample size they still require a critical look. A cerebellar stroke can lead to a great number of possible symptoms [6]. The four patients do not represent this full set of symptoms. As the data show, even within the patient group, diversity can occur. For example, the high performance and gain of patient 1, is inconsistent with the other patients' data. This implies that every case must

be evaluated individually. Still, the credibility of results of patients can be supported with theory and previous findings. The high delay can be attributed to the working principle of the cerebellum [2]–[4] and the increased damping ratio has been found previously for PD patients [24].

The results from the age-matched control group can be validated by the larger, healthy young adult group. For the key parameters of this experiment, the medians of both groups are almost equal. The gain of age-matched control subjects is only 1.4% higher than that of the young adults. The medians of the visual time delay of age-matched control subjects (3.4% higher) and damping ratio (9.6% lower) are also close to the corresponding medians of young adults. For the lead time constant, the median of young adults is 28% higher, which is still below the median of the patients. For these four parameters, the group of age-matched control produces data that is fairly representative for healthy subjects.

C. Applicability of the task

The preview task proposed in this paper, is able to detect impairment based on the control behaviour of subjects. That leaves the question as to whether or not the preview task is suitable for cerebellar patients and patients with brain

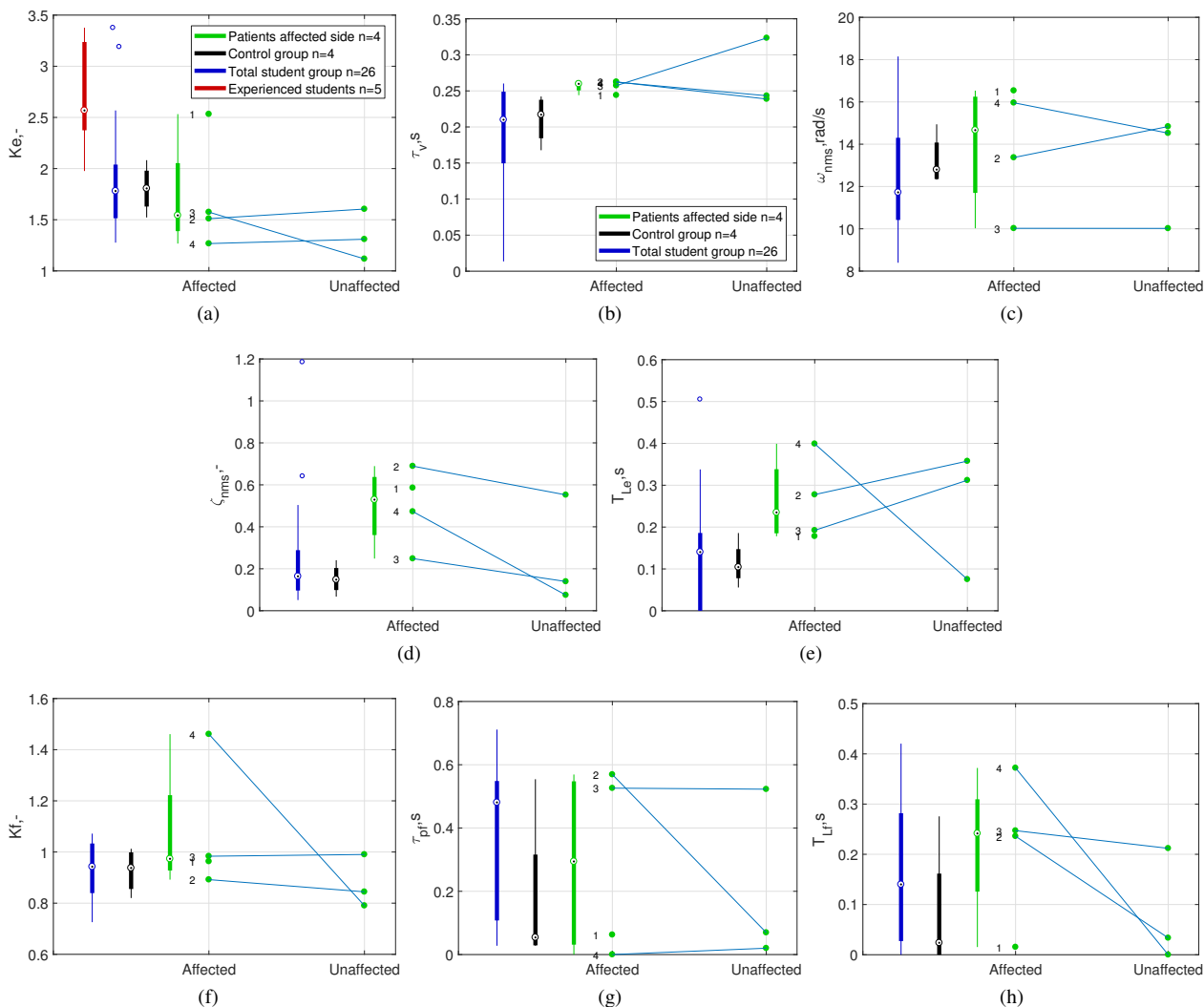


Fig. 11. Control parameters

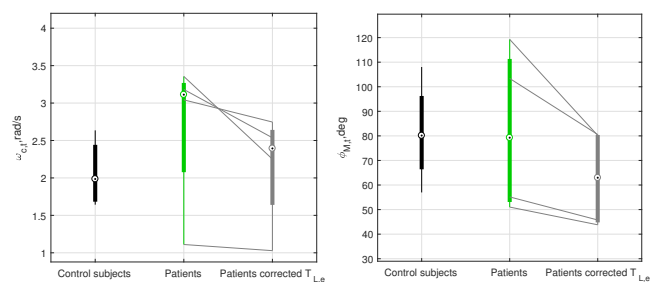


Fig. 12. Crossover frequency and phase margin

disorders in terms of difficulty and workload. In the current setting, the task seems too complex and too demanding. By removing the preview however, a deeper insight in manual tracking behaviour, that preview tracking offers, will be lost. Simplifying the task seems an easy solution, but several consequences should be considered. The forcing function could be simplified by leaving out some high frequency sinusoids. This method would increase the subjects performance [47]. However, the neuromuscular peak

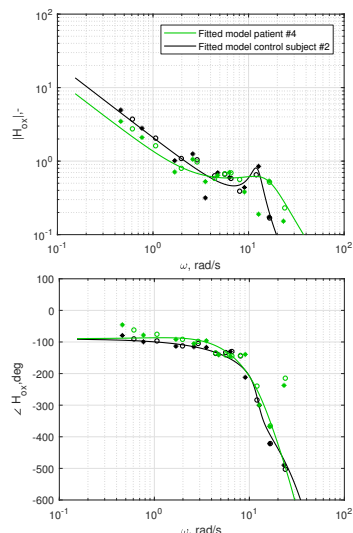


Fig. 13. An example of the difference between strategies of patients and age-matched control subjects

occurs at high frequencies. If these frequencies are omitted, the frequency range might not be broad enough to capture the neuromuscular peak at high frequencies. The damping ratio, an important parameter for the quantification of impairment, can then not be determined. By changing the controlled element dynamics to a higher order, the neuromuscular peak might reappear at a lower frequency [48]. However, this could lead to problems with touch-screen tracking. Tracking with higher order CE dynamics feels unnatural to inexperienced subjects, leading to LOC incidents and a more demanding task. Another option to simplify the task, is by allowing the subjects more practise runs. This is however, difficult to combine with the other eye-hand tasks.

VII. RECOMMENDATIONS

More research can be done to improve the current experiment. First of all, the input device should be addressed. Although the touch-screen interface is user-friendly, loss of contact affects the quality of the results. An alternative set-up could be splitting the display and the input screen. By adding a flat laying input touch-screen, LOC due to fatigue could be decreased. Also, fittings could be used, such as a stylus or a thimble, to decrease LOC due to friction.

When the LOC problem is fixed, more attention should be paid to the preview problem. The additional required cognitive processing makes the preview preferable to a pursuit task. Experiments should be performed to identify what factors influence inexperienced subjects ability to use preview. For example, the learning curve of older patients in a preview task could be investigated. Other factors could be the visibility, size and location of the target and preview line on the display. Another method to motivate subjects to use preview is to make the task more recognizable. For example, the tracking task could imitate a car driving task.

Also, the small sample size should be dealt with. For now, a very specific patient group has been selected; those with cerebellar dysfunction due to stroke. Perhaps, it is not necessary to restrict the experiment to such a specific condition. Loss of motor skill is attributed to many neurological disorders. Including cerebral disorders and tumors. Another larger group could be tested, or groups could be combined to increase sample size if the symptoms are alike. The current experiment is not accurate enough to differentiate between different conditions, it detects loss of motor skill in general.

VIII. CONCLUSION

The goal of the current experiment, was to develop a preview tracking task to quantify loss of motor skills after a cerebellar stroke. Four patients, four age-matched control subjects and 26 young adults participated in a preview experiment on a touch-screen. The results of patients and control subjects have been compared, to identify differences in tracking behaviour. The results show that patients deploy a more cautious control strategy. They generate additional lead to compensate for their low gain. Thereby, they increase stability. The effects of a cerebellar stroke are also described by the increased damping

ratio and increased visual time delay.

The tracking task is a capable tool for the quantification of loss of motor skill.

REFERENCES

- [1] "Patiëntenversie richtlijn beroerte," Brochure, 2008.
- [2] E. R. Kandel, *Principles of Neural Science*, 5th ed. McGraw-Hill, 2013.
- [3] M. Kawato, K. Furukawa, and R. Suzuki, "A hierarchical neural-network model for control and learning of voluntary movement," *Biological Cybernetics*, vol. 57, no. 3, pp. 169–185, 1987.
- [4] K. Ito, "Neurophysiological aspects of the cerebellar motor control system," *International journal of neurology*, vol. 7, no. 2, pp. 162–176, 1970.
- [5] D. M. Wolpert and M. Kawato, "Multiple paired forward and inverse models for motor control," *Neural Networks*, vol. 11, no. 7-8, pp. 1317–1329, 1998.
- [6] C. M. Fredericks, *Disorders of the cerebellum and its connections*, 1996.
- [7] P. Trouillas, T. Takayanagi, M. Hallett, R. Currier, S. Subramony, K. Wessel, A. Bryer, H. Diener, S. Massaquoi, C. Gomez, P. Coutinho, M. Ben Hamida, G. Campanella, L. Filla, A. Schut, D. Timann, J. Honorat, N. Nighoghossian, and B. Manyam, "International Cooperative Ataxia Rating Scale for pharmacological assessment of the cerebellar syndrome," *Journal of the Neurological Sciences*, vol. 145, no. 2, pp. 205–211, 1997.
- [8] D. T. McRuer and H. R. Jex, "A Review of Quasi-Linear Pilot Models," *Human Factors in Electronics, IEEE Transactions on*, vol. HFE-8, no. 3, pp. 231–249, 1967.
- [9] K. Flowers, "Lack of prediction in the motor behaviour of parkinsonism," *Brain*, vol. 101, pp. 35–52, 1978.
- [10] J. D. Cooke, J. D. Brown, and V. B. Brooks, "Increased dependence on visual information for arm movement in patients with Parkinson's disease," *Extrapyramidal System and its Disorders*, vol. 24, no. 4, pp. 185–189, 1979.
- [11] H. Beppu, M. Suda, and R. Tanaka, "Analysis of Cerebellar Motor Disorders By Visually Guided Elbow Tracking Movement," *Brain*, vol. 107, pp. 787–809, 1984.
- [12] R. D. Jones and I. M. Donaldson, "Measurement of integrated sensory-motor function following brain damage by a computerized preview tracking task," *International rehabilitation medicine*, vol. 3, no. 2, pp. 71–83, 1981.
- [13] B. L. Day, J. P. R. Dick, and C. D. Marsden, "Patients with Parkinson's disease can employ a predictive motor strategy," *Journal of neurology, neurosurgery, and psychiatry*, vol. 47, no. 12, pp. 1299–1306, 1984.
- [14] R. D. Jones and I. M. Donaldson, "Measurement of sensory-motor integrated function in neurological disorders: three computerised tracking tasks," *Medical & biological engineering & computing*, vol. 24, no. 5, pp. 536–540, 1986.
- [15] J. L. Vercher and G. M. Gauthier, "Cerebellar involvement in the coordination control of the oculo-manual tracking system: effects of cerebellar dentate nucleus lesion," *Experimental brain research*, vol. 73, pp. 155–166, 1988.
- [16] B. L. Morrice, W. J. Becker, J. A. Hoffer, and R. G. Lee, "Manual tracking performance in patients with cerebellar incoordination: effects of mechanical loading," *Can J Neurol Sci*, vol. 17, no. 3, pp. 275–285, 1990.
- [17] P. van Donkelaar and R. G. Lee, "Interactions between the eye and hand motor systems: disruptions due to cerebellar dysfunction," *Journal of neurophysiology*, vol. 72, no. 4, pp. 1674–85, 1994.
- [18] P. Soliveri, R. G. Brown, M. Jahanshahi, T. Caraceni, and C. D. Marsden, "Learning manual pursuit tracking skills in patients with Parkinson's disease," *Brain*, vol. 120, no. 8, pp. 1325–1337, 1997.
- [19] K. C. Engel, J. H. Anderson, C. M. Gomez, and J. F. Soechting, "Deficits in ocular and manual tracking due to episodic ataxia type 2," *Movement Disorders*, vol. 19, no. 7, pp. 778–787, 2004.
- [20] L. A. Boyd and C. J. Winstein, "Cerebellar Stroke Impairs Temporal but not Spatial Accuracy during Implicit Motor Learning," *Neurorehabilitation and Neural Repair*, vol. 18, no. 3, pp. 134–143, 2004.
- [21] M. H. Heitger, T. J. Anderson, R. D. Jones, J. C. Dalrymple-Alford, C. M. Frampton, and M. W. Ardagh, "Eye movement and visuomotor arm movement deficits following mild closed head injury," *Brain*, vol. 127, no. 3, pp. 575–590, 2004.
- [22] R. C. Miall, D. J. Weir, and J. F. Stein, "Visuo-motor tracking during reversible inactivation of the cerebellum," *Experimental brain research*, vol. 65, pp. 455–464, 1987.

- [23] M. M. K. Oishi, P. Talebifard, and M. J. McKeown, "Assessing manual pursuit tracking in parkinson's disease via linear dynamical systems," *Annals of Biomedical Engineering*, vol. 39, no. 8, pp. 2263–2273, 2011.
- [24] R. de Vries, "Using Human Operator Modeling for Quantifying Loss of Motor Skills due to Parkinson's Disease," Master's thesis, Delft University of Technology, 2016.
- [25] K. Hiramatsu and H. Uno, "Older drivers' performance with variation of preview time in tracking task," *Technical Notes/JSAE Review*, vol. 17, pp. 65–77, 1996.
- [26] K. Ito and M. Ito, "Tracking Behaviors of the Human Operator in Preview Control Systems," *Electrical Engineering in Japan (Translated from Dedd Cakkai Ronbunshi)*, vol. 95, no. 1, pp. 120–127, 1975.
- [27] L. D. Reid and N. H. Drewell, "A pilot model for tracking with preview," in *Proc. 8th Annu. Conf. Manual Control*, 1972, pp. 191–204.
- [28] R. A. Hess and A. Modjtahedzadeh, "A preview control model of driver steering behavior," *Systems, Man and Cybernetics*, pp. 504–509, 1989.
- [29] T. B. Sheridan, "Three Models of Preview Control," *IEEE Transactions on Human Factors in Electronics*, vol. 7, no. 2, pp. 91–102, 1966.
- [30] M. Tomizuka and D. E. Whitney, "The human operator in manual preview tracking (an experiment and its modeling via optimal control)," *Journal of Dynamic Systems, Measurement, and Control*, vol. 98, pp. 407–413, 1976.
- [31] K. van der El, D. M. Pool, H. J. Damveld, M. M. van Paassen, and M. Mulder, "An Empirical Human Controller Model for Preview Tracking Tasks," *IEEE Transactions on Cybernetics*, pp. 1–13, 2015.
- [32] R. Miall and G. Reckess, "The Cerebellum and the Timing of Coordinated Eye and Hand Tracking," *Brain and Cognition*, vol. 48, no. 1, pp. 212–226, 2002.
- [33] R. Jones and I. Donaldson, "Tracking tasks and the study of predictive motor planning in Parkinson's disease," in *Engineering in Medicine and Biology Society*, no. 11, 1989, pp. 1055–1056.
- [34] R. D. Jones, "Measurement and Analysis of Sensory-Motor Performance: Tracking Tasks," in *Human performance engineering*, 2014, pp. 31–1–27.
- [35] P. M. T. Zaal, D. M. Pool, J. de Bruin, M. Mulder, and M. M. van Paassen, "Use of Pitch and Heave Motion Cues in a Pitch Control Task," *Journal of Guidance, Control, and Dynamics*, vol. 32, no. 2, pp. 366–377, 2009.
- [36] K. van der El, S. Barendswaard, D. M. Pool, and M. Mulder, "Effects of Preview Time on Human Control Behavior in Rate Tracking Tasks," in *13th IFAC/IFIP/IFORS/IEA Symposium on Analysis, Design, and Evaluation of Human-Machine Systems*, Kyoto, Japan, 2016.
- [37] E. Rezunenko, "Validating a Human Controller Model for Preview Tracking Tasks," Master's thesis, Delft University of Technology, 2016.
- [38] M. F. Folstein, S. E. Folstein, and P. R. McHugh, "Mini-mental state: a practical method for grading the cognitive state of patients for the clinician. Journal," *Journal of psychiatric research*, vol. 12, no. 4, pp. 189–198, 1975.
- [39] C. Vision, "Chronos Visio." [Online]. Available: www.chronos-vision.de
- [40] C. De Boer, J. Van der Steen, R. J. Schol, and J. J. M. Pel, "Repeatability of the timing of eye-hand coordinated movements across different cognitive tasks," *Journal of Neuroscience Methods*, vol. 218, no. 1, pp. 131–138, 2013.
- [41] D. Muilwijk, S. Verheij, J. J. M. Pel, A. J. Boon, and J. van der Steen, "Changes in Timing and kinematics of goal directed eye-hand movements in early-stage Parkinson's disease." *Translational neurodegeneration*, vol. 2, no. 1, p. 1, 2013.
- [42] C. de Boer, J. van der Steen, F. Mattace-Raso, A. J. Boon, and J. J. M. Pel, "The Effect of Neurodegeneration on Visuomotor Behavior in Alzheimer's Disease and Parkinson's Disease." *Motor control*, vol. 20, no. 1, pp. 1–20, 2016.
- [43] Y. Haartsen, "Quantifying loss of motor skills after cerebellar stroke: Control behavior of cerebellar patients in a preview tracking task," Master's thesis, Delft University of Technology, 2017.
- [44] M. M. van Paassen and M. Mulder, "Identification of human operator control behaviour in multiple-loop tracking tasks," in *Proc. 7th IFAC/IFIP/IFORS/IEA Symp. Anal. Design Eval. Man Mach. Syst.*, Kyoto, Japan, 1998, pp. 515–520.
- [45] J. R. Leigh and D. S. Zee, *The neurology of eye movements*, 3rd ed. New York: Oxford University Press, 1999.
- [46] R. J. Wasicko, D. T. McRuer, and R. E. Magdaleno, "Human Pilot Dynamic Response in Single-loop Systems with Compensatory and Pursuit Displays," Air Force Flight Dynamics Laboratory, Tech. Rep., 1966.
- [47] H. J. Damveld, G. C. Beerens, M. M. Van Paassen, and M. Mulder, "Design of Forcing Functions for the Identification of Human Control Behavior," *Journal of Guidance, Control, and Dynamics*, vol. 33, no. 4, pp. 1064–1081, 2010.
- [48] K. van der El, D. M. Pool, M. M. van Paassen, and M. Mulder, "Effects of Preview on Human Control Behavior in Tracking Tasks With Various Controlled Elements," *IEEE Transactions on Cybernetics*, 2017.

Part II

Preliminary report

Chapters 2 to 8 have been graded as part of AE4020

The cerebellum and its functions

The goal of this research is to conduct a tracking experiment with patients that suffered from a cerebellar stroke and an age-matched control group. To design a suitable task and be able to interpret the results, it is important to know how the cerebellum works. This chapter is dedicated to the cerebellum. Section 2-1 explains the anatomy and general functions of the cerebellum. Section 2-2 further elaborates on the functions of the cerebellum related to the vestibular system. Next, Section 2-3 does the same for functions related to voluntary movement. Section 2-4 describes possible consequences of a cerebellar stroke. The relation between the cerebellum and the basal ganglia is explained in Section 2-5. This helps to relate the current project to the one previously conducted at the Erasmus MC [3, 4]. Finally, in Section 2-6 the current assessment methods are explained.

2-1 Cerebellar anatomy and pathways

The cerebellum is located at the back of the brain as depicted in Figure 2-1. The main function of the cerebellum is to assist the cerebrum in coordinating movement. It projects via the thalamus to the motor cortex. Thereby the cerebellum transforms input from several nuclei into output for accurate and efficient movement. Functions attributed to the cerebellum are; maintenance of balance and posture, coordination of voluntary movements, motor learning and cognitive functions [10]. These functions are linked to three functional parts of the cerebellum. The first part is the vestibulocerebellum, it projects to the vestibular nuclei in the brain stem, more about this part of the cerebellum can be found in Figure 2-2. Another part is the spinocerebellum, an essential part that coordinates muscles in the torso and maintains balance and posture. It projects to the brainstem motor nuclei. The last part is the cerebrocerebellum, this part contributes to coordination of voluntary movements. It projects to the cortex via the thalamus.

The functional parts of the cerebellum are incorporated in three highly foliated chains; the central vermis and two hemispheres. Within these chains there are many lobes. Figure 2-2 gives an anatomical overview of the cerebellum. A schematic, functional overview can be found in Figure 2-3.

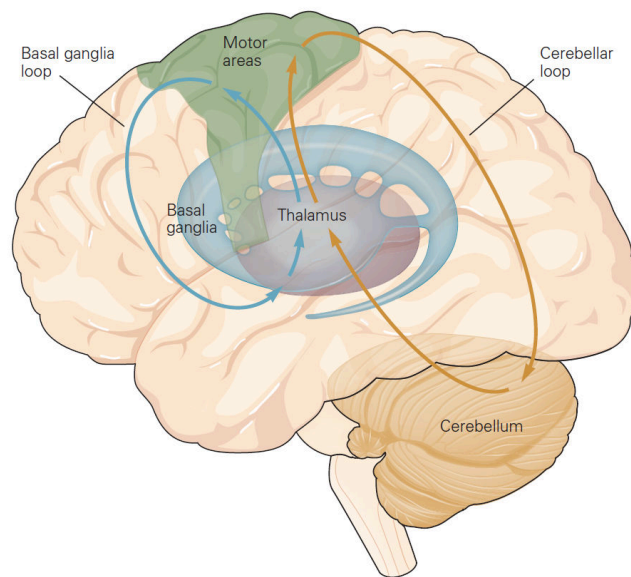


Figure 2-1: The major subcortical brain systems that initiate and control motor actions [11]

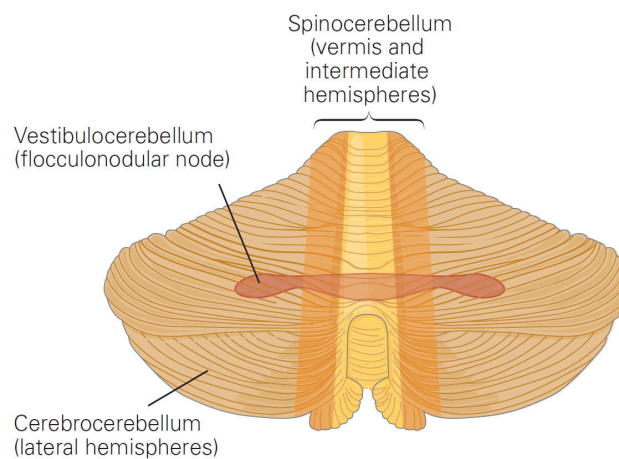


Figure 2-2: Anatomical overview of the cerebellum [11]

2-2 Vestibular ocular reflex

In the vermis and hemispheres, the flocculus, paraflocculus, nodulus and ventral ovula form the vestibulocerebellum. They are closely related to the vestibular system and play an important role in the control of eye movements. Based on how the lobules are connected, their functions can be derived. The flocculus and paraflocculus contribute to vestibulo-ocular reflexes and smooth pursuit respectively. The nodulus and ventral ovula influence the vestibulo-ocular reflex (VOR) at low frequencies [12]. When the head is moved by an external stimulus, the VOR causes a fixed gaze. The cerebellum compensates head movement by moving the eyes. For example, when a subject looks at a screen while the head is forced to rotate left and right, the VOR ensures that the eyes of the subject remain fixed on the screen. Another part of the

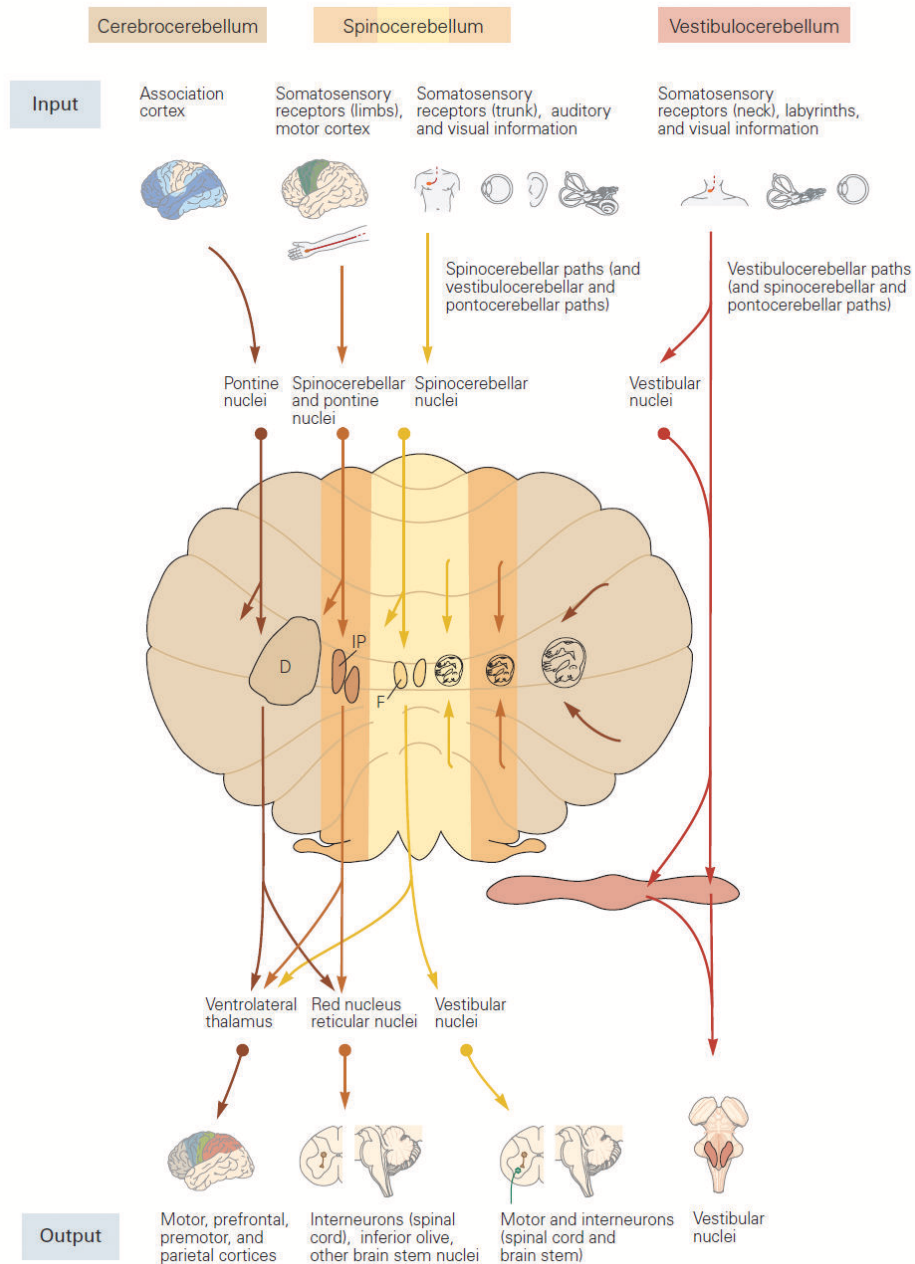


Figure 2-3: Schematic overview of functional anatomy of the cerebellum [11]

dorsal vermis is responsible for saccades; fast eye movements between to fixation points.

2-3 Motor control in the cerebellum

The dentate nucleus, located in the cerebrocerebellum, regulates voluntary movement. Visually guided movement appears to originate in this section as well. Miall et al. [13] observed that, after inactivation of the cerebellum, tracking accuracy decreased. Vercher and Gauthier

[1] conducted tracking tasks with trained monkeys. The monkeys had to track a target in four different ways; only with the eyes, with eyes and hand using a lever, with eyes and hand while the hand was masked, by moving the target themselves. The monkeys performed the tasks in healthy conditions and after lesioning of the dentate nucleus. For the eye-alone tracking of an unpredictable target the researchers found a delay of 200ms. If a healthy monkey actively moved the target itself, the delay between hand and eye movements decreased to 30ms. As if a copy of the hand movement was sent to the eye motor system to ensure synchronization of hand and eye movements. After lesioning, the delay between hand and eye movements for this task, increased to 200ms. The eye motor system was no longer able to benefit from information, that allowed for prediction of arm motion. To explain the increasing delay between hand- and eye movements after inactivation of the cerebellum, several theories have been proposed.

2-3-1 The forward model

The first theory suggests that the cerebellum acts as a forward model in a feedback-error-learning system [14]. A schematic representation of the system can be found in Figure 2-4. A plan to move is send to the motor cortex. The motor cortex generates a command and sends it to the actuator. The final outcome of the command is fed back to the motor cortex by sensory systems such as the visual system, proprioceptive system and vestibular system. The sensory feedback loop is indicated by the grey lines. Sensory feedback is slow, only relying on this feedback loop, leads to long delays. Therefore an efferent copy of the motor command is send to the cerebellum. The cerebellum predicts what the final outcome of the command would be and sends internal feedback to the motor cortex. The internal feedback is much faster than the sensory feedback loop. The fast flow of corrective commands leads to smooth movement. The more the movement is repeated, the better the cerebellum becomes at predicting the final state of the actuator. At first the movement will be slow, but it becomes faster as the internal model is formed. In the end the sensory feedback signal becomes redundant and the movement can be performed almost automatically.

2-3-2 The inverse model

Another theory is the inverse model developed by Kawato et al. [15]. Kawato et al. propose a hierarchical neural network model for the cerebellum, similar to Figure 2-5. When a task is performed for the first time, movement is slow and inaccurate due to long-loop sensory feedback. After repeating the movement a few times, the task can be executed more precise and more rapidly. According to Kawato et al., an inverse dynamics model of the of the controlled limb is formed. By learning from the predicted movement signal of the internal model, the inverse model is constructed. This works as a feed-forward controller where the inputs are the desired trajectory and motor command and the output is the motor command that will be send to the motor cortex. Thereby the cerebellum omits the long-loop feedback delays.

Since the feed-forward inverse dynamics model is never perfect the internal dynamics model still plays an important role in motor control.

Since Kawato et al. [15] others have extended the hierarchical neural network model. Wolpert and Kawato suggested a multiple paired forward and inverse model [16]. This model exists of

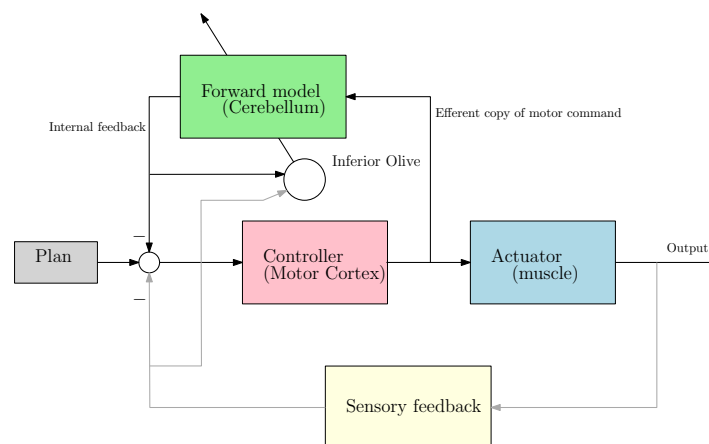


Figure 2-4: Cerebellum as forward model in feedback-error-learning system

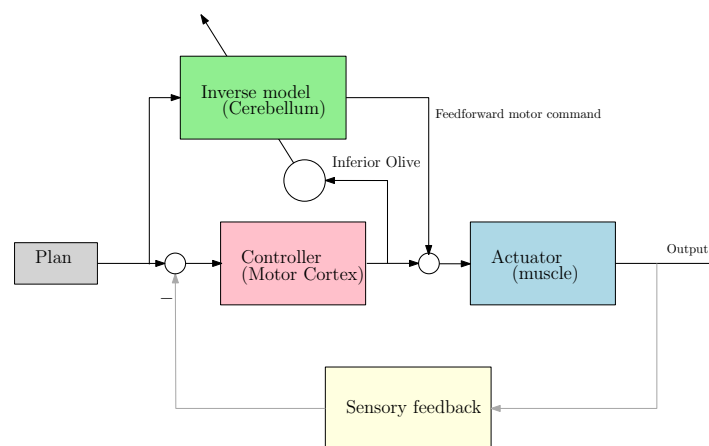


Figure 2-5: Cerebellum as inverse model in feedback-error-learning system

multiple inverse models accompanied by a corresponding forward model. The outputs of both models are weighted by the responsibility predictor to determine to which degree each model can contribute to the resulting motor command. Meanwhile the inverse model receives the motor feedback command, weighted by the responsibility predictor, for learning purposes. The motor learning process starts with the slow sensory feedback loop. After a while the internal feedback loop takes over and movement becomes faster. Finally the inverse dynamics model takes over. Figure 2-6 shows the multiple paired model. The dotted lines represent training signals sent to the forward- and inverse models, dashed lines show the output of the responsibility predictor. Haruno added a learning rule and successfully simulated the model [17].

2-4 Consequences of lesions in the cerebellum for eye and hand movements

The cerebellum is connected to several systems in the human body. How a lesion in the cerebellum influences these systems, depends highly on its location. Whether it is in the left

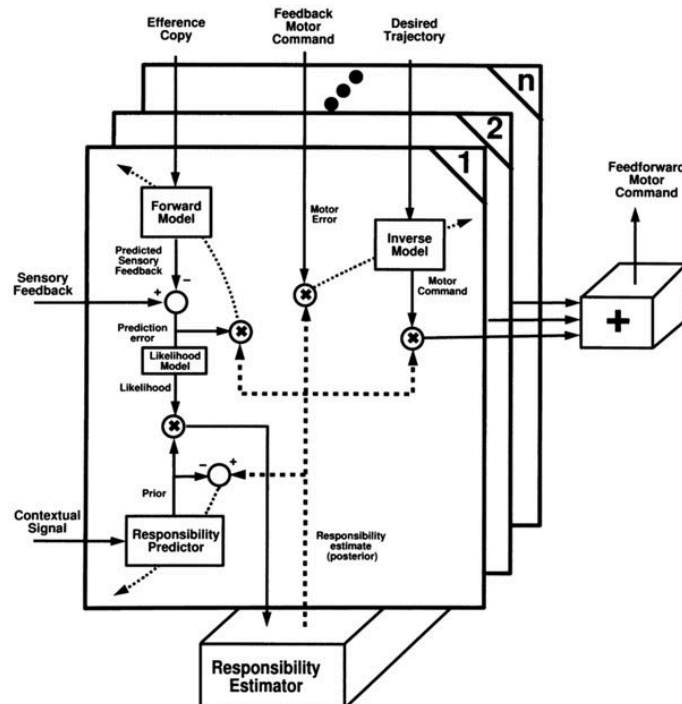


Figure 2-6: Multiple paired internal model of the cerebellum [16]

or right side of the brain and whether it occurs in the vermis, hemisphere or flocculus. When the lesion occurs on one side of the brain (*unilateral*), limbs on the same side (*ipsilateral*) are affected. So a lesion in the right hemisphere would lead to impairment in limbs on the right side of the body.

Four symptoms indicate cerebellar disorders [11,18]. A general symptom of cerebellar dysfunction is *ataxia*, derived from the Greek word meaning "lack of order". Movements of patients are uncoordinated and results in errors in speed and direction. Ataxia is reflected in gait, speech, limb movement and eye movement, depending on the location of the lesion. If the damage occurs in the outer hemisphere, voluntary movement of limbs is affected. A lesion in the floccolondular lobes may result in balance problems but also in problems with head posture and eye movements. For example nystagmus, vertigo, nausea and vomiting. These are symptoms similar to those caused by a damaged vestibular system.

If the lesion is close to the vermis the trunk and legs are most likely affected. Patients are unsteady, walk uncertain and experience balance problems. Sometimes unsupported sitting or walking is impossible. This is called *astasia-abasia*.

During a target-reaching task the arm movement of the patient is characterized by *dysmetria*; overshoot (*hypermetria*) and undershoot (*hypometria*). To compensate for all the errors, instead of one smooth movement the patient executes multiple small movements. For a task that requires a lot of precision, all these small movements result in an *intention tremor*.

The final symptom is *hypotonia*. The patient suffers from decreased muscle tone; decreased resistance to passive stretching of a muscle. For example, if a healthy leg is stretched, the flexor muscles will quickly respond to the movement by contracting. When the knee is flexed again, it comes to rest immediately. In case of hypotonia the knee keeps swinging back and

forth for a couple of times before it comes to rest.

Besides motor problems a damaged cerebellum could also lead to cognitive dysfunctions. In some cases patients have trouble speaking and learning.

The above mentioned symptoms do not only affect the limbs. If the lesion occurs in the vermis, eye movement will be affected too. Two types of eye movement originate from the cerebellum [11]. Saccadic eye movements direct the gaze quickly from one object to another. Smooth pursuit eye movement, on the other hand, fixes the gaze on a moving target. For example, when a target shifts horizontally on a screen, the eyes move at the same speed as the moving target, maintaining object fixation. After a cerebellar stroke, smooth pursuit is impaired. Engel et al. [19] studied ocular and manual tracking behaviour of patients with ataxia. In case of cerebellar dysfunction, ocular tracking resulted in saccadic eye movements.

2-5 Relation to basal ganglia

The cerebellum and basal ganglia reside in the motor system structure. Both components communicate to the motor cortex through the thalamus and coordinate voluntary movement. They work together to create smooth, efficient movements. There are however a few differences between the basal ganglia and the cerebellum. The basal ganglia excite and inhibit movement. When movement is necessary, the basal ganglia select and release the specific movement. They play an important role in timing of movements [20]. The cerebellum on the other hand, produces smooth, skilled movement. It corrects online errors in the ongoing motor command.

The difference between the functions of both systems can be recognized in symptoms of patients with Parkinson's disease and cerebellar deficits. Parkinson's disease is a result of a lack of dopamine production in the basal ganglia [21]. A well known symptom of Parkinson's disease is the tremor at rest. Patients also have difficulties with the initiation of movement (*akinesia*), they show a slow shuffling gait. Only if the movement is triggered by external stimuli the patient can perform it relatively normal. Patients with cerebellar deficits do not experience difficulties with the initiation of movements, instead they show errors in size and speed during moving (*ataxia*). Patients have an unsteady gait which is sometimes referred to as "drunken sailor gait". Instead of the tremor at rest which is evident in Parkinson's patients, cerebellar patients suffer from an intention tremor. They execute uncoordinated movements during voluntary movement.

2-6 Assessment of cerebellar dysfunction

Symptoms of a cerebellar stroke are difficult to distinguish. Patients may experience problems with movement, impaired speech, dizziness, nausea or a headache. In many cases, these symptoms are not recognized as a stroke because they can also be interpreted as a regular flu. Only after experiencing persistent physical complaints, patients search for medical help. After diagnosis, the recovery trajectory starts. Half of the patients is considered to function normally after 6 months [22]. After two weeks a patient is allowed to drive again, provided that there are no interfering cognitive or physical deficits. If there are deficits, a patient is

tested again after three months and six months. At the Erasmus MC, two tests are applied for cognitive and motor assessment; the Montreal Cognitive Assessment and the International Cooperative Ataxia Rating Scale.

2-6-1 Montreal Cognitive Assessment (MoCa)

The Montreal Cognitive Assessment is a 10-minute test to identify mild cognitive impairment. It was developed by Nasreddine et al. [23] and administered to patients that score sufficient on the Mini-Mental State Examination (MMSE). The MoCa is more sensitive than the MMSE, a test that indicates dementia. The MoCa treats several different categories: attention and concentration, executive functions, memory, language, visuoconstructional skills, conceptual thinking, calculations, and orientation. Tasks are for example: draw a clock at ten past nine, remember and repeat a list of words, explain what two given words have in common, give the current date. The medical expert gives a score based on MoCa standards. Scores between 26 and 30 points indicate that there is no cognitive impairment.

2-6-2 International Cooperative Ataxia Rating Scale

The ICARS has been developed at the Vancouver Neurology Congress [2]. It is a scale that semi-quantifies cerebellar ataxia symptoms in a reasonable amount of time. The test can be divided in several domains of cerebellar ataxia: postural and stance disturbances; limb movements disturbances; speech disorders; and oculomotor disorders. Each category has a different weight factor. Limb ataxia contributes more to the score than oculomotor disorder. The scores add up to a total of 100 points where 0 indicates no cerebellar deficits. A patient has to, for example: walk, sway with eyes open and closed, point at his nose, and trace an Archimedes spiral.

The downsides of the ICARS test is that it is semi-subjective, has a low resolution and does not assess fine motor skills in detail, such as eye-hand coordination.

Manual tracking tasks

An occupation in which well-controlled eye-hand movements are vital, is flying an aircraft. In the field of aerospace engineering, manual control tasks are used to study and optimize the performance of pilots. McRuer et al. presented a general method to describe human controller (HC) dynamics [24]. His work still serves as a basis for research on HC behaviour. This chapter explains the necessary theory for developing and analysing the results of the preliminary and final experiment. Several types of manual tracking tasks exist. This chapter will only consider theory related to pursuit and preview tasks. First, Section 3-1 will introduce the HC, Section 3-2 describes the two tasks, Section 3-3 the input functions. Section 3-4 explains how the response of the HC is obtained. Pilot describing models will be given in Section 3-5. Finally the model fitting and parameter estimation methods will be described in Section 3-6.

3-1 The human controller

To investigate control behaviour of the HC, it would be convenient if every HC acted the same. In an ideal world, a single model could be constructed to summarize human behaviour while steering a dynamic system. In reality, HCs learn and adapt their behaviour to the system. They show a variety of control strategies and characteristics [25], highly dependent on the type of task. A specifically designed manual tracking task can be used to compare control behaviour between subjects.

3-2 Tracking behaviour in pursuit and preview tasks

A man-machine system is treated as a closed-loop system. Figure 3-1 shows the block diagram of the pursuit task adapted from the model proposed by Wasicko et al. [26]. The display is

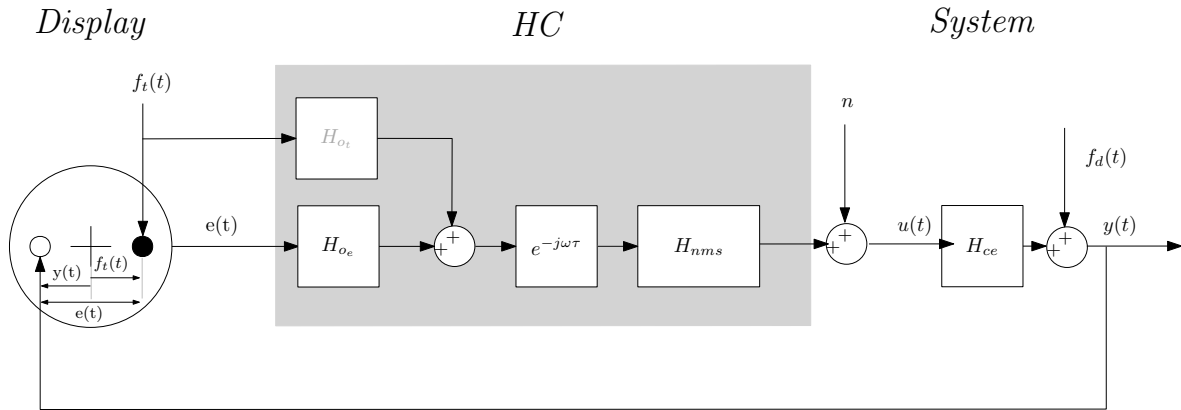


Figure 3-1: Block diagram of pursuit tracking task, adapted from original model by [26]

included in the figure. The HC steers the *controlled element* to minimize the distance between the *controlled element* and the *target*. The HC itself (in grey on Figure 3-1) is represented by a linear, mathematical model. The remnant signal (n) is added to the output of the HC to account for non-linear behaviour [24]. The HC observes the controlled element, the target and indirectly the error, because $e(t) = f_t(t) - y(t)$. Due to this linear dependency the model is overdetermined. Therefore, it is rewritten to a two-channel model. In other words, the HC responds to two of three inputs. Wasicko et al. [26], proposed the model in Figure 3-1 where the HC responds to the error and the target. Wasicko et al. then concluded that the HC performing a pursuit task with single integrator dynamics, does not use the target input function. Therefore, the H_{o_t} loop can be omitted. For system identification purposes the HC is considered as a single-input-single-output system.

Figure 3-2 shows two block diagrams of the preview task performed by Van der El et al. [9]. The top diagram represents the bottom diagram in a simplified form. Part of the target function is shown above the target, allowing the HC to look-ahead and compensate for his own time-delay. Consequently, performance increases [27]. In this case the HC tries to minimize the error $e^*(t)$ between the controlled element and the target at a far-view point $f_{t,f}^*(t)$. The HC observes the controlled element and target, similar to the pursuit task, and additionally a part of the target function. A pursuit task is actually a preview task with zero preview. For the pursuit task with single integrator dynamics, the HC can be modelled as a single-input-single-output system. For the preview task however, the HC is expected to respond to the target and controlled element [9]. This is represented in the simplified model in Figure 3-2.

3-3 Forcing functions

Forcing functions are pre-set signals inserted into the closed-loop system. They excite the system and are needed to estimate the response of the HC [28]. A quasi-random, multi-sine signal, constructed using Equation (3-1), gives a suitable input function. A_t denotes the amplitudes, ω the excitation frequencies, and ϕ the phases shifts. The forcing function has power at the frequencies of the sinusoids. In the pursuit task, depicted in Figure 3-1, the HC is only responding to the error, given that the system has single integrator dynamics. This

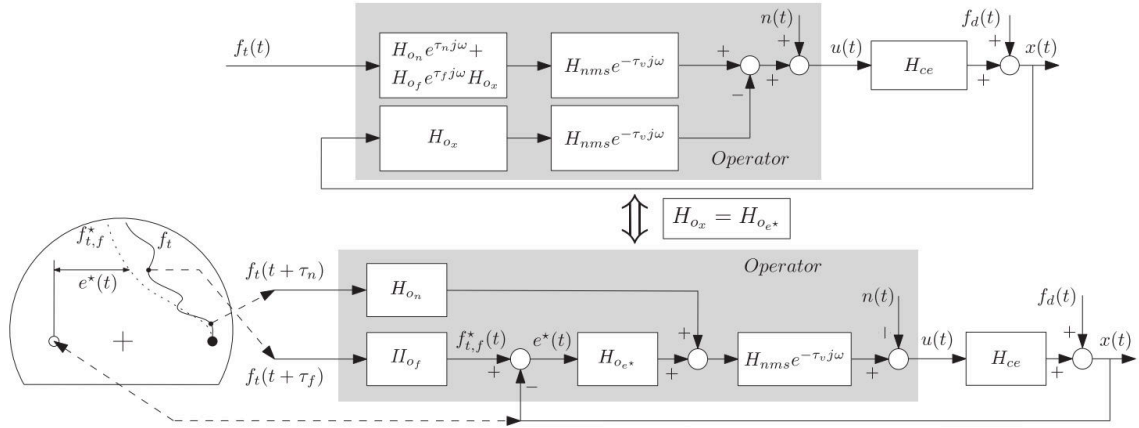


Figure 3-2: Block diagram of HC behavior preview tracking task developed by Van de El et al. [9]

requires only one input forcing function that controls the target, $f_d(t) = 0$.

$$f_t = \sum_{k=1}^{N_t} A_t(k) \sin(\omega_t(k)t + \phi_t(k)) \quad (3-1)$$

In the preview tracking task the HC responds to the target and the controlled element. This requires two forcing functions [28]. The first being the target forcing function. The second forcing function is the disturbance f_d , applied to the controlled element.

3-4 System identification

To investigate control behaviour, the operator response has to be estimated. The Fourier Coefficient method (FCM) is a black-box identification method that gives an estimation of the operator response in the frequency domain [28]. It can be applied to the system without prior knowledge of the HC describing function. After Fourier transforming the inputs and outputs close to the HC, Equation (3-2) can be derived.

$$U(j\omega) = H_{o_e}(j\omega)E(j\omega) + N(j\omega) \quad (3-2)$$

The remnant accounts for non-linear behaviour. The HC responds to a multi-sine signal with a significant amount of power at the frequencies of the input sines. At these frequencies the contribution of the remnant in the operator response, $N(j\omega_t)$, is small. Therefore, it can be neglected at the input frequencies and the operator response can be estimated with the instrument variable method for this simple case given by Equation (3-3).

$$\hat{H}_{o_e}(j\omega_t) = \frac{U(j\omega_t)}{E(j\omega_t)} \quad (3-3)$$

In case of a preview tracking task the HC may respond to both the target and the error at a far view point. The two-channel identification method allows for separation of the two responses [28]. Now, Equation (3-2) should be expressed as in Equation (3-4).

$$U(j\omega) = H_{o_t}(j\omega)F_t(j\omega) + H_{o_x}(j\omega)X(j\omega) + N(j\omega) \quad (3-4)$$

The remnant can be ignored at the input frequencies of the target and disturbance forcing function. The estimation of $\hat{H}_{o_e}(j\omega_t)$ and $\hat{H}_{o_x}(j\omega_t)$ can be found in Equation (3-5). The same method can be applied to estimate the response at the disturbance frequencies ω_d .

$$\begin{aligned}\hat{H}_{o_e}(j\omega_t) &= \frac{\tilde{U}(j\omega_t)X(j\omega_t) - U(j\omega_t)\tilde{X}(j\omega_t)}{\tilde{F}_t(j\omega_t)X(j\omega_t) - F_t(j\omega_t)\tilde{X}(j\omega_t)} \\ \hat{H}_{o_x}(j\omega_t) &= \frac{\tilde{U}(j\omega_t)F_t(j\omega_t) - U(j\omega_t)\tilde{F}_t(j\omega_t)}{\tilde{F}_t(j\omega_t)X(j\omega_t) - F_t(j\omega_t)\tilde{X}(j\omega_t)}\end{aligned}\quad (3-5)$$

3-5 Pilot models

In the previous section the operator response has been estimated using the input and output of the HC. McRuer and Hex [25] represented the HC itself with a quasi-linear describing function. They concluded that the response of the non-linear HC can be split into two parts. The first part is the linear response to the input. The second part is the remnant, the difference between the linear part of the response and the actual response of the HC. The blocks that form the HC model of a pursuit task can be found in Figure 3-1. The mathematical expression of the HC model is given in Equation (3-6).

$$H_{p_e}(j\omega) = K_p \frac{T_L j\omega + 1}{T_l j\omega + 1} e^{-j\omega\tau} \frac{(j\omega)^2}{(j\omega)^2 + 2\zeta_{nms}\omega_{nms}j\omega + \omega_{nms}^2} \quad (3-6)$$

- K_p indicates the pilot gain
- T_L indicates the lead time constant
- T_l indicates the lag time constant
- τ indicates the visual time delay
- ω_{nms} indicates the neuromuscular frequency
- ζ_{nms} indicates the neuromuscular damping ratio

The pilot parameters are depicted in grey, they describe the control characteristics of the HC. McRuer et al. [24] stated that the HCs adjust their behaviour to the system to achieve optimal performance. The lead and lag constants are adjusted such that the open loop transfer function shows a -20dB/decade slope. This means that, if the controlled element has single integrator dynamics (K_c/s), the lead and lag time constants (T_L, T_l) are 0, thus the HC acts as a gain. If the system has gain dynamics (K_c), the HC generates lag to achieve the -20dB/decade slope, $T_l > 0$.

The pilot model for a preview tracking task, as proposed by Van der El et al. [9], can be

found in Equation (3-7) and Figure 3-2.

$$\begin{aligned}
H_{nms}(j\omega) &= \frac{(j\omega)^2}{(j\omega)^2 + 2\zeta_{nms}\omega_{nms}j\omega + \omega_{nms}^2} \\
H_{o_{e^*}}(j\omega) &= K_e \frac{1 + T_{L,e}j\omega}{1 + T_{l,e}j\omega} \\
H_{o_n}(j\omega) &= K_n \frac{j\omega}{1 + T_{l,n}j\omega} \\
H_{o_f}(j\omega) &= K_f H_{o_{e^*}}(j\omega) \frac{1}{1 + T_{l,f}j\omega} \\
\hline
H_{o_t}(j\omega) &= \left(H_{o_n}(j\omega)e^{j\omega(\tau_n - \tau_v)} + H_{o_f}(j\omega)e^{j\omega\tau_f} \right) H_{nms}(j\omega)e^{j\omega(-\tau_v)} \\
H_{o_x}(j\omega) &= H_{o_{e^*}}(j\omega)H_{nms}(j\omega)e^{j\omega(-\tau_v)}
\end{aligned} \tag{3-7}$$

The HC tracks the high frequencies of the target signal by reacting to a near-viewpoint. This point lies τ_n seconds ahead of the target. $H_{o_n}(j\omega)$ describes the response to the near-viewpoint. To track the low frequencies the HC responds to the far-viewpoint, τ_f seconds ahead of the target. $H_{o_f}(j\omega)$ describes the response to the far-viewpoint.

3-6 Model fitting and parameter estimation

Section 3-4 provided information about the HC with an estimation of the operator response based on black-box system identification. Section 3-5 considered the pilot describing model with pilot parameters to describe control behaviour. By combining both, the pilot parameters can be estimated. A cost function fits the pilot describing model to the estimated operator response. It minimizes the difference between the operator response and the model by constantly changing the pilot parameters, until a global minimum of J is found. The outcome highly depends on the initial values. To prevent the function from only producing local minima the optimization is repeated for 50-100 sets of initial parameter values.

$$J(\theta) = \sum_{k=1}^N |\hat{H}_{p_e}(j\omega[k]) - H_{p_e}(j\omega[k]; \theta)|^2 \tag{3-8}$$

Equation 3-8 can be used for pursuit tasks. A cost function that can be used for two-channel tasks such as preview tasks, is given by Equation (3-9). The Fourier coefficients are weighted by $|\hat{H}_{o_x}|^2$ to put emphasis on the high frequencies.

$$J(\theta) = \sum_{k=1}^N \frac{|\hat{H}_{o_t}(j\omega[k]) - H_{o_t}(j\omega[k]; \theta)|^2}{|\hat{H}_{o_t}|^2} + \sum_{k=1}^N \frac{|\hat{H}_{o_x}(j\omega[k]) - H_{o_x}(j\omega[k]; \theta)|^2}{|\hat{H}_{o_x}|^2} \tag{3-9}$$

Measuring visuomotor deficits

The ICARS test [2] from Section 2-6 gives a semi-quantitative score on cerebellar deficits. To get a finer, and more objective result, patients can conduct several predefined tasks where eye and hand movements are recorded. This chapter describes two types of experiments that are conducted at the Erasmus. It also proposes a new task. The tapping task is described in Section 4-1. Section 4-2 describes the pursuit task and finally, in Section 4-3 a new task will be introduced.

4-1 Tapping tasks

At the dept. Neuroscience at the EMC an additional tool has been developed. It precisely quantifies the timing of eyes and hands during fine motor tapping tasks under different cognitive conditions, such as reflexive tapping, memory tapping and decision tapping. The goal is to test the integrity of the visual motor network. In the past it was used to study the effects of Alzheimer's disease [29] and PD [3, 21, 30, 31]. The setup of the experiment can be found in Figure 4-1. The infrared eye-tracking system (Chronos Vision, Berlin, DE) measures the location of the gaze for each eye individually. To ensure a fixed distance to the screen, the subject places his/her head on a chinrest. A 32 inch touch screen (ELO Touch Solutions, Milpitas, CA) displays the task and accurately measures finger position. The touchscreen does not record the actual movement of the arm and hand. This is done by the infrared motion detection system (Vicon Motion Systems, Oxford, UK). All systems are synchronised using a trigger controlled by MATLAB

With this setup the reaction time and accuracy of movement can be determined. An example of an eye-hand task is the pro-tapping task, depicted in Figure 4-2. The subject sits in front of the screen and is instructed to look at the white dot at the center of the screen and hold his/her finger within the blue rectangle. When the rectangle and white dot disappear, a blue dot appears at a random position on the screen. The subject has to direct his gaze to the blue dot and touch it as fast and accurately as possible. After a maximum of three test trials the task is repeated for eight times. Other tasks also include memory and inhibition. Study shows

that Alzheimer's patients experience difficulties with the execution of movement. They also need more time to complete the movement and make many small saccades before reaching the target. PD patients show increased hand movement times [21].



Figure 4-1: The setup at the EMC used for measuring loss of eye-hand coordination and cognitive skills. (1) touch screen, (2) infrared eye-tracking system, (3) infrared motion detection system [31]

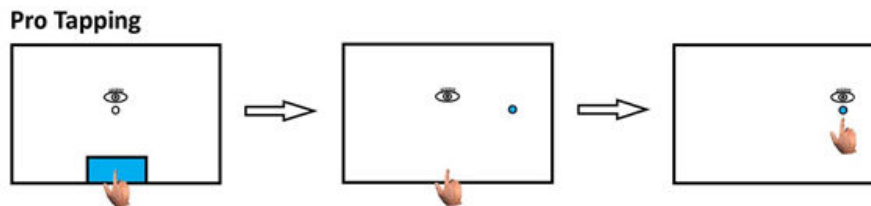


Figure 4-2: Pro-tapping task performed at the EMC [31]

4-2 Pursuit tracking

The tapping tasks only record movement for a short period of time and can only assess fine motor skills to a limited degree. In 2016 a new task was introduced by De Vries [4], to measure loss of motor skills in PD. By using a combination of a manual tracking task and human controller modelling, loss of fine motor skills can be quantified by even more detail than with tapping tasks. It is not the first time that tracking tasks have been applied to patients with impaired motor planning and execution [1, 19, 32–42]. In 2011, Oishi et al. even proposed a second-order linear dynamical system to quantify tracking behaviour in PD patients [43].

The setup at the Erasmus from Figure 4-1 was expanded with a customized HOTAS Warthog joystick (Thrustmaster, Hillsboro, Oregon, USA). The subjects perform a target following task. The display is depicted in Figure 4-3. A blue circle, the target, moves horizontally on the screen, following a semi-random, sinusoidal input signal. The subject uses the joystick to control a red dot, the controlled element, that also moves horizontally on the screen. The goal is to minimize the distance between the target and the controlled element. The controlled

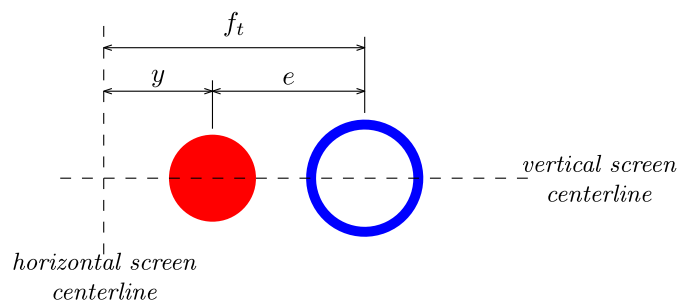


Figure 4-3: Tracking task display [3]

element has single integrator system dynamics. In the previous study at the EMC by Pool et al. [3], four PD patients participated in the experiment. The system identification and model fitting processes were applied successfully. From the results followed that the patient group performed significantly worse than the healthy control group. Analysis of the HC model parameters also showed reduced control gain and increased neuromuscular damping for patients.

4-3 Preview tracking

The target following task held potential as tool to detect early stage PD. To gain even more insight in tracking behaviour, a preview task can be conducted. Many others have implemented preview in their experiments [6–9, 27, 44, 45]. An advantage of using preview tracking tasks is that it represents everyday tasks. Cycling and driving a car are examples of such a task. The intended path of the vehicle is visible and the operator can anticipate future events.

There has been limited research to neurological disorders in combination with a preview tracking task. Jones has incorporated preview tasks for the assessment of motor functions in patients with a neurological disorder [5, 35, 37, 46]. Jones also recognizes the technical difficulty of implementing preview in a tracking task. This might be a reason to dismiss preview tracking. According to Jones and Donaldson *"...the preview tracking task has the advantage of allowing the patient to react to a changing stimulus and to be able to anticipate the nature and magnitude of the responses needed. It thus simulates conditions that patients meet in everyday life better than previous tests."* [35]. A more theoretical motivation for using preview tracking to quantify motor skills in patients with neurological disorders has not been found. In 1989 Jones and Donaldson conducted experiments where PD patients performed manual tracking tasks. One of the tasks was a random input preview task [5]. The experiments showed that predictive motor planning was impaired when involving preview. Some doubts existed to whether there were visuospatial deficits influencing the tracking behaviour during preview tasks. Later, Jones et al. proved that the contribution of visual impairment to the tracking performance of PD patients is small [47]. The research conducted by Jones leads to believe that a preview tracking task might reveal impaired tracking skills for patients with motor system problems.

Preliminary Experiment 1: Comparison between joystick tracking task and touch screen tracking task

Three preliminary tests have been conducted to support decisions regarding chosen settings and form of the final experiment. This chapter describes the first preliminary experiment, where two different types of control devices were compared; touchscreen and joystick.

5-1 Introduction

Manual tracking tasks have been widely used to model control behavior of pilots [24, 26, 27]. Since the early days, manual tracking tasks were performed using a stick [24], steering wheel [6] or lever [48]. This resembles the "real" environment in which a controller would find himself while controlling a vehicle. Manual tracking tasks have also been performed for medical purposes. These test were performed to investigate impairment of visuo-motor skills for Parkinson's disease patients [5, 36, 49, 50], and patients suffering from a stroke [38, 41]. Researchers used various types of control equipment to collect data. For example steering wheels, joysticks or manipulandums.

Increased application of the popular touchscreen interface offers new possibilities for test equipment. The user-friendliness of a touchscreen interface allows for easy application in different situations such as, machine control [51] and medical research [21, 29, 30]. Some simple tracking tasks have been performed using a touchscreen to investigate similarities in the response of hand- and eye tracking tasks [19, 52, 53] Kivila et al. [52] compared a joystick and three different interfaces on a touchscreen. Subjects had to track a target that moved horizontally according to a semi-random forcing function. The authors observed that the tracking error could best be minimized using the joystick. Also, subjects showed the highest gain and lowest time delay while using the joystick.

The tracking task developed at the dept. of Neuroscience at the EMC [3], proved to be an

effective tool to quantify loss of motor skills. For vulnerable subjects, however, a touchscreen interface may be preferable because of its user-friendliness and intuitiveness. Therefore, steps will be taken to replace the joystick task with a touchscreen based manual tracking task. To describe tracking behaviour, it is important to investigate if the identification methods from Chapter 3 can also be applied to the touchscreen interface. Furthermore it is important to check whether touchscreen tracking tasks are comfortable for subjects, since the final experiment will involve inexperienced, vulnerable subjects.

5-2 Method

5-2-1 Subjects

Eight subjects participated, six males and two females. They were between 18 and 44 years old (mean=25.6, SD=7.9). Two subjects were left-handed. Three subjects considered themselves experienced with manual control tasks, two did not have any experience. The remaining subjects had average experience. Six subjects were working at the Neuroscience lab at EMC, two subjects were from Delft University of Technology. None of the subjects suffered from major hand/arm injuries or visual impairment.

5-2-2 Apparatus

The experiment setup at the EMC, presented in Figure 4-1, was used for testing. The infrared eye-tracker and infrared motion detection system were excluded from the setup. The gaze-data is not essential for this experiment and might cause unnecessary distractions from the task. As for the motion detection system, the touchscreen provides enough information on hand motions of subjects.

All tasks were performed in right-handed setting despite the varying handedness of subjects. When subjects found it difficult to maintain contact with the screen during a touchscreen task, they were asked to perform the test using a motion capture glove (Vicon Motion Systems, Oxford, UK). It was left to the subject whether to use the armrest and the chinrest during the experiment.

5-2-3 Experiment

Four tracking tasks were presented to each subject, as depicted in Table 5-2. The pursuit display was designed by De Vries [4]. A blue circle moved on the horizontal axis according to the forcing function, see Figure 4-3. The subject was instructed to pursue the blue circle with a red dot that could be controlled with either the joystick or the touchscreen, see Figure 5-1. The controlled element had gain and single integrator dynamics. The forcing function was taken originally from Zaal et al. [54]. The testing time was decreased from 81.92 to 40.96 seconds because the original testing time might be too long for patients. To enable a better identification of the neuromuscular peak, the signal has been extended by one sine wave in the high frequency region [4]. The forcing function is a sum of 11 sinusoids, which will have a variance of $\sigma = 1 \text{ deg}^2$. ω_t indicates the frequencies at which the target signal gives power and ϕ is the phase of the signal. Table 5-1 shows the properties of the target function. To avoid

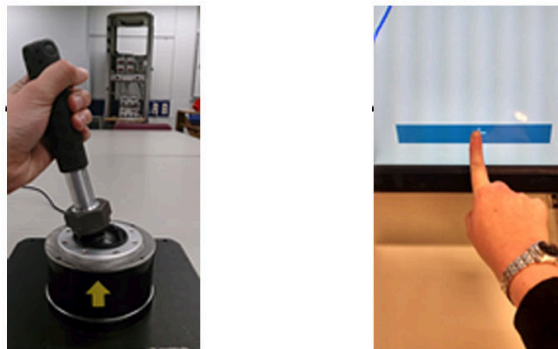
Table 5-1: Target signal properties

<i>Target f_t</i>			
$n_{t,-}$	$\omega_t, \text{rad/s}$	A_t, deg	ϕ_t, rad
4	0.614	1.079	7.239
7	1.074	0.776	0.506
11	1.994	0.391	7.860
17	2.915	0.225	8.184
23	4.449	0.117	9.012
29	5.676	0.082	6.141
37	6.596	0.066	6.776
53	8.130	0.051	6.265
79	12.118	0.035	4.432
109	16.720	0.028	2.672
157	24.084	0.024	8.009

false comparison of tracking tasks, they were conducted in semi-random order as indicated by the latin square in Appendix A. Each subject completed eight runs of every task.

The error signal $e(t)$ was measured as the difference between the target function $f_t(t)$ and the location of the controlled element $x(t)$. The HC output $u(t)$ was the scaled and translated position of the HC finger on the screen.

After testing each subject completed a questionnaire where the most and least difficult task had to be chosen.

**Figure 5-1:** Control devices**Table 5-2:** Experimental conditions preliminary experiment 1

	Touch screen	Joystick
K_c	$G - T$	$G - J$
K_c/s	$SI - T$	$SI - J$

5-3 Results

The results have been produced using the identification and parameter estimation methods for pursuit tasks explained in Chapter 3. The first three trials are considered as practice-trials and will not be considered during the analysis.

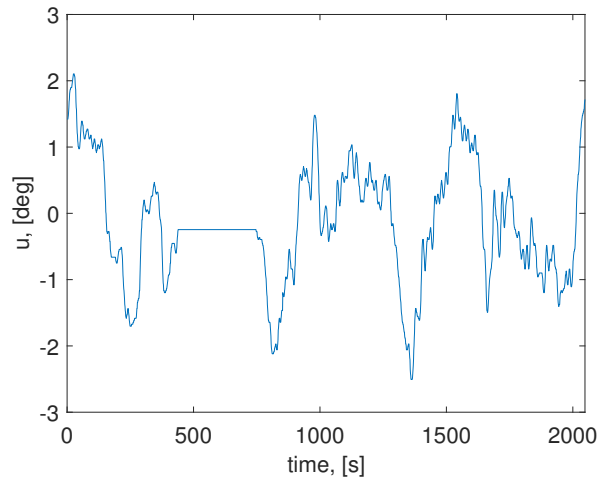


Figure 5-2: Example of loss of contact incident during trial

5-3-1 Questionnaire

Figure 5-3 shows the results of the questionnaire. Overall, the winner is the gain touchscreen task. The gain joystick task was marked as least difficult but for some subjects this task was the most difficult. Most subject considered the single integrator touchscreen task as the most difficult.

5-3-2 Results in the time domain

Before applying identification methods the signal can be plotted in the time domain to detect any problems with data. A drawback of using a touchscreen interface is the contact with the screen. It can be quite difficult to maintain contact with the screen during the whole experiment. The subjects arm could get tired, causing him to relax the arm and loose contact. Also, the friction with the screen might lead to short instances of loss of contact. An example of such an incident can be found in Figure 5-2. For this experiment loss of contact leads to loss of data. In Chapter 6 the influence of the loss of contact incidents on the data will be investigated. For the remainder of the current experiment, all data will be analysed, including data with loss of contact incidents.

5-3-3 Tracking performance and control activity

Figure 5-4 shows the tracking performance per subject for the gain and single integrator. The performance is expressed in variance of the error (σ_e^2) normalized by the variance of the target forcing function ($\sigma_{f_t}^2$). If $\frac{\sigma_e^2}{\sigma_{f_t}^2} < 1$ the subject is trying to reduce the error. For the single integrator one bin is missing. The touchscreen data of subject #1 could not be retrieved due to an error during testing. For the gain, the performance using the touchscreen and joystick, is almost equal. The single integrator dynamics on the other hand, causes differences in performance. Subjects perform better on the joystick task. This is corresponds to results of the post-experiment questionnaire, which can be found in Figure 5-3. Most subjects found the

single integrator touchscreen task the most difficult.

Another method to determine performance is the crossover frequency. At the crossover frequency the open loop magnitude is 1; $|H_{OL}(j\omega_c)| = 1$. The higher the crossover frequency, the better the performance of the subject. Crossover frequency is related to the phase margin, which indicates stability [24]. The phase margins of the joystick tasks and touchscreen tasks showed similar results, as depicted in Figure 5-7. For the crossover frequency, however, the results for the joystick increased by a factor of 1.5 compared to the touchscreen. They are depicted in Figure 5-6. Nevertheless, the difference is small and not represented in Figure 5-4. Therefore it will not be considered as significant.

The control activity for both tasks is depicted in Figure 5-5. In this case, the operator output (σ_u^2) is normalized by the variance of the target forcing function ($\sigma_{f_i}^2$). For the gain task, there is hardly any difference between the touchscreen and joystick. Also between subjects, control activity results are similar. For the single integrator task however, the control activity of the touchscreen task lies higher than for the joystick task. This could explain why subjects regarded this task as difficult; they put a lot of effort in following the target.

There are important mechanical differences between a touchscreen and a joystick that could also explain the difference in control activity. The joystick has a break-out force and gives some mechanical feedback on how far the stick is deflected. This makes it easy to find the zero-position of the device. During a single integrator task, the subject uses both visual feedback and mechanical feedback to move the controlled element. For the touchscreen the subject relies mostly on visual input. There is some friction between the fingertip and the screen, this could give an indication of velocity but a subject cannot derive the nul-position. Adding a line that marks the nul-position leads to unnecessary eye-movements between the fingertip and the controlled element.

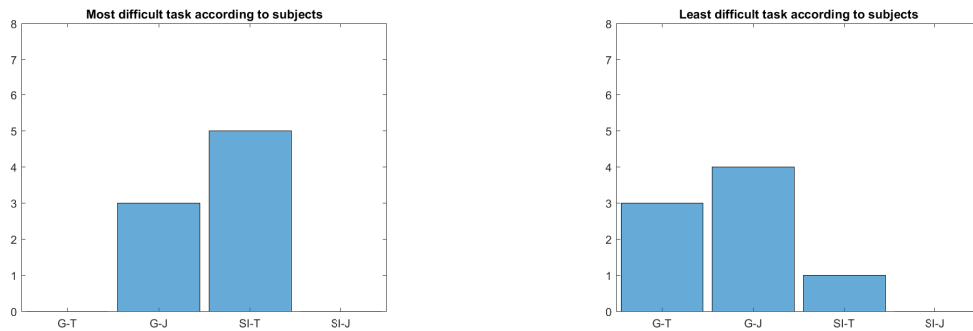


Figure 5-3: Results of post-experiment questionnaire

5-3-4 Model fitting

System identification was performed using the Fourier Coefficient method (FCM). The frequency response of each subject was estimated using the instrument variable method, then a model was fitted to the fourier coefficients in the frequency domain. The pilot describing model is adapted from Equation (3-6). It can be found in Equation (5-1). In case of the gain task the HC generates lag. Therefore, a lag term was added ($T_l \neq 0$). The pilot describing

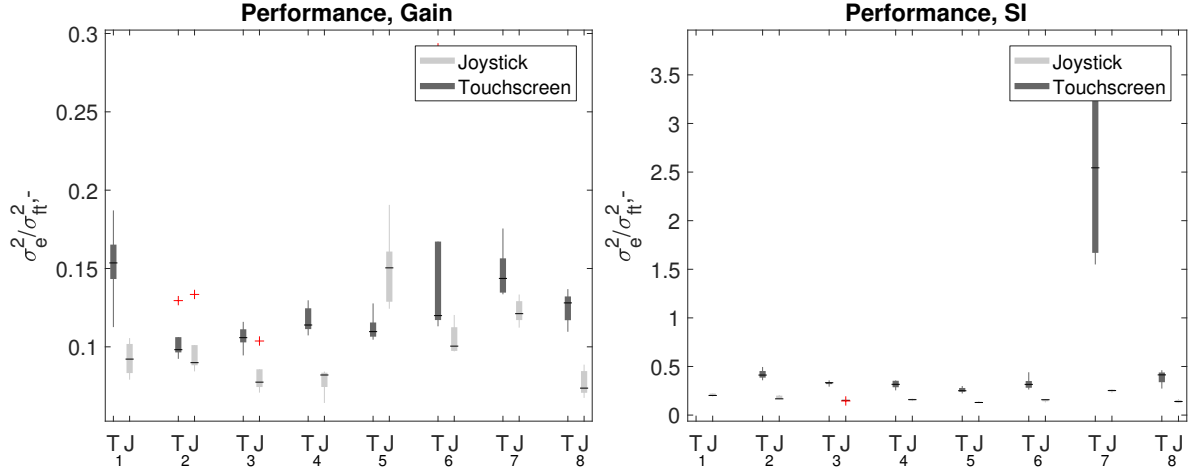


Figure 5-4: Tracking performance per subject on Touchscreen (T) and Joystick (J)

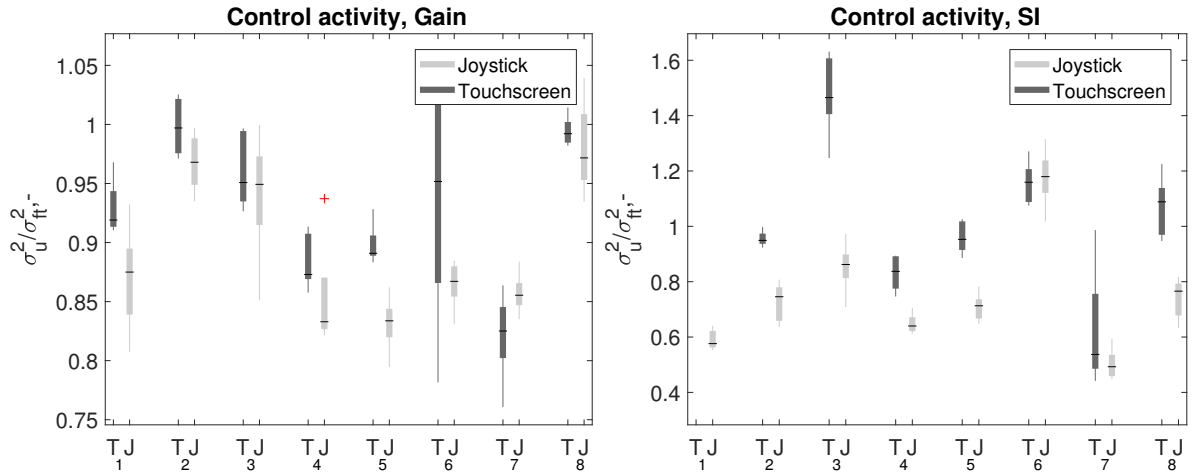


Figure 5-5: Control activity per subject on Touchscreen (T) and Joystick (J)

parameters in Equation (5-1) are depicted in grey.

$$H_{pe}(j\omega) = K_p \frac{1}{T_i j\omega + 1} (j\omega) e^{-j\omega\tau} \frac{(j\omega)^2}{(j\omega)^2 + 2\zeta_{nms}\omega_{nms}j\omega + \omega_{nms}^2} \quad (5-1)$$

Appendix B shows the final fitted model for every subject per task. The figures show that the operator response functions of touchscreen and joystick tasks are similar between subjects and the pilot model fits well to the measured responses. For one subject, however, see Figure (B-3), the neuromuscular peak was not described by the fitted model for a gain-touchscreen task. This leads to a very high neuromuscular damping ratio and neuromuscular frequency. The quality of the fit can be calculated using the Variance Accounted For (Eq. (5-2)).

$$VAF = \left(1 - \frac{\sum_{k=1}^N |u(k) - \hat{u}(k)|^2}{\sum_{k=1}^N u(k)^2}\right) * 100\% \quad (5-2)$$

This variable gives a percentage that indicates what part of the measured input is explained by the modelled input. The VAFs for this experiment can be found in Figure 5-8. A percentage

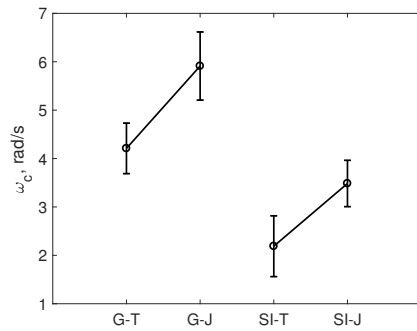


Figure 5-6: Crossover frequencies of Joystick (G-J,SI-J) and Touchscreen (G-T,SI-T) tasks, average of 8 subjects

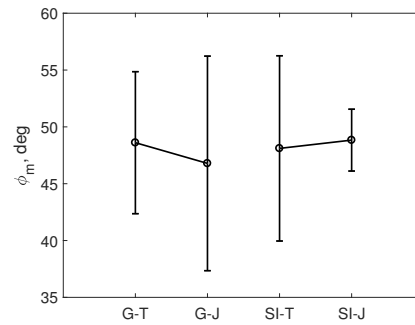


Figure 5-7: Phase margin of Joystick (G-J,SI-J) and Touchscreen (G-T,SI-T) tasks, average of 8 subjects

of 100% suggests that the model perfectly describes the measured data. Figure 5-8 shows that there is no significant difference between the control devices when it comes to the quality of the fit. The fitting method can be applied to both control devices.

5-3-5 Parameter Estimation

To get an idea of the difference between tracking behaviour for a manual tracking task using a joystick and a touchscreen, the pilot parameters can be compared. Three parameters are of interest and depicted in Figure 5-9. The first parameter is the gain. It represents how much effort the operator puts in following the target. From Figure 5-9 can be concluded that the gain K_P is similar for touchscreen and joystick. The second parameter is the lead time constant T_l . For single integrator tasks $T_l = 0$. The lead time constant for the touchscreen task is higher than for the joystick task. The third plot shows the time-delay τ . The largest time-delay value corresponds to the single integrator task. This might be explained by the difficulty of the tasks. Subjects considered the S-T task as most difficult, hence, this task shows a larger time delay. The bottom two parameters are neuromuscular parameters. Steering a joystick requires the operator to move his/her hand in a different way than when using a touchscreen. Therefore it is important to check whether these parameters match as well for both control devices. Figure 5-9 shows the neuromuscular damping ratio and neuromuscular frequency. As explained earlier, for one subject these parameters ended up very high for the gain-touchscreen task, due to fitting problems. Without this incorrect data the neuromuscular parameters are very similar for the touchscreen and joystick task. Despite the different steering methods, neuromuscular characteristics do not vary.

5-4 Conclusion

The goal of the preliminary test was to investigate the differences between human tracking behaviour for a manual tracking task, using a joystick and a touch screen interface. These control devices have been tested with gain and single integrator system dynamics. Four tasks were performed by eight subjects from the EMC and the TU Delft. The results were analysed using the FC method and frequency domain parameter estimation. The results show that

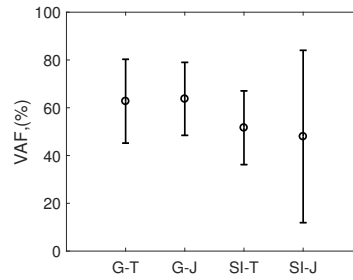


Figure 5-8: Variance Accounted For (VAF) for all 8 subjects for gain-touchscreen (G-T), gain-joystick (G-J), single integrator-touchscreen (SI-T) and single integrator-joystick (SI-J)

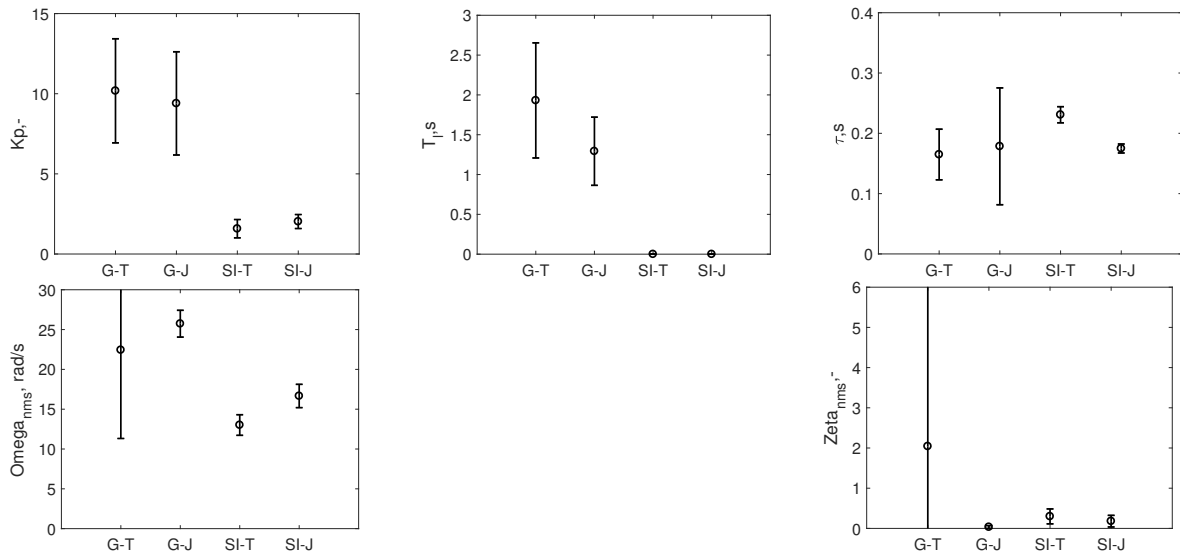


Figure 5-9: Estimated model parameters of all 8 subjects for gain-touchscreen (G-T), gain-joystick (G-J), single integrator-touchscreen (SI-T) and single integrator-joystick (SI-J)

the single integrator-touchscreen task required the most effort from subjects. They rated this task as the most difficult and performed worst. Therefore, the SI-T configuration is least preferable.

For the gain there was no significant difference between touchscreen and joystick in terms of performance and control activity, also both tasks were regarded as relatively easy by subjects.

The crossover frequencies of the joystick tasks were higher than those for the touchscreen tasks. Also, the lead time constant of the touchscreen task was higher than that of the joystick task. Preferably, the final experiment will involve a touchscreen interface because it is most suitable for the subjects. Therefore a gain-touchscreen task is most preferable for the final experiment.

The pilot model was fitted successfully to almost every operator response function. Only one case failed because the model did not fit a neuromuscular system. Ignoring this case, the estimated pilot parameters of the touchscreen task are very similar to that of the joystick task. This leads to the conclusion that the methods by which we describe manual tracking behaviour, apply to both control devices.

Preliminary experiment 2: Simulation to investigate influence of lost data

This chapter describes the second preliminary experiment. It further expounds on the results discussed in Section 5-3-2, from the previous experiment. The same pursuit tracking task will be simulated to investigate the effects of loss of data in a touchscreen task on the quality of HC identifiable results.

6-1 Introduction

In Chapter 5 a comparison has been made between joystick tracking tasks and touchscreen tracking tasks. During a joystick tracking task the output of the system u is continuous. The signal is never interrupted. For touchscreens on the other hand a loss of contact with the screen can occur. If the subject accidentally lifts his finger off the screen, no input data is available. The output of the system freezes until contact is established again. This leads to flat sections in the HC output data u . An example of such an output signal can be found in Figure 5-2. The disrupted signal leads to distorted results after system identification when the Fourier coefficient method is used. To investigate the effect of "loss of contact" during a touchscreen tracking task, a human HC was simulated in a pursuit target tracking task.

6-2 Method

The simulation was carried out in MATLAB/Simulink. A schematic overview of the setup can be found in Figure 6-1. The touchscreen tracking tasks from Chapter 5 were used for the design of the simulation experiment. Also, the HC models and parameters were taken from the results of Chapter 5, specifically from subject 5. Simulation time is based on the real tracking task executed experimentally.

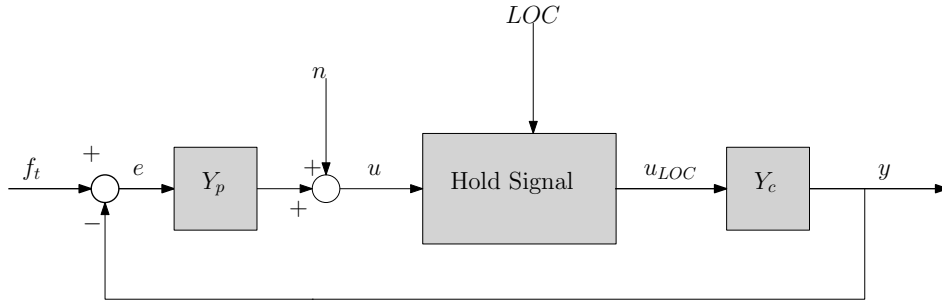


Figure 6-1: Loss of contact simulation, schematic overview

Table 6-1: HC model parameters

	K_p	τ	ζ_{nms}	ω_{nms}	T_L
K_c	2.5448	0.1898	0.1960	20.3712	1.7654
$K_{c/s}$	0.678	0.2090	0.4523	12.4465	-

6-2-1 Remnant

To account for non-linear behavior, white noise is led through a low pass filter and added to the HC output. The remnant filter and relevant parameters were taken from Zaal et al. [55]. The gain K_n is chosen such that σ is approximately 0.1. The characteristics of the remnant filter are similar to those of a third-order low-pass filter with a damping coefficient, the filter can be found in Eq 6-1.

$$H_n(j\omega) = \frac{K_n \omega_n^3}{((j\omega)^2 + 2\zeta_n \omega_n j\omega + \omega_n^2)(j\omega + \omega_n)} \quad (6-1)$$

6-2-2 HC describing models

Two types of tracking tasks were simulated. In the first task the HC controlled a single integrator, the second was a gain controlled task. To obtain the HC parameters, two stable performing subjects were selected as Y_p . The HC model parameters for both tasks can be found in Table 6-1.

6-2-3 LOC scenarios

To simulate an incident where loss of contact occurs, four scenarios were considered. The first scenario is one where no incident occurs. The second scenario simulates only a few incidents, the third multiple and the fourth represents a worst-case-scenario. In each simulation, the control input is held for a few seconds, causing flat sections in the signal, similar to those seen in 5-2. The signals of the scenarios can be found in Appendix C-1, they were randomly constructed. For every scenario there is a certain amount of data loss:

- No LOC: 0%
- Good: 8%

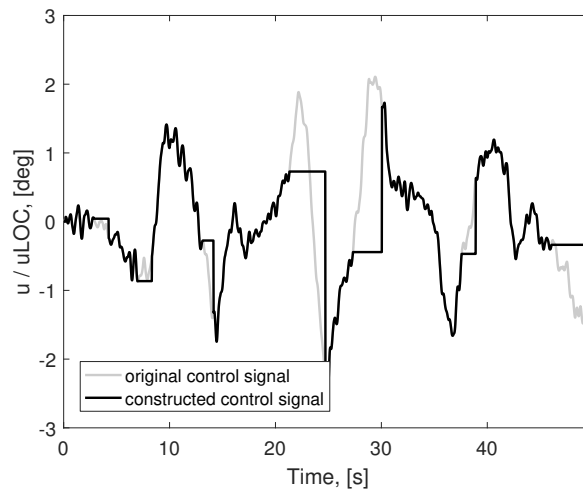


Figure 6-2: Original control signal and constructed control signal after Bad LOC scenario was applied

- Moderate: 12%
- Bad: 29%

The Good scenario is the most realistic in experiments. An example of a simulated control input signal is given in Figure 6-2. The experiment is repeated for eight trials. Over these trials the HC model and scenario remain the same. The remnant signal varies over the trials.

6-3 Results

6-3-1 Single integrator dynamics

Time domain

First, the four scenarios will be compared in the time domain. The LOC scenarios are applied to the HC output. To get an idea of the effect of LOC on the system output the scenarios are compared in Figure 6-3. The ideal situation is one without loss of contact. Such a situation is depicted left. The system output is similar to the forcing function. The next figure shows a situation where only a few loss of contact incidents occur, this would be a Good situation. There are some discrepancies between the forcing function and output signal at the locations where the human loses contact but these are acceptable. The Moderate situation shows quite some undershoot and overshoot in regions with high amplitudes. There does not seem to be that much difference between these two situations. The Moderate situation has more incidents but for the good situation two of the three incidents are very close together. This might have an effect on the results.

The Bad scenario shows two instances of very large overshoot. At these locations the amplitude of the forcing function is very high. The reconstructed control signal has to make a big

leap to catch up to the original control signal. From the results in the time domain, it can be concluded that a Bad scenario is highly undesirable. Just three or four short incidents might not have such an influence on the output of the system. The effect on system identification will have to be evaluated.

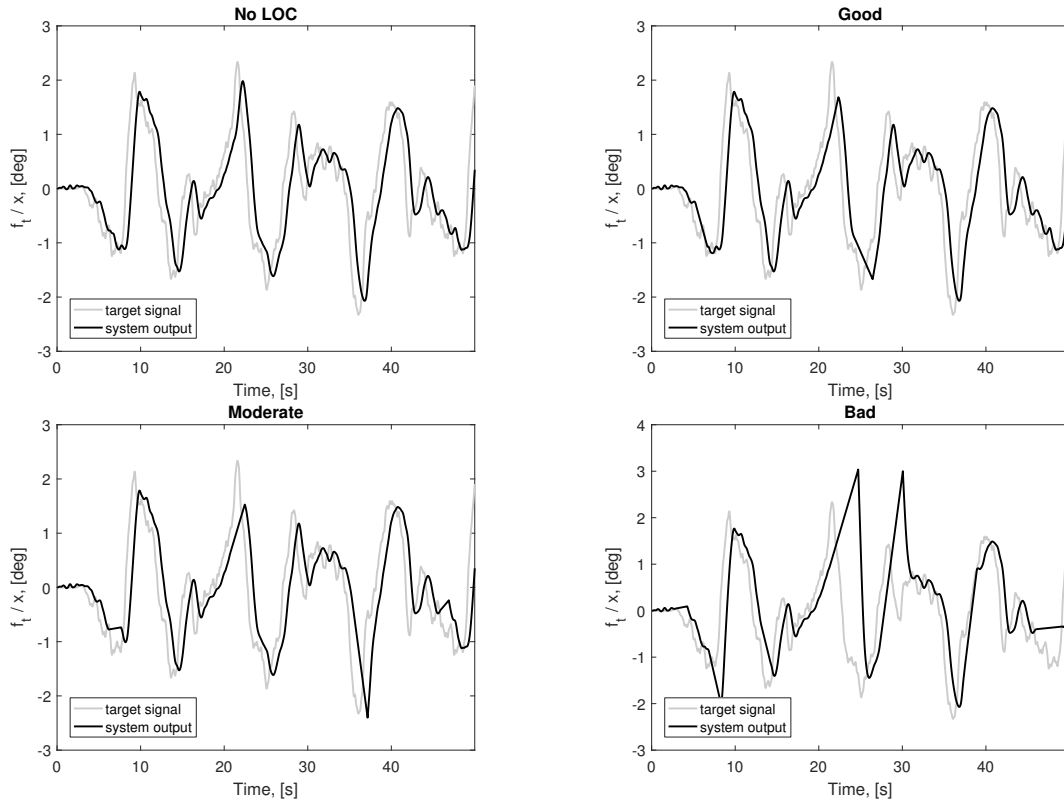


Figure 6-3: System output and forcing function for all LOC scenarios, single integrator

PSD analysis

The error and control signals will be used for identification. In an ideal situation without loss of contact these signals should deliver a significant amount of power on the same frequencies as the forcing function. In that case the remnant can be ignored at these frequencies and the signals can be used to estimate the HC response. The power spectral density function is a method to calculate the power intensity of the signal. At the power frequencies there should be clear peaks visible. Figure 6-4 shows the average power intensity for each scenario for signal U (reconstructed control input). The PSDs for signal E (error) can be found in Appendix C-3. The star indicates the position of the power frequencies. For the scenario without LOC in Figure 6-4 the peaks can be clearly distinguished from the noise region, signal-to-noise ratio is high. For the good and moderate situation a few peaks at high frequencies are sinking towards the noise. The bad situation has a low signal to noise ratio.

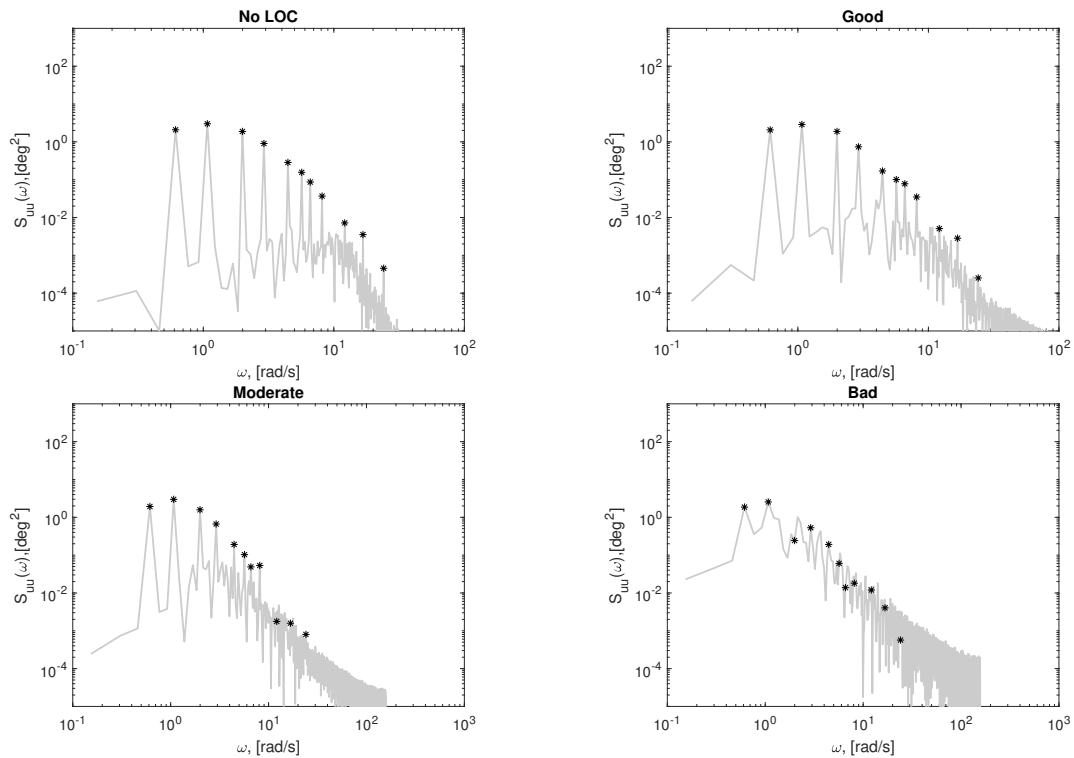


Figure 6-4: PSD of reconstructed control input for all LOC scenarios, averaged over 5 trials, single integrator dynamics

System identification

To identify the HC response, the instrument variable method has been used. Figure 6-5 shows the HC response and the original HC model, which served as input for the simulations for each scenario. The original model and response of the case without loss of contact almost coincide. The good scenario shows some dissimilarities in the magnitude. In the two bottom figures, the differences between the simulated HC response and original model increase. Even the phase starts to show disruptions. The Variance Accounted For (Eq. 5-2), will give a more objective impression of the results. It gives the percentage of the simulated response that is explained by the original HC model. Obviously, this percentage will be lower for a situation with LOC. Table 6-2 shows the average VAF for every situation. The remnant has a power of 0.1. Meaning that it describes 10% of the HC output. The other 90% follows from the HC model. Thus a situation without LOC has a VAF of 90%. The VAF drastically drops for the worst situation. Before that, there seems to be little effect.

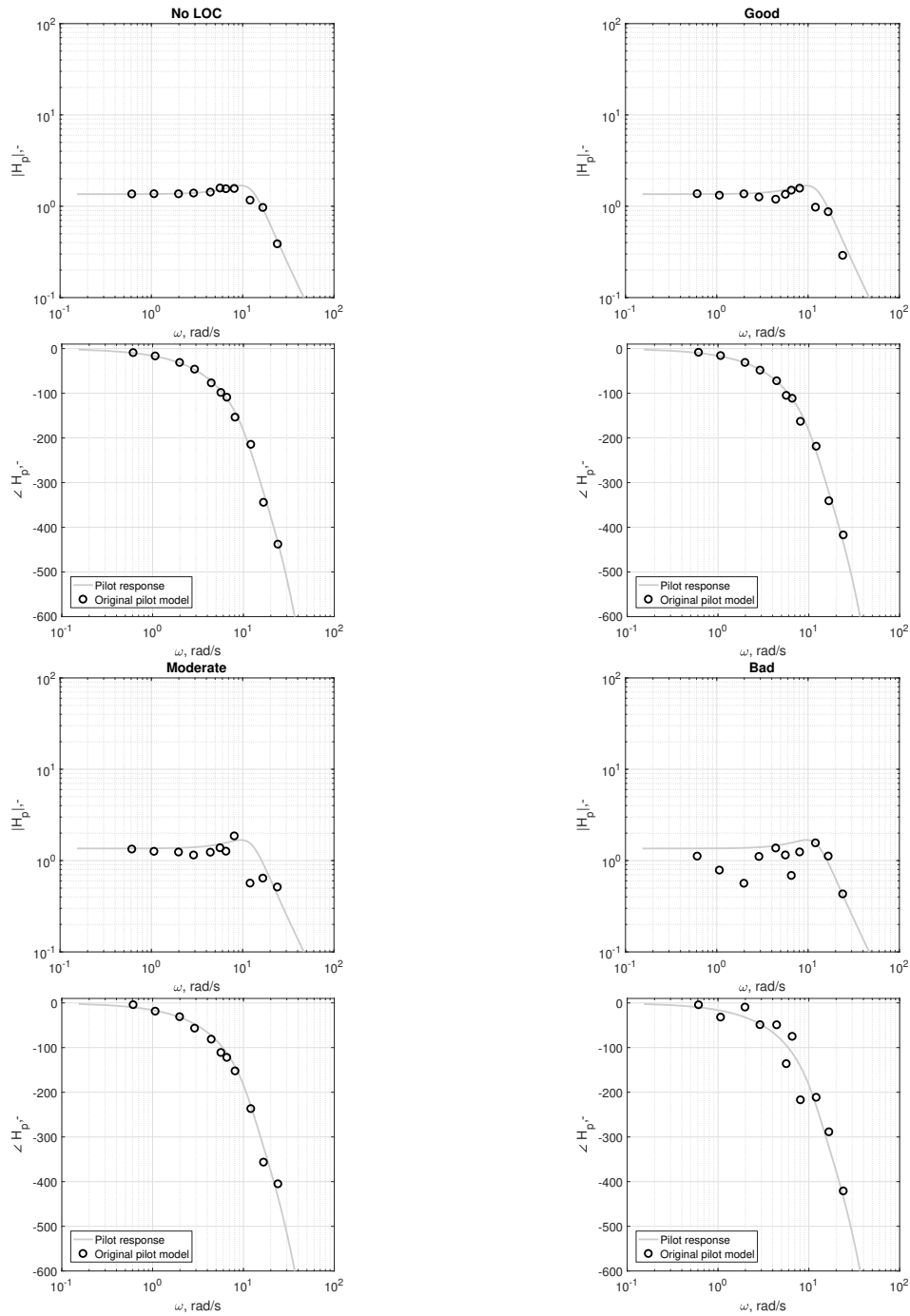


Figure 6-5: HC response and originally fitted HC model, single integrator dynamics

Table 6-2: Single integrator VAF

<i>LOC scenario</i>	<i>VAF, %</i>
No LOC	89.29
Good situation	85.38
Moderate situation	77.31
Bad situation	23.11

6-3-2 Gain dynamics

Time domain

For the gain dynamics the control behaviour of the HC is different from that of the single integrator. The input is position based. Where the system output of single integrator showed cases of overshoot and undershoot, the system output of the gain task is flat. This does not affect the identification process, since this process only requires the control input and error signal. The system output and forcing function are depicted in Figure 6-6. From the figure it can be concluded that the data close to the LOC incidents is also affected. When contact is restored the HC tries to catch up with the target signal and tends to overshoot it.

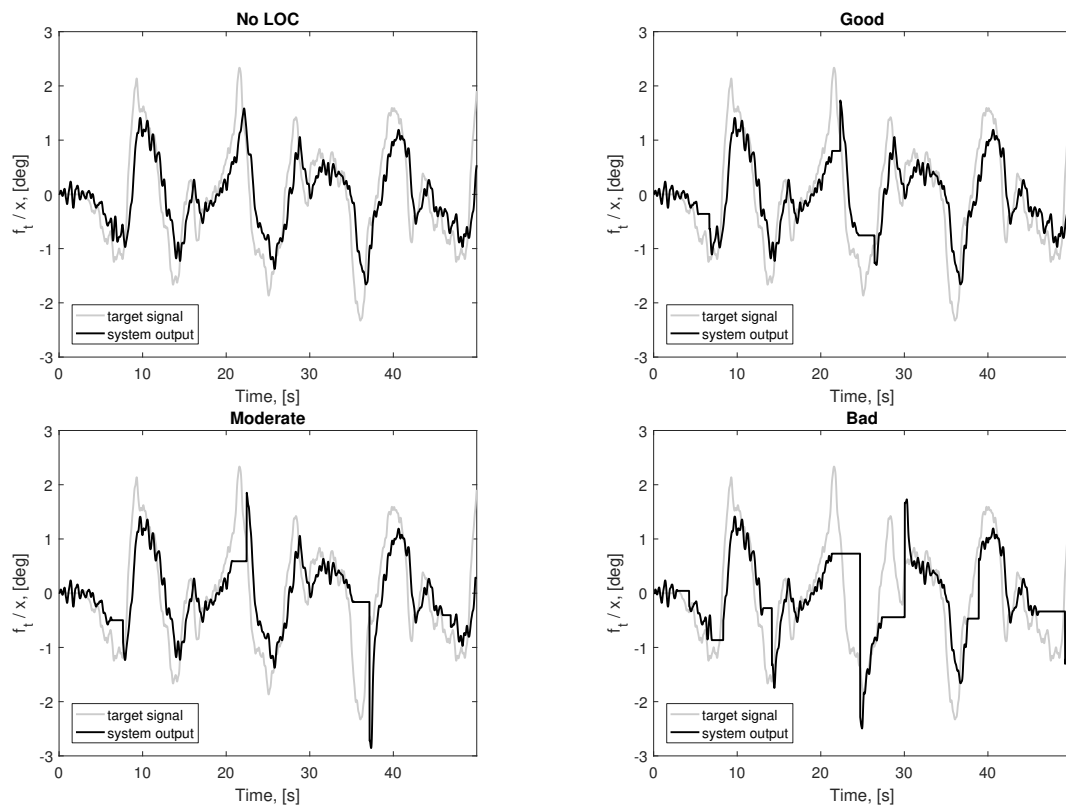


Figure 6-6: System output and forcing function for all LOC scenarios, averaged over 8 trials, gain dynamics

PSD analysis

The power spectral density plots of the reconstructed control input can be found in Figure 6-7. PSD data of the error signal can be found in Appendix C-2. The peaks are a lot tougher to identify than for the single integrator case for both the control output and the error signal. For the situation without loss of contact, at high frequencies, the signal to noise ratio is already low. This is caused by the HC model. During a gain dynamics task the HC generates lag. The HC acts as a low pass filter and does not put effort into following the high frequencies. This means that the contribution of the remnant is high at these locations. If the signal-to-noise ratio becomes too small the remnant can not be ignored in the system identification process.

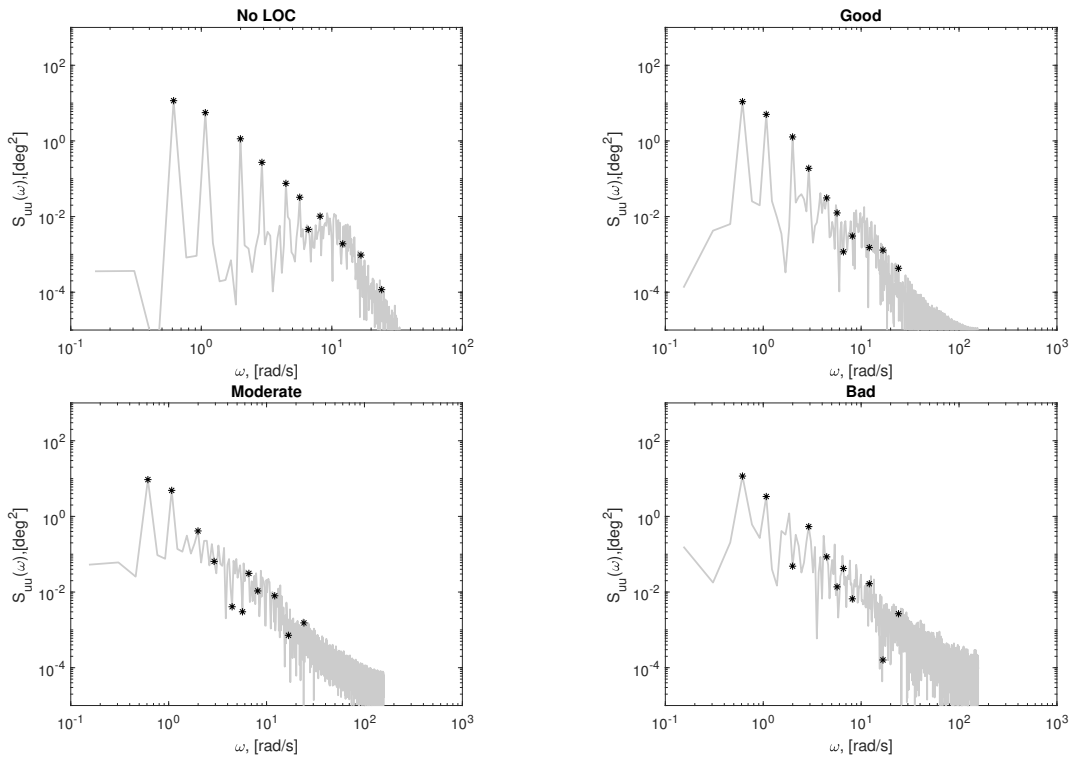


Figure 6-7: PSD of reconstructed control input for all LOC scenarios, average of 5 trials, gain dynamics

System identification

The system identification follows the same procedure as for the single integrator. The only difference is the HC model. For gain dynamics a lag term T_L is added to the model. The simulated HC response and original HC model can be found in Figure 6-7. The HC response estimate is a lot worse than for the single integrator. This gives a result that is very different from the original model. The VAF can be found in Table 6-3. For the scenario without LOC the VAF is again 90%.

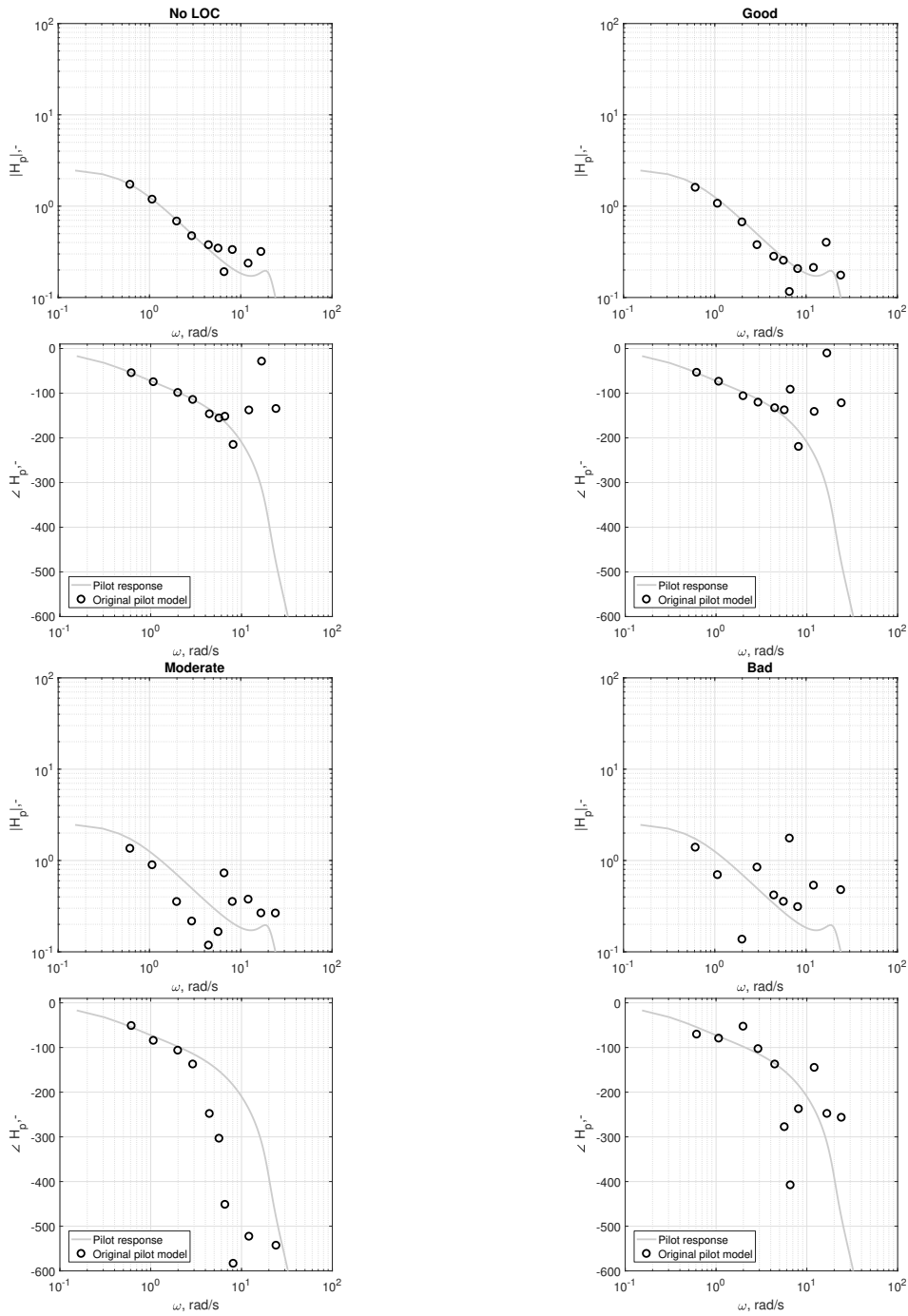


Figure 6-8: HC response and originally fitted HC model, gain dynamics

Table 6-3: Gain VAF

<i>LOC scenario</i>	<i>VAF, %</i>
No LOC	89.10
Good situation	85.98
Moderate situation	66.24
Bad situation	56.28

6-4 Conclusion

In this chapter a pursuit task was simulated to investigate the consequences of data loss due to loss of contact with the touchscreen. The results show that loss of contact is highly undesirable. Since a limited group of subjects is available, data is already very scarce. Once obtained, data must be of good quality in order to complete the identification en fitting process. The Variance Accounted For suggests that a few LOC incidents are acceptable. The good scenario, with 8% data loss, produces HC output that imitates the original HC output for 85%. From then on the HC response becomes unreliable.

To compensate lost data the HC output signal could be reconstructed using interpolation. The click-up and click-down events are logged during the experiment. They indicate the start and ending of LOC incidents. During the experiment a LOC incident can be very confusing for the subject. He might try to regain contact by swiping or pressing at different positions on the screen. This causes disrupted data around the LOC incident. The disrupted data is then used for the interpolation process, leading to a completely messed up reconstructed signal. Therefore, the interpolation process has to be completed with great care. In extreme cases, when the HC output shows too many LOC incidents and interpolation makes the data worse, the trial will have to be excluded from the analysis.

Preliminary experiment 3: Effect of disturbance signal on human tracking behaviour in a preview tracking task

7-1 Introduction

The differences between a touchscreen tracking task and a joystick tracking task have been investigated in Chapter 5. The next step was to determine the effect of Loss of Contact during a run, as explained in Chapter 6. Before the configuration of the final task can be determined, preview tracking control behaviour of inexperienced subjects will be investigated. First of all, the addition of the disturbance signal needs to be considered. This signal is necessary since the HC's responds to the target and the controlled element, as explained in Section 3-3. However, adding a disturbance signal might feel abnormal in a touchscreen based tracking task. Especially for an inexperienced, vulnerable patient group. Secondly, an inexperienced subject might not deploy a preview strategy. Simply because he does not understand how this preview information has to be treated to improve the score. If a subject does not use the preview, the preview parameters cannot be estimated and the task would return to the pursuit tracking task. In this chapter the effect of a disturbance signal and preview information on human control behaviour will be studied. Also, the acquired eye-tracking samples shall be analysed to validate the response of the human controller to a preview tracking task.

7-2 Method

7-2-1 Subjects

In total, nine subjects participated. For one subject the test was terminated after the first task due to a headache. To complete the latin square, a ninth participant performed the



Figure 7-1: Infrared eye-tracker system [56]

terminated set. The subjects that eventually participated were between 21 and 44 years old (mean=27.9, SD=7.7). Five of them were working at the Neuroscience lab at Erasmus MC, the other three were from the Control and Simulation department at Delft University of Technology. None of the subjects suffered from major hand injuries or visual impairment. All subjects were right-handed. Four subjects considered themselves as experienced with manual control tasks (2,4,5,8) three subjects had no experience (1,6,7) and one considered herself as medium experienced (3).

7-2-2 Apparatus

The setup that was used is similar to that of Chapter 5, except for two parts. First of all, the tracking input was solely recorded on the touchscreen. Second, the eye-tracker (Chronos Vision, Berlin, DE [56]) was used to also collect eye data. The system is depicted in Figure 7-1. It consists of a helmet that can be adjusted to headsize and interpupillary distance of the subject. The eyes are recorded individually by two cameras through a dichroic mirror. The measurement resolution is better than 0.05 deg.

7-2-3 Experiment

For the current experiment, four tasks were performed by each subject. The latin square can be found in Appendix A. The conditions were either single integrator or gain dynamics, both performed with or without a disturbance signal. This way, the effect of the disturbance signal on the performance of the HC could be investigated. Table 7-1 shows the conditions of the experiment.

The display used can be found in Figure 7-2. The target and controlled element were shifted downwards to allow space for the preview line.

Since there are two cues, the preview task calls for multi-channel identification. In this case there are two independent signals needed to separate the responses of the human controller: a target signal (f_t) and a disturbance signal (f_d). The latter perturbs the controlled element. These signals have been constructed using a low-pass filter as proposed by Zaal et al. [54]. The

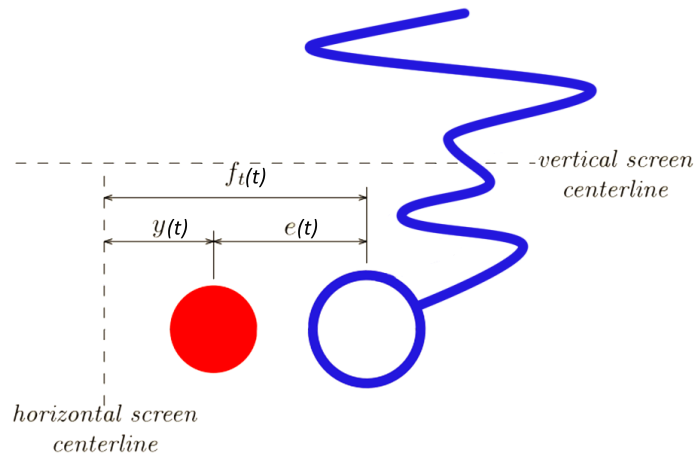


Figure 7-2: Preview tracking display, adapted from [3]

disturbance signal should not be too strong to prevent the task from becoming a disturbance-rejecting task. Therefore the amplitudes were scaled such that for f_t the variance is 1 deg^2 and for f_d the variance is 0.5 deg^2 . The characteristics of the signals can be found in Table 7-2.

Table 7-1: Experimental conditions preliminary experiment 3

	With f_d	Without f_d
K_c	$G - fd$	G
K_c/s	$SI - fd$	SI

7-2-4 Preview time

The length of the preview line, shown above the target, influences the control behaviour of the HC [27]. The performance of the HC improves as preview time increases, until an optimal preview time is reached. After this time, the performance stabilizes. Appropriate preview times have been determined in previous studies [6, 44, 57]. While Jones and Donaldson [5] use 8 seconds of preview time for Parkinson's disease patients, Van der El et al. [57] showed that critical preview is between 0.5 and 0.75 seconds. A subject does not use information beyond 1 second. Hiramatsu and Uno [44] suggested 0.5 to 2.0 seconds of preview time where the 2.0 seconds is considered appropriate for elderly subjects. The current experiment will be conducted with inexperienced subjects, therefore the preview time was set to 1.0 seconds.

7-3 Results

Considering practice trials, only the last 5 trials were analysed in the results.

Table 7-2: Forcing function signal properties

<i>Target f_t</i>							
$n_{t,-}$	$\omega_t, \text{rad/s}$	A_t, deg	ϕ_t, rad	$n_{d,-}$	$\omega_d, \text{rad/s}$	A_d, deg	ϕ_d, rad
4	0.614	1.079	7.239	3	8.948	0.507	8.948
7	1.074	0.776	0.506	5	0.030	0.420	0.030
11	1.994	0.391	7.860	11	0.773	0.210	0.773
17	2.915	0.225	8.184	17	4.199	0.115	4.199
23	4.449	0.117	9.012	23	3.680	0.072	3.680
29	5.676	0.082	6.141	31	1.705	0.046	1.705
37	6.596	0.066	6.776	41	1.585	0.031	1.585
53	8.130	0.051	6.265	59	5.650	0.020	5.650
79	12.118	0.035	4.432	83	7.711	0.014	7.711
109	16.720	0.028	2.672	107	8.125	0.012	8.125
157	24.084	0.024	8.009	151	9.458	0.011	9.458

7-3-1 Performance and control activity

When a disturbance is added the HC has to compensate for the disturbance and the target input. This leads to a decreasing performance and increasing control activity, see Figures 7-3 and 7-4. The plots show the average from eight subjects for each task. This gives a general idea of the performance and control activity. The performance and control activity are expressed in variance of the error and HC output signal. As expected, the variance of the error signal increases when the disturbance signal is added, thus performance decreases. The control activity increases as the disturbance signal is added. Thus, subjects put more effort in executing the task because they have to compensate for two input signals. This leads to the conclusion that the intensity of the disturbance signal is sufficient.

To investigate the effect of the disturbance input in more detail, the contribution of all input

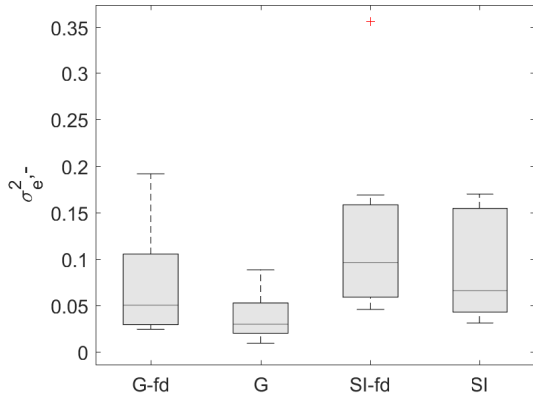


Figure 7-3: Performance per subject for all tasks

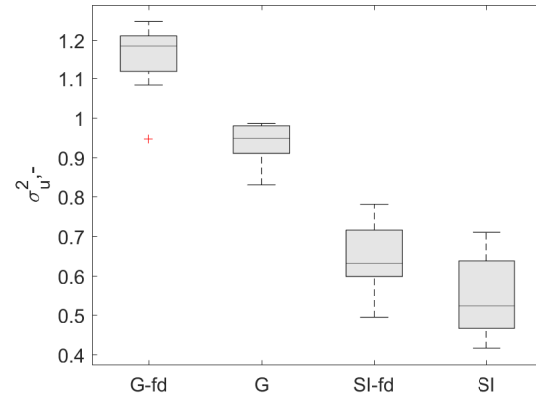


Figure 7-4: Control activity per subject for all tasks

signals to the total variance can be determined. Based on the frequency integers at which they occur, σ_{uft}^2 and σ_{ufd}^2 can be calculated. The remaining variance contribution comes from the remnant, σ_{un}^2 . The split error and control variances for each subject can be found in Appendix E. For every subject, the variance contributions of the remnant n and forcing func-

tion f_t to the total control variance σ_u^2 remain approximately the same when a disturbance function f_d is added. The same holds for the error variance σ_e^2 in case of gain dynamics. The variance of the disturbance signal adds to the total variance without affecting the other two signal variances. An example can be found in Figure 7-5.

For the error variance σ_e^2 , in case of single integrator dynamics, different scenarios are possible. For subjects 2, 3 and 6 (Figures 7-6,7-7 and 7-8), the total variance of the error is higher without added disturbance. This can be explained by the order in which tasks were performed. These subjects performed the SI task before the SI-fd task. In Chapter 5 it was established that inexperienced HCs find the single integrator task difficult. It takes some trials to overcome the first shock and get used to the dynamics. This explains why the performance of the SI task is worse than for the SI-fd, if it is carried out before. For the same reason, subjects 4 and 7 (Figures 7-9 and 7-10) show a high variance for the SI-fd task.

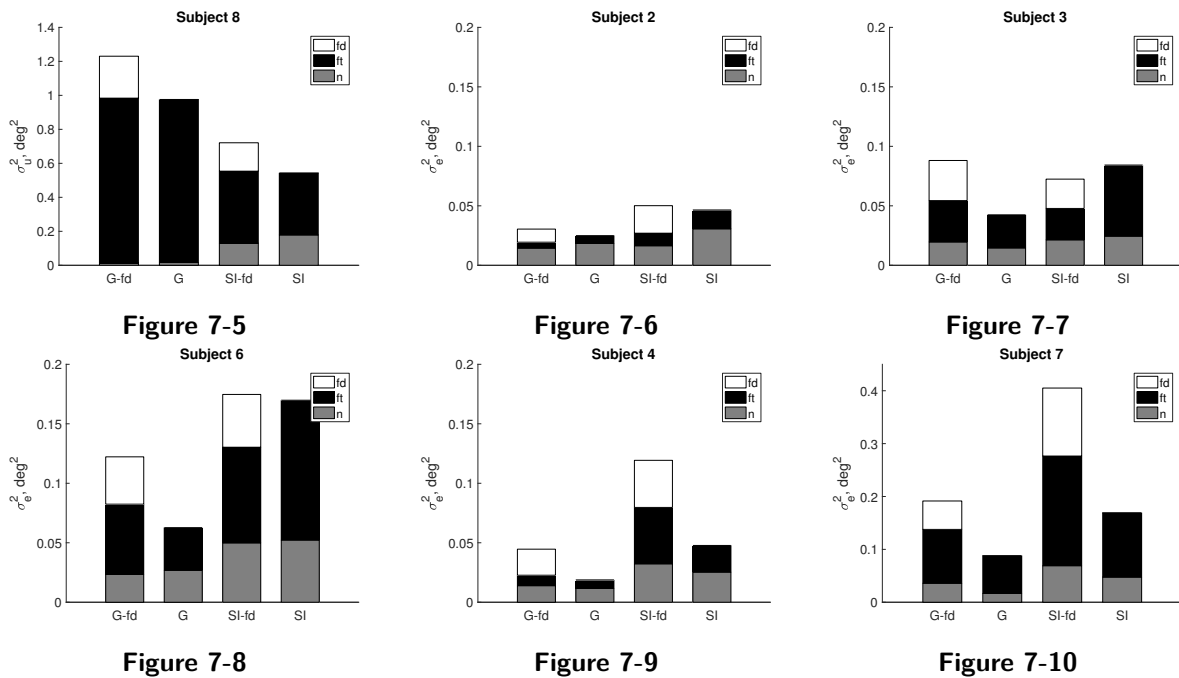


Figure 7-11: Control variance and error variances

7-3-2 System Identification

The results from the tasks with a disturbance function on the controlled element, have been obtained using multichannel system identification methods. For the tasks without a disturbance function the instrument variable method was used. The HC describing functions can be found in Appendix D. On the left, the responses for the task with disturbance are plotted, on the right the response for the task without disturbance. The shade of the plot indicates the order in which the trials were performed. The last trial has a black color, the first is depicted in light grey. This could reveal a learning effect.

One of the goals of this task was to find out whether inexperienced controllers use a preview strategy. The use of a preview strategy becomes clear from the operator response in two ways. First, by the phase of the target response. During a pursuit task the phase lag decreases due

to increasing time delay. A preview line gives the HC the opportunity to compensate for the time delay. The phase response remains the same and might even increase. Another method to detect a preview strategy is by comparing the magnitudes of the responses to the target and the controlled element. If both magnitude plots are exactly the same, the HC reacts equally to the target f_t and the controlled element y . Basically, he is only using the error e information during the task. On the other hand, if the magnitude plots differ the HC puts more effort in following the preview line than responding to the disturbance.

For example, subject 1 in Figure 7-12 does not show signs of a preview strategy. The responses H_{o_t} and H_{o_x} have similar magnitude and the phase lag of the target response decreases. Subject 5, depicted in Figure 7-13, is using a preview strategy. The target phases of both the gain and single integrator task increase. Also the magnitudes of the responses differ.

By comparing the responses of the tasks with disturbance and without disturbance, the added

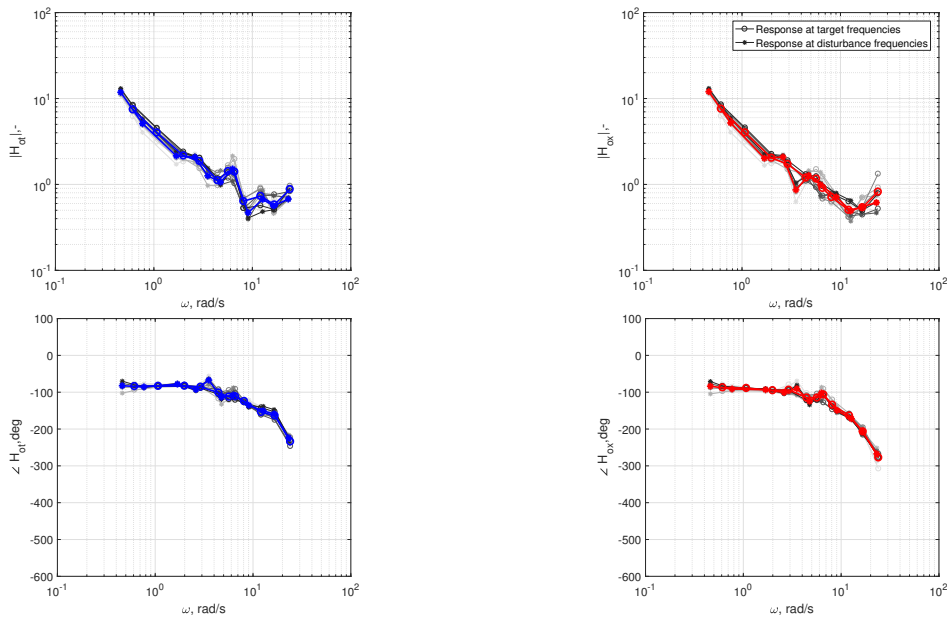


Figure 7-12: HC response data for subject 1, gain dynamics

value of the disturbance function becomes clear. Without the disturbance signal, results are inconsistent and responses fluctuate randomly. This especially applies to the responses of experienced controllers. These subjects use both the error and preview information. An example can be found in Figures 7-14 and 7-15. While the results of the inexperienced subject are somewhat consistent, the results of the experienced subject show strong variations. The task has been performed with various controlled element system dynamics. The human operator adjusts his control behaviour to the system. If the system has higher order controlled element dynamics, the HC has to compensate for the larger phase lag. The preview information gives the HC the opportunity to compensate his own lag and the phase lag of the system. Thus, in case of higher order dynamics, the HC should make more use of the preview [57]. At first glance, it seems that experienced subjects look further ahead along the preview line during the task with single integrator dynamics. Also, for two of the inexperienced subjects (6 and 3), the phase of the target response is slightly larger than for the controlled element.

As for learning, there does not seem to be a recognizable trend. From the eight trials, trial 4 to 8 are used for analysis. The first three trials offer the subject some opportunity to practice.

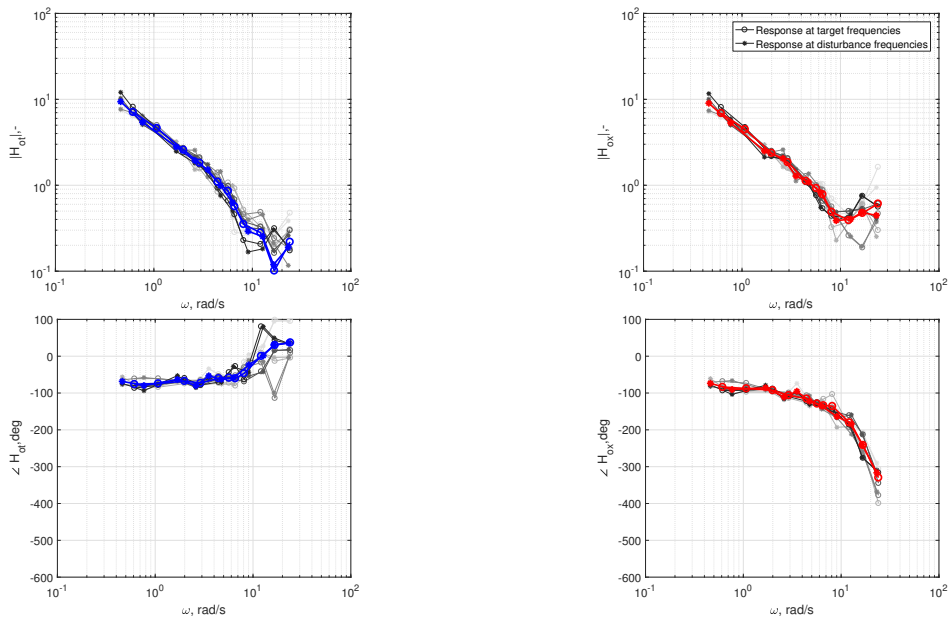


Figure 7-13: HC response data for subject 5, gain dynamics

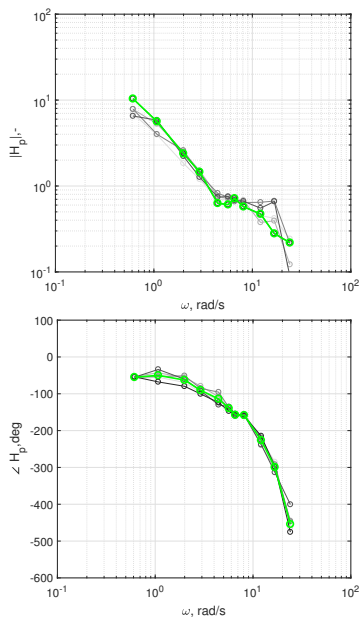


Figure 7-14: HC response data without f_d from inexperienced subject, gain dynamics

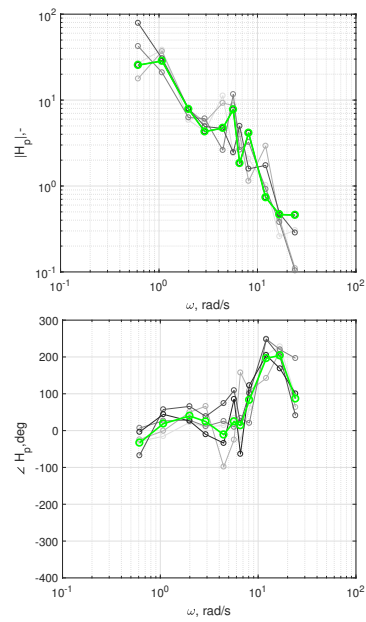


Figure 7-15: HC response data without f_d from experienced subject, gain dynamics

These trials seem to be enough to stabilize the performance of inexperienced patients.

7-3-3 Model fitting and parameter estimation

Based on the results, the final experiment will focus on a task with gain dynamics and a disturbance. Therefore, these results will be considered for the HC model fitting process. The model of Equation (3-7) is adapted such that it fits the HC responses.

Some subjects use the near-viewpoint response H_{o_n} , to track the target at high frequencies [9]. For the current experiment and the final experiment, inexperienced subjects will be tested. These subjects are not expected to track high frequencies. The K_n parameter is likely to end up close to 0. For efficiency purposes the response to the near-viewpoint will be omitted.

Another part of the model that can be excluded is the lag term $T_{l,e}$. At low frequencies the subjects behave as an integrator instead of a low pass filter. Therefore $1/(1 + T_{l,e}j\omega)$ becomes $1/(j\omega)$. Finally, the neuromuscular peak is difficult to identify. It might be located beyond the measured frequencies. For PD patients the neuromuscular characteristics indicated impairment of fine motor skills. A similar outcome is expected for cerebellar patients. Preferably, the model also estimates a neuromuscular system. Both situations will have to be evaluated; a model with and without H_{nms} .

The final HC model for a task with gain dynamics can be found in Equation (7-1), with HC parameters in grey.

$$\begin{aligned}
 H_{o_{e*}}(j\omega) &= K_e \frac{1}{j\omega} \\
 H_{o_f}(j\omega) &= K_f H_{o_{e*}}(j\omega) \frac{j\omega}{1 + T_{l,f}j\omega} \\
 \hline
 H_{o_t}(j\omega) &= H_{o_f}(j\omega) e^{j\omega\tau_f} e^{j\omega(-\tau_v)} \\
 H_{o_x}(j\omega) &= H_{o_{e*}}(j\omega) e^{j\omega(-\tau_v)}
 \end{aligned} \tag{7-1}$$

Table 7-3 shows the estimated parameters for the case without the neuromuscular system. The estimated preview parameters are relatively low compared to the results of the experiments conducted by Van der El et al. [9]. Overall, experienced subjects show higher look-ahead time τ_f , higher gain K_e and highly consistent data.

Table 7-3: Estimated model parameters of experienced (grey) and inexperienced (white) subjects for task with gain dynamics, H_{nms} excluded

Subject #	K_e	τ_v	K_f	τ_f	$T_{l,f}$
1	1.47	0.10	1.02	0.04	0
2	1.93	0.13	0.95	0.31	0.14
3	0.93	0.18	0.82	0.26	0.09
4	1.15	0.11	0.95	0.32	0.09
5	1.49	0.13	1.02	0.31	0.08
6	0.90	0.24	0.93	0.11	0.01
7	0.56	0.11	0.96	0.12	0.07
8	1.48	0.12	0.94	0.32	0.13

7-4 Gaze data

During the preview experiment, gaze data has been recorded. For now, the data will validate the HC responses in terms of preview use. In Figure 7-16, gaze data from one of the experienced subjects is shown. Beside, Figure 7-17 shows gaze data from an inexperienced subject. The dotted line represents the zero line; the location of the controlled element and the target. The y-axis represents the distance in degrees between the gaze and the zero line. From the tracking data was derived that experienced subjects make more use of preview data. The gaze data seems to support this hypothesis. The data from the experienced subject shows strong variations in vertical distance; the subject looks far along the preview line and follows the target signal back to the zero line. This is clearly indicated by the sawtooth pattern. For the inexperienced subject in Figure 7-17 the variance of the vertical gaze data is small. This subject mainly focuses on the area around the zero line.

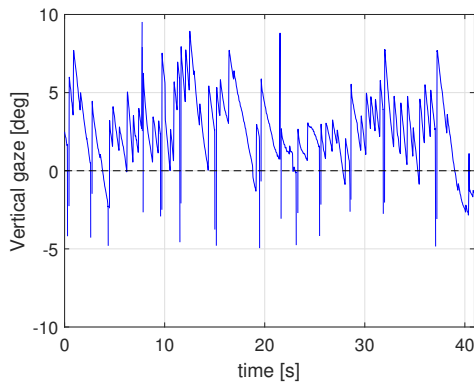


Figure 7-16: Vertical gaze data of one trial from experienced subject

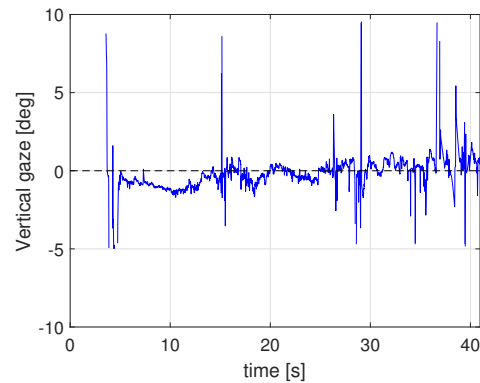


Figure 7-17: Vertical gaze data of one trial from inexperienced subject

7-5 Conclusion

The goal of this chapter was to investigate the effects of a disturbance signal and preview information on human control behaviour. Furthermore, recorded vertical gaze data was used to support HC behaviour results. Overall, the results of experienced and inexperienced subjects have been compared.

The information in Appendix D shows that experienced subjects use a preview strategy while the other subjects use a compensatory strategy (error reducing). It is not obvious that inexperienced controllers use preview information when it is presented on the display. HCs cannot be 'forced' to deploy a preview strategy, only motivated. Therefore subjects need to be instructed properly. Furthermore, the display must be designed such that it motivates subjects to use the preview information.

Since subjects find the task with single integrator dynamics difficult, the task with gain dynamics is preferable. Furthermore, the addition of the disturbance signal does not have a significant effect on control behaviour. The final experiment will have gain dynamics and a disturbance signal.

Chapter 8

Project plan

The plan for the final experiment was constructed using the outcomes of the literature study and preliminary experiments. This chapter describes the planned final experiment.

8-1 Conclusions leading to the final experiment

In Chapter 2, functions of the cerebellum and consequences of a cerebellar stroke have been described. The location of a lesion determines the possible symptoms. A one-sided lesion would result in symptoms in body parts on the affected side of the brain. To compare the affected hand and unaffected hand, the tracking task should be performed with both hands. After a cerebellar stroke both manual and ocular tracking can be impaired. Hands will suffer from tremors and dysmetria, in the eyes, the smooth pursuit will turn into saccadic eye movements.

Chapter 5 compared two input devices and system dynamics. Results showed that the touch-screen task with gain dynamics is the most comfortable. Also, system identification methods based on joystick tracking tasks, can be applied to touchscreen tracking tasks as well.

From Chapter 6 was concluded that loss of contact during the experiment affects the quality of the HC response. Therefore, loss of contact is highly undesirable.

In Chapter 7, the effect of a disturbance signal to a preview tracking task was studied. The performance and control activity of subjects did not show abnormalities when the disturbance signal was added. From results was concluded that experienced subjects tend to make more efficient use of the preview information than inexperienced subjects.

8-2 Research questions and hypotheses

As mentioned in Chapter 1, the objective of the project is to develop a preview tracking task that may be used as an additional tool for the detection of degraded eye-hand coordination after a cerebellar stroke using system identification methods. To develop such a tool, the

following question has to be answered:

What are the differences in preview tracking behaviour between patients who suffered from a cerebellar stroke and healthy subjects?

Two types of data are available to answer this question. First, the tracking data from the tracking task itself performed on a touchscreen. Using system identification techniques and model fitting the tracking characteristics can be obtained. The second source is an eye-tracker. Eye data can support the tracking data, provide insight in tracking behaviour of the eyes and thereby detect possibly degraded eye movements in patients.

8-2-1 Tracking

The tracking data will be used to answer the following questions:

- 1) *Do cerebellar patients use preview?*
- 2) *How are performance and control activity affected for cerebellar patients?*
- 3) *What do HC parameters reveal about preview tracking behaviour of cerebellar patients?*

From the information and results presented in this report the following hypotheses can be derived:

- 1) *Ideally, cerebellar patients would use the preview information to optimize their performance. Therefore, patient would use more preview than control subjects. In reality, patients are inexperienced controllers. Therefore they will make limited use of preview.*
- 2) *Due to ataxia, the performance of patients is expected to be lower than that of control subjects, for the same reason, control activity might be lower too.*
- 3) *Due to ataxia, cerebellar patients show lower gains and higher delays, neuromuscular damping ratio will be lower due too.*

8-2-2 Gaze

Analysis of the eye-data will support the following questions:

- 1) *Do cerebellar patients use preview?*
- 2) *Where are the fixation points on the preview line for cerebellar patients and healthy control subjects?*
- 3) *How is smooth pursuit affected in cerebellar patients?*

The corresponding hypotheses are:

- 1) *The same hypothesis as for the tracking data can be considered. Patients will make limited use of preview.*
- 2) *Patients will make limited use of the preview. The fixation point will be located at zero preview time.*
- 3) *Patients will show saccadic eye movements while control subjects show smooth pursuit eye movements.*

8-3 Subjects

The cerebellar patients participate in a clinical project at the dept. of Neurology at the EMC; COgnitive DEficits in Cerebellar Stroke. During this project patients are clinically tested on cognitive impairment after three and six months of revalidation. The current eye-hand coordination project will be an extension of the CODECS-study. Patients will be tested after six months or more. They are not obligated to participate in both studies. For now at least 7 patients and 7 healthy controls will be expected before the end of April 2017. From then on the experiment will be combined with polyclinical appointments to recruit new participants. The aim is to test 10 patients and 10 healthy control subjects.

8-4 Apparatus

In Figure 4-1 the setup at the Erasmus can be found. The eye-tracker and touchscreen will provide the required data. Patients will be asked to wear gloves to remove friction between screen and finger but movement will not be recorded by the infrared motion tracker. Extra effort has been put into ensuring accurate timing of the system.

8-5 Experiment

The final experiment is similar to the gain with target and disturbance function task of Chapter 7. The main difference between the two tasks is that (from the second patient onwards) the preview line on the display only shows 0.5 seconds of the future. Also, the experiment will consist of eight trials repeated two times. Eight trials using the dominant hand, followed by eight trials with the non-dominant hand. This will reveal impairment of the affected in relation to the unaffected hand and help cope with the inherent spread in symptoms over this patient population. Both forcing function signals are the same as in Chapter 7.

Influence of left and right hand on control behaviour

A cerebellar stroke can occur on either side of the brain. This chapter will discuss whether the hand with which the task is performed, has an influence on control behaviour of subjects.

9-1 Introduction

In case of a unilateral, cerebellar stroke only one side of the brain is affected. Consequently, the patient experiences problems on the ipsilateral side of the body. For the experiment described in Part I, the affected hand was not necessarily the dominant hand of the patient. Intuitively, one might expect better results for the dominant hand because this hand is preferred for fine motor tasks. In this chapter, an experiment will be conducted to investigate the influence of the left vs. right hand on control behaviour for left- and right-handed subjects.

9-2 Method

9-2-1 Subjects

In total, 26 subjects have been tested. Two groups can be distinguished; dominant right ($n=16$, age 17-34, $\mu = 23.2$, $\sigma = 4.4$) and dominant left ($n=10$, age 21-31, $\mu = 23.9$, $\sigma = 3.1$). Three left-handed subjects and two right-handed subjects were considered as experts because they had previous experience with tracking tasks. The dominant hand of subjects was determined as the hand used for writing.

9-2-2 Apparatus

The setup used for the test has been described in Section 7-2-2.

9-2-3 Experiment

The task that had to be performed is similar to the gain dynamics task, described in Section 7-2-3. Preview time was set to 0.5 seconds of the future path of the target. Each subject had to perform the same task 16 times. First eight with the dominant hand, then eight with the non-dominant hand. The last six trials were used for analysis.

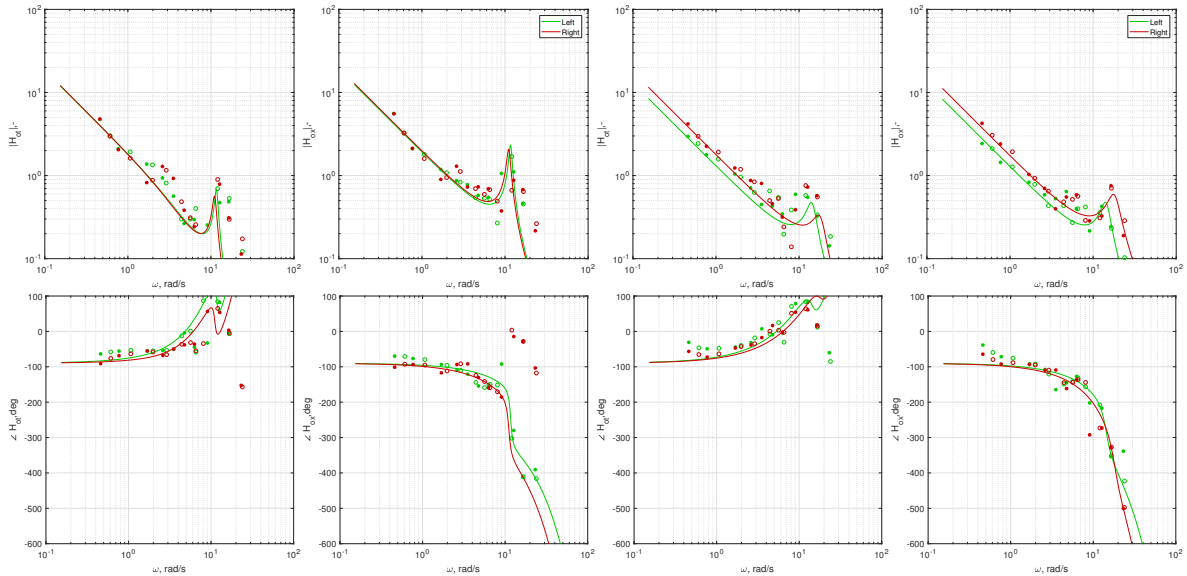


Figure 9-1: Response and model of left-handed student 4

Figure 9-2: Response and model of left-handed student 13

9-3 Results

The average response of the subjects for both hands can be found in Appendix F. For a few subjects the responses and fitted models of both hands are almost the same. For example for right-handed student 4 depicted in Figure 9-1. Another example can be found in Figure F-10. Many students show a response similar to that of right-handed student 13, depicted in Figure 9-2. The general appearance of the responses of both hands is similar, however, the response of the non-dominant hand is shifted downwards, indicating a lower gain. The same holds for student depicted in Figures F-7, F-9, F-19, F-21.

Performance and control activity results can be found in Figures 9-3 and 9-4. As for control activity, all subjects show similar control activity for both hands. When comparing both hands for left-handed subjects, the performance is very similar. For the right-handed subjects performance decreases for the left hand.

For the left-handed subjects all HC parameters of both hands are similar. The right-handed subjects show a lower gain in Figure 9-5 for the left hand and a higher visual delay in Figure 9-6.

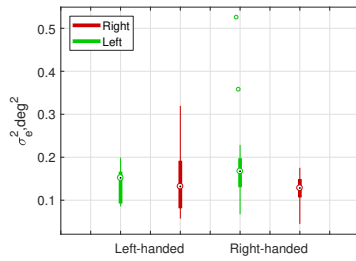


Figure 9-3

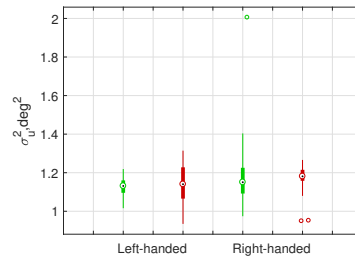


Figure 9-4

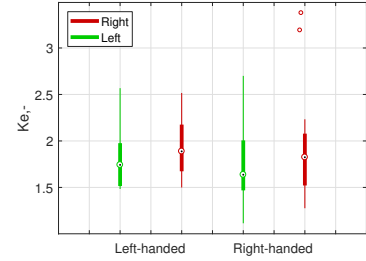


Figure 9-5

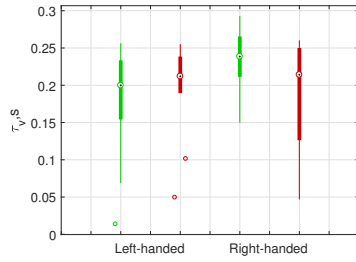


Figure 9-6

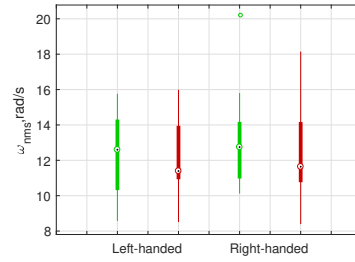


Figure 9-7

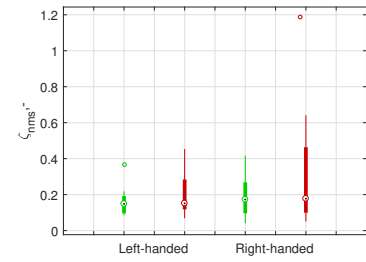


Figure 9-8

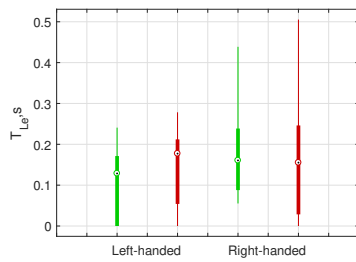


Figure 9-9

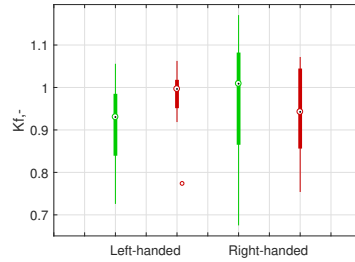


Figure 9-10

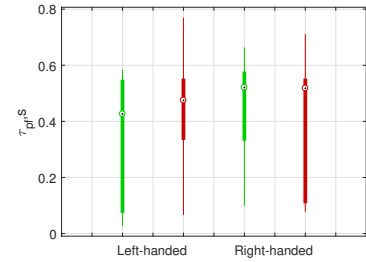


Figure 9-11

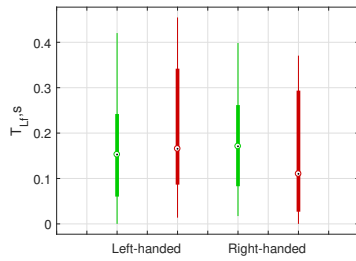


Figure 9-12

Figure 9-13: Control parameters

9-4 Discussion

For the left-handed students there is no clear difference in control behaviour for the left and right hand. Right-handed students show differences in the performance and related parameters. Namely the performance itself, gain and visual time delay. There are several theories that could explain these results.

9-4-1 Social influence

Approximately 10% of the world population is left-handed [58]. In today's society many tools are designed to be handled with the right hand. For example the location of a doorknob, scissors, a computer mouse, the refrigerator door and more. Although left handed versions exist, in many cases left-handed people are forced to adapt and thereby train their non-dominant hand to perform complex tasks. This could explain why left-handed people show similar results for both hands.

9-4-2 Brain lateralization

A more biological explanation factor that could lead to the good performance with the right hand for left-handed subjects, is hemispheric lateralization [59–61]. According to this theory, both hemispheres of the brain play a specific role in motor actions. The left hemisphere is predominant for language and motor skills while the right hemisphere is associated with spatial functions. This theory suggest that the right hand, strongly connected to the left hemisphere, is better at performing motor tasks in terms of planning and coordination. This would explain the relatively good performance of the right hand for left-handed students.

9-5 Conclusion

Whether the left or right hand is used to perform the experiment, influences the results if the subjects is right-handed. On average, for right-handed subjects the performance decreased for the left hand. Right-handed subjects also showed a lower gain and higher delay for the left hand. For left-handed subjects all parameters were similar for both hands. The current experiment was performed with young, healthy subjects. For the control behaviour of the patients in Part I, it is not possible to determine whether the effect of the steering hand is stronger than the consequences of the lesion. However, the results of the current experiment could clarify inexplicable differences between hands in the performance of patients.

Part III

Appendices

Chapters A to E have been graded as part of AE4020

Appendix A

Latin square design

Table A-1: Latin square designed for preliminary experiment 1 in Chapter 5

	Subject 1	Subject 2	Subject 3	Subject 4	Subject 5	Subject 6	Subject 7	Subject 8
Task 1	SI-J	G-T	G-T	SI-J	SI-T	G-J	SI-T	G-J
Task 2	G-T	SI-T	SI-T	G-T	G-J	SI-J	G-J	SI-J
Task 3	SI-T	G-J	G-J	SI-T	SI-J	G-T	SI-J	G-T
Task 4	G-J	SI-J	SI-J	G-J	G-T	SI-T	G-T	SI-T

Table A-2: Latin square designed for preliminary experiment 3 in Chapter 7

	Subject 1	Subject 2	Subject 3	Subject 4	Subject 5	Subject 6	Subject 7	Subject 8
Task 1	SIfd	SI	SI	G	Gfd	Gfd	SIfd	G
Task 2	Gfd	G	G	SIfd	SI	SI	Gfd	SIfd
Task 3	SI	SIfd	SIfd	Gfd	G	G	SI	Gfd
Task 4	G	Gfd	Gfd	SI	SIfd	SIfd	G	SI

Appendix B

Touchscreen vs Joystick operator describing functions

The following pages show the fourier coefficients (black circles) and fitted operator model (grey) for all subjects and tasks.

B-1 Gain-Touchscreen

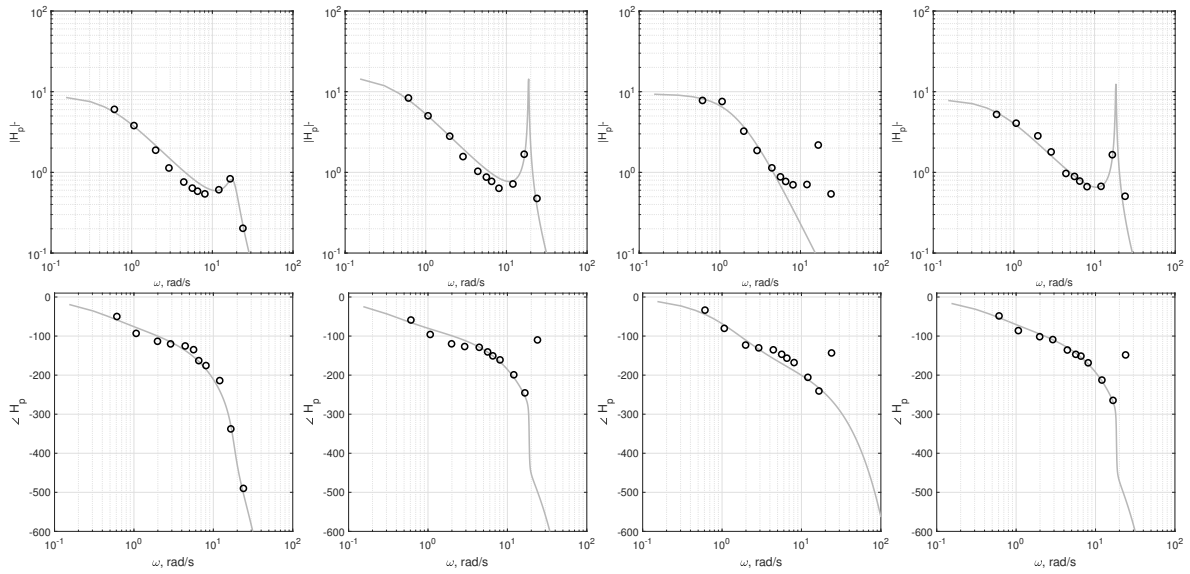


Figure B-1:
Subject 1

Figure B-2:
Subject 2

Figure B-3:
Subject 3

Figure B-4:
Subject 4

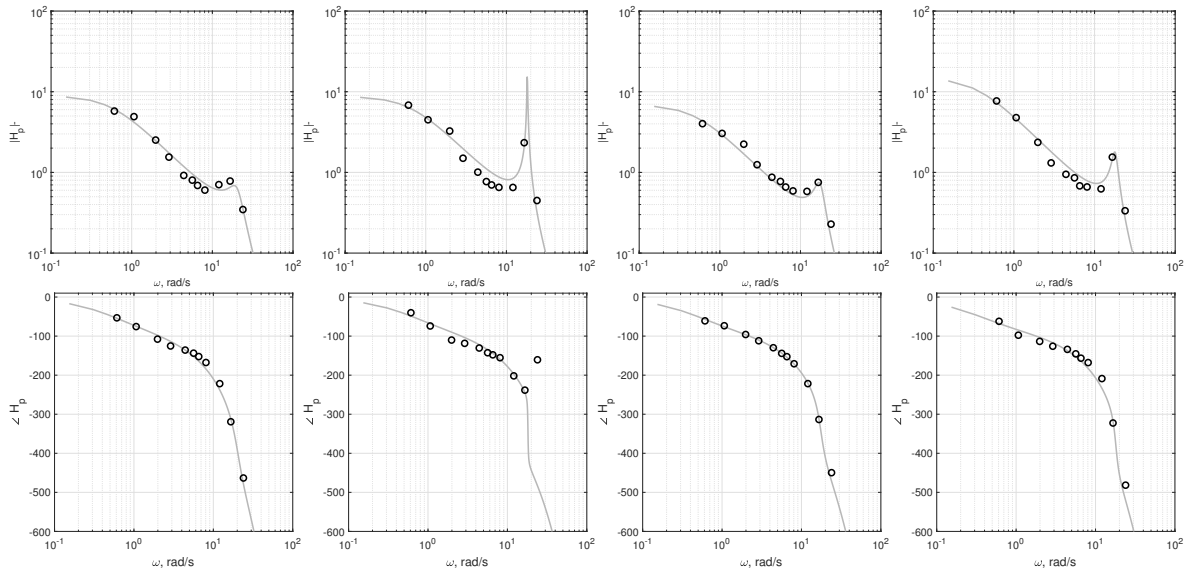


Figure B-5:
Subject 5

Figure B-6:
Subject 6

Figure B-7:
Subject 7

Figure B-8:
Subject 8

B-2 Gain-Joystick

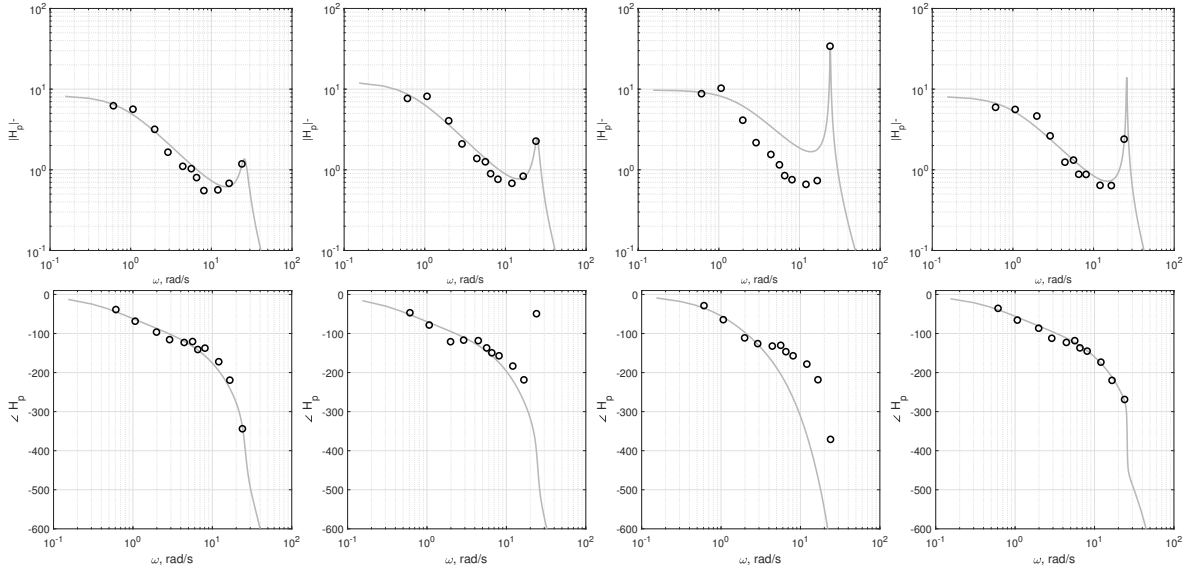


Figure B-9:
Subject 1

Figure B-10:
Subject 2

Figure B-11:
Subject 3

Figure B-12:
Subject 4

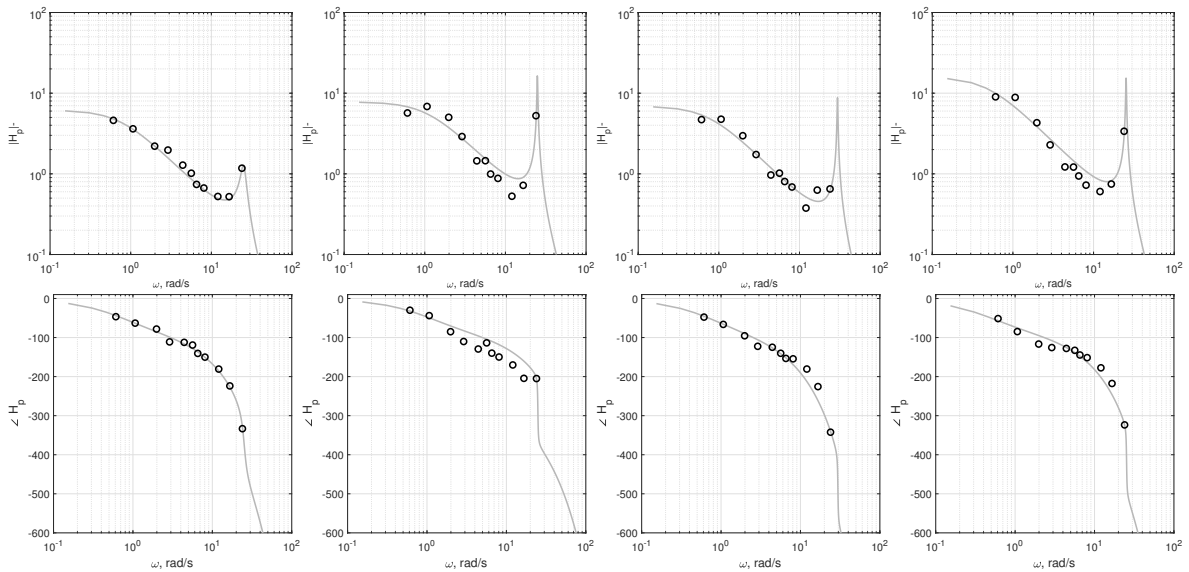


Figure B-13:
Subject 5

Figure B-14:
Subject 6

Figure B-15:
Subject 7

Figure B-16:
Subject 8

B-3 Single integrator-Touchscreen

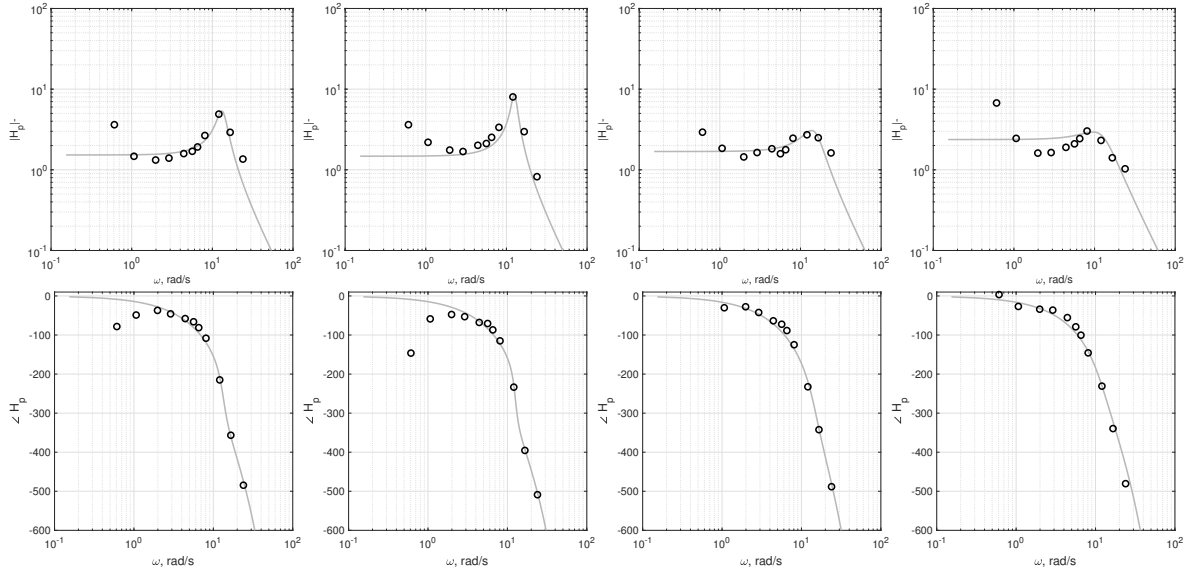


Figure B-17:
Subject 2

Figure B-18:
Subject 3

Figure B-19:
Subject 4

Figure B-20:
Subject 5

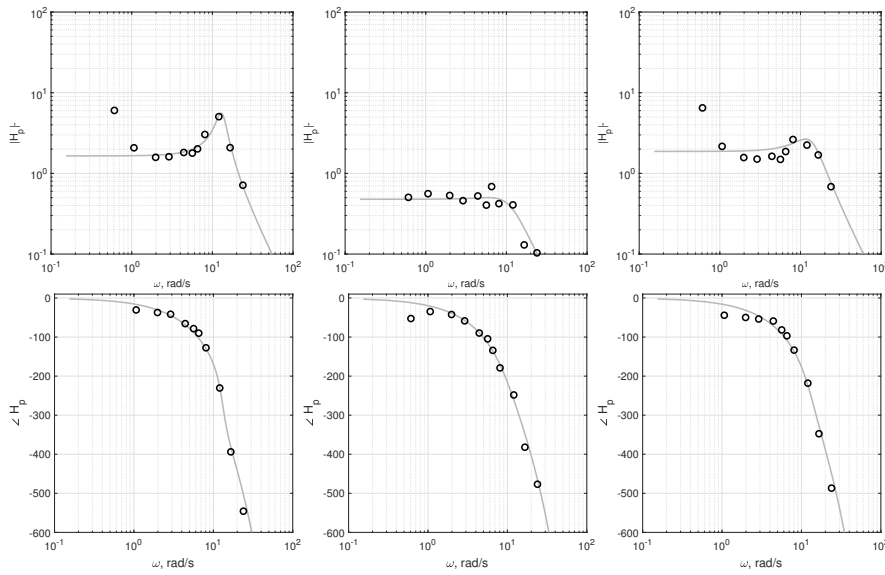


Figure B-21:
Subject 6

Figure B-22:
Subject 7

Figure B-23:
Subject 8

B-4 Single integrator-Joystick

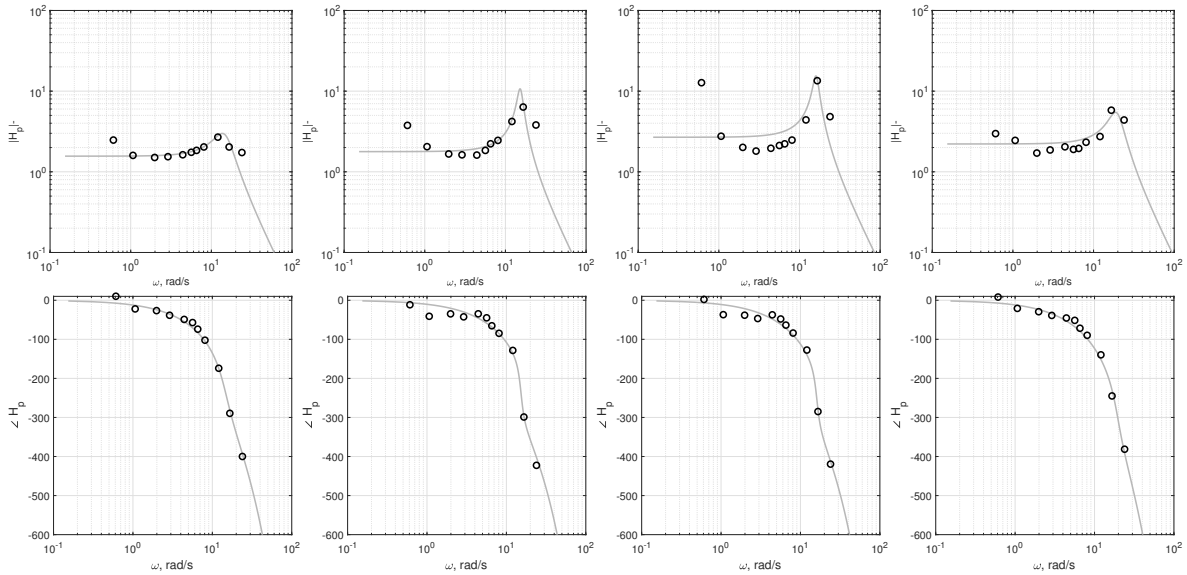


Figure B-24:
Subject 1

Figure B-25:
Subject 2

Figure B-26:
Subject 3

Figure B-27:
Subject 4

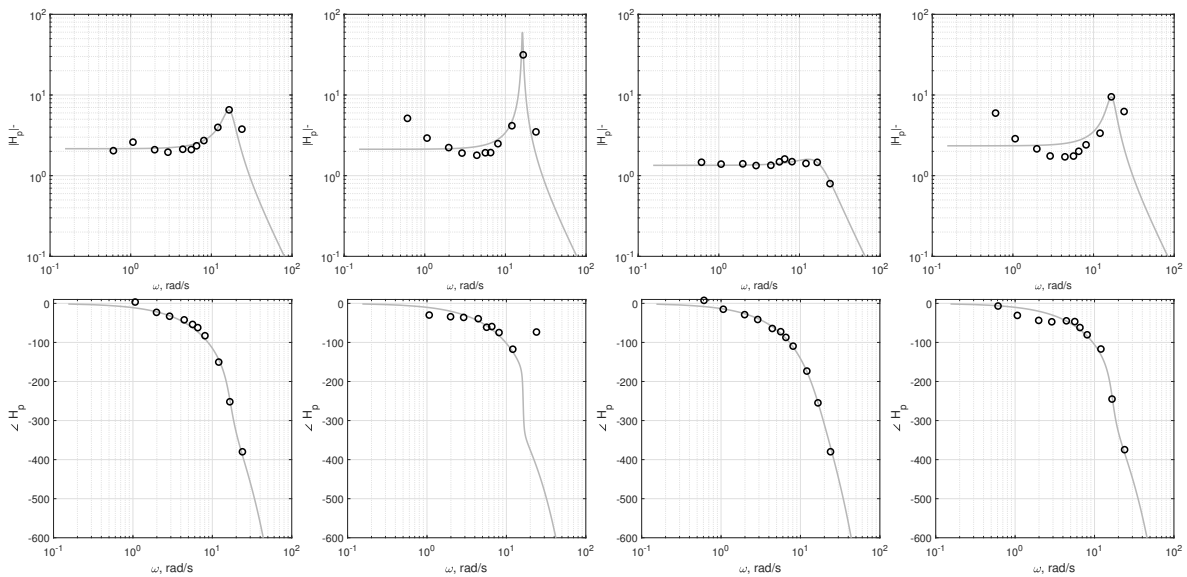


Figure B-28:
Subject 5

Figure B-29:
Subject 6

Figure B-30:
Subject 7

Figure B-31:
Subject 8

Appendix C

Loss of contact

This chapter presents additional results from Chapter 6. Section C-1 shows the randomly created LOC scenarios. In Section C-2 the Power Spectral density plots of the error signal are depicted.

C-1 LOC scenarios

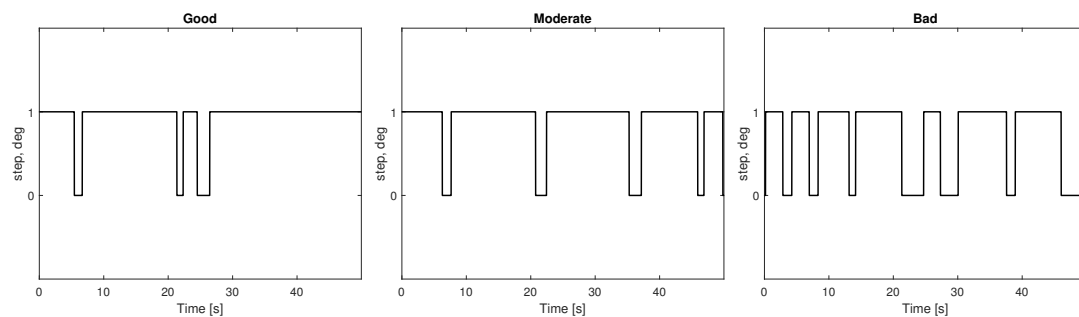


Figure C-1: Loss of contact scenarios

C-2 PSD error signal for all LOC scenarios

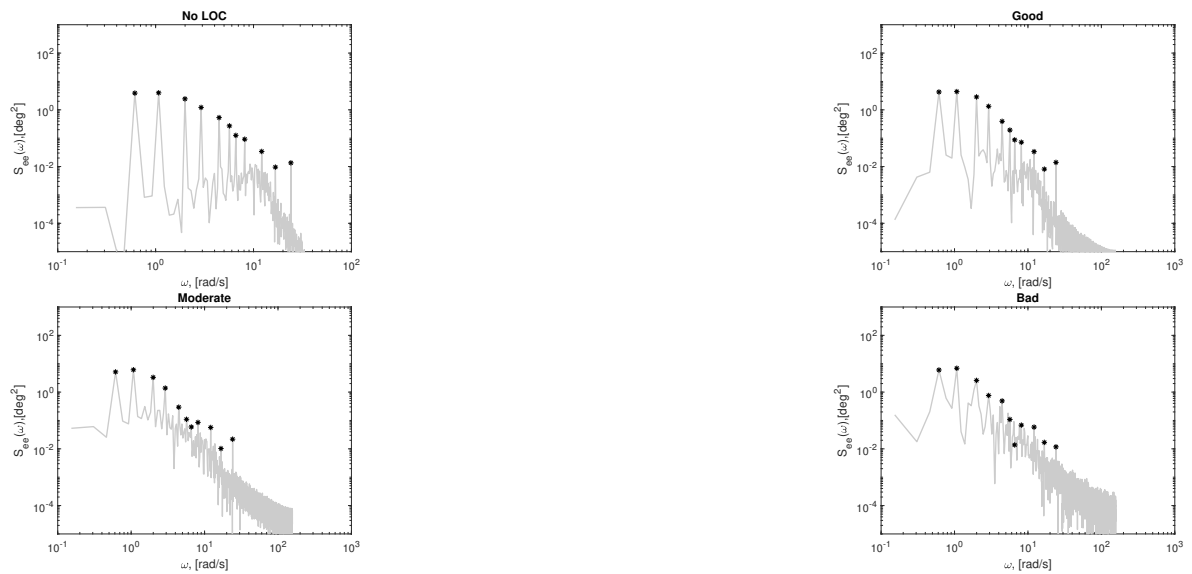


Figure C-2: Power spectral density of error signal, Gain dynamics

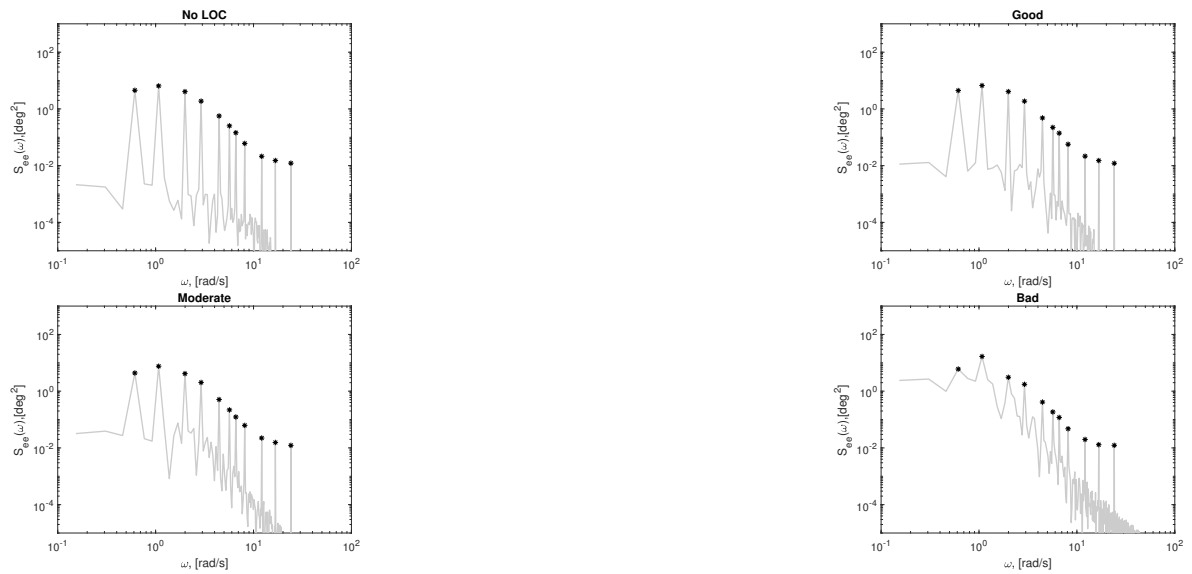
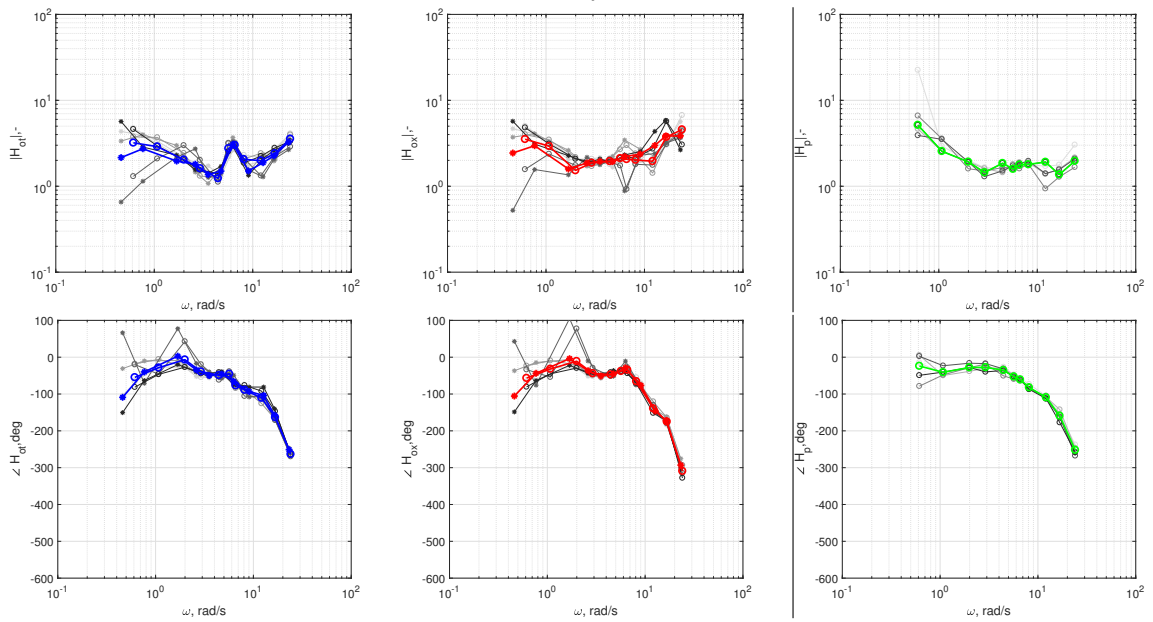
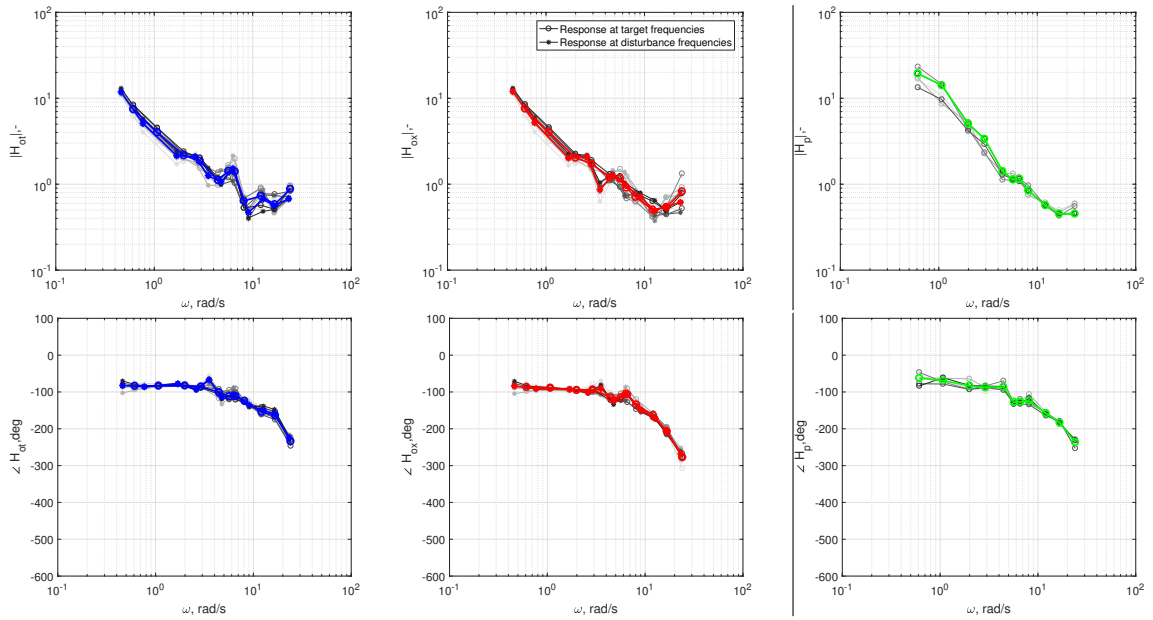


Figure C-3: Power spectral density of error signal, Single integrator dynamics

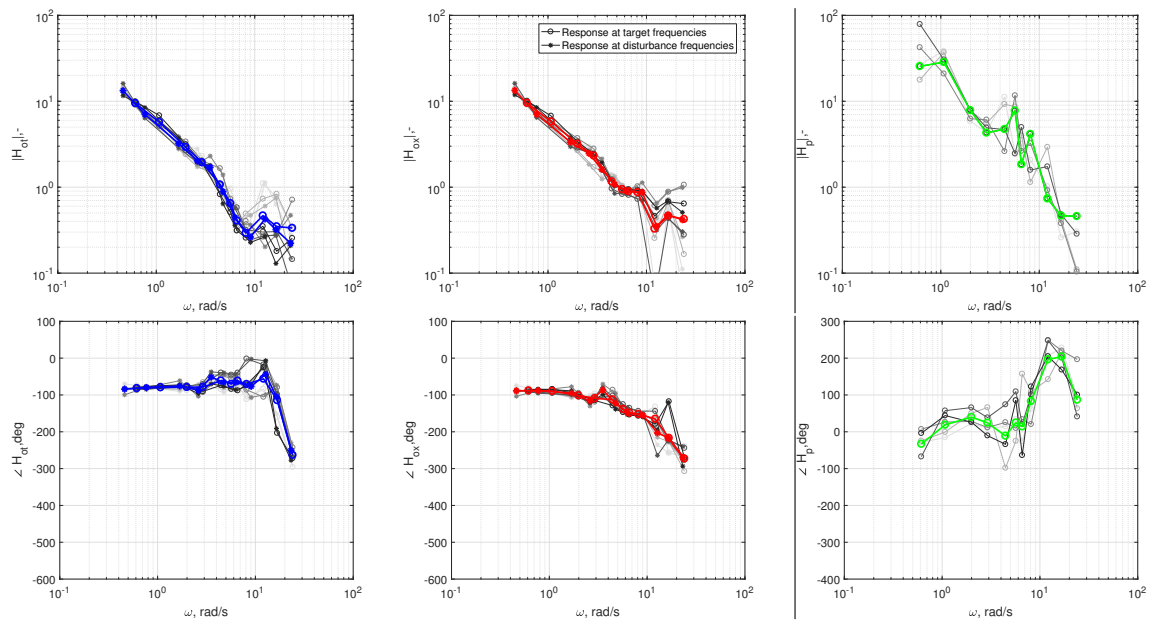
Appendix D

Preview test operator describing functions

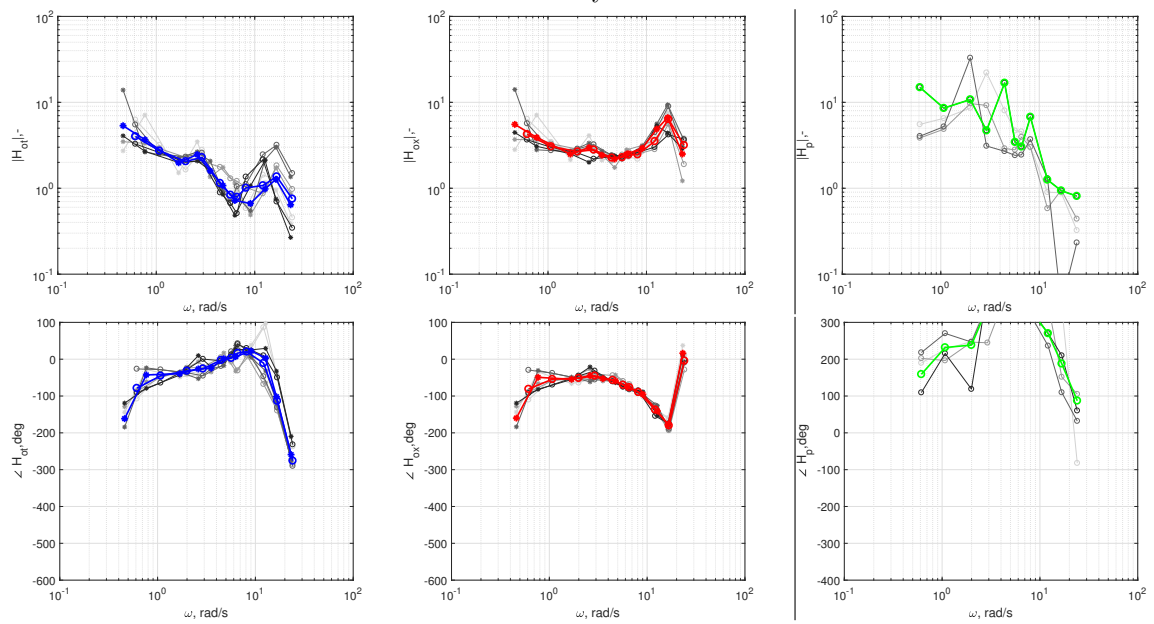
This chapter presents the operator describing functions. Every page is dedicated to a subject. The top of the page shows the bode plots for the tasks with gain dynamics, the bottom graphs depict the tasks with single integrator dynamics. On the left side of the vertical line the operator response to the target H_{ot} and controlled element H_{ox} are presented. On the right side of the vertical line, the response for the tasks without a disturbance function are shown. The circles (o) indicate the response at the target frequencies, the stars (*) the response at disturbance frequencies. Every trial is depicted on the plots. The first trial is depicted in light grey, the second is slightly darker, etc. The last trial is shown in black. The thick lines indicate the mean of all trials.



a: Subject 1

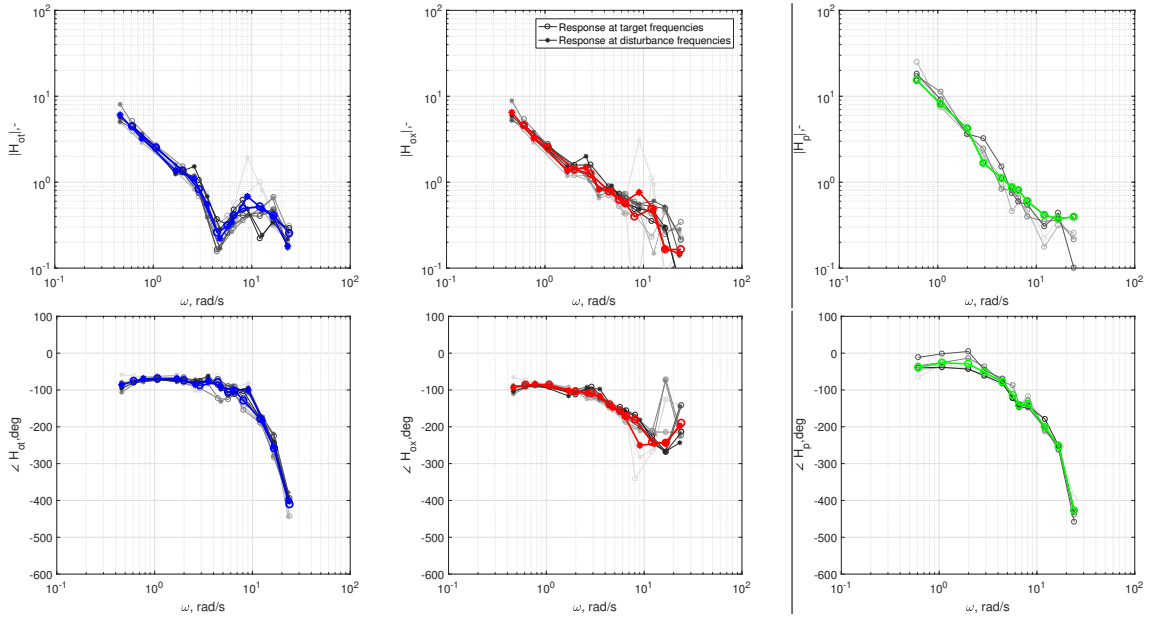


Gain dynamics

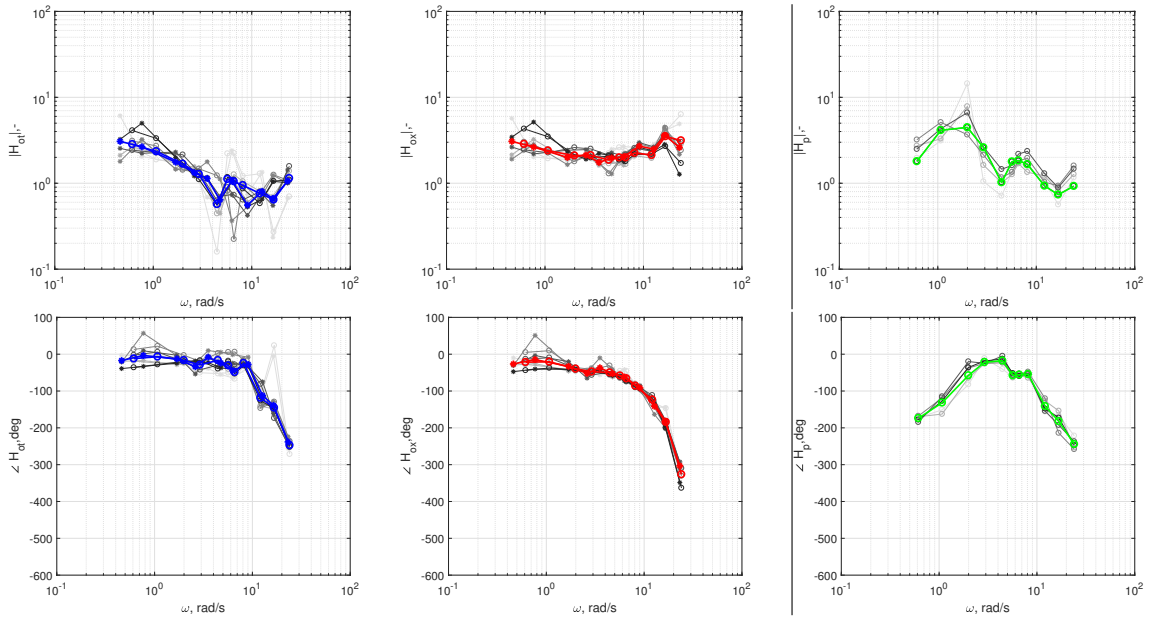


Single integrator dynamics

b: Subject 2

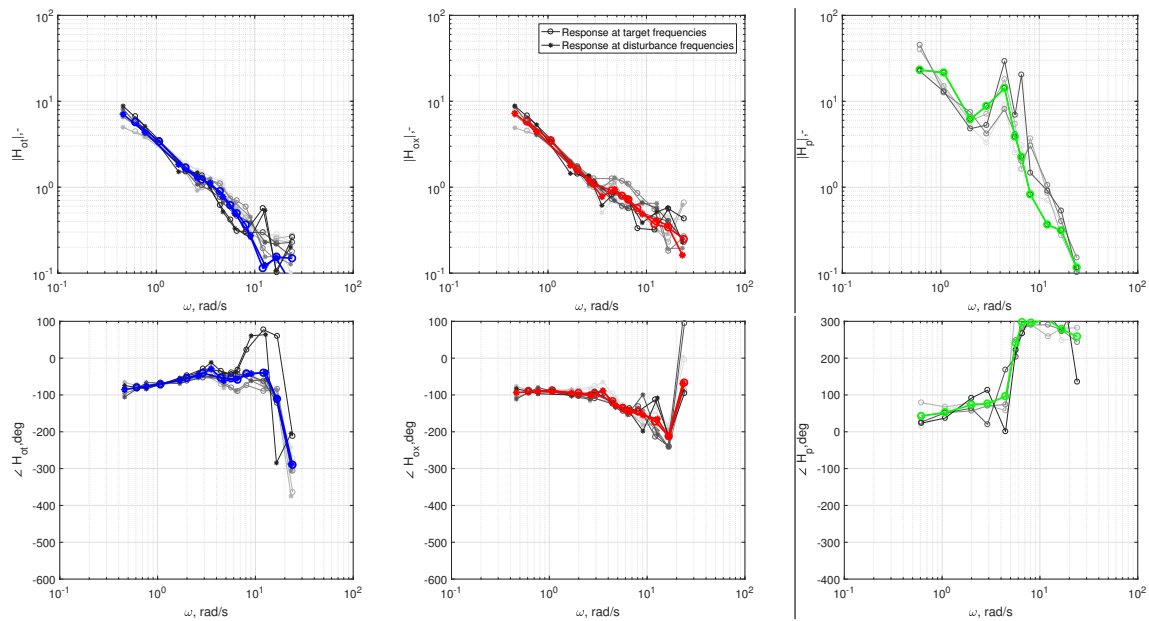


Gain dynamics

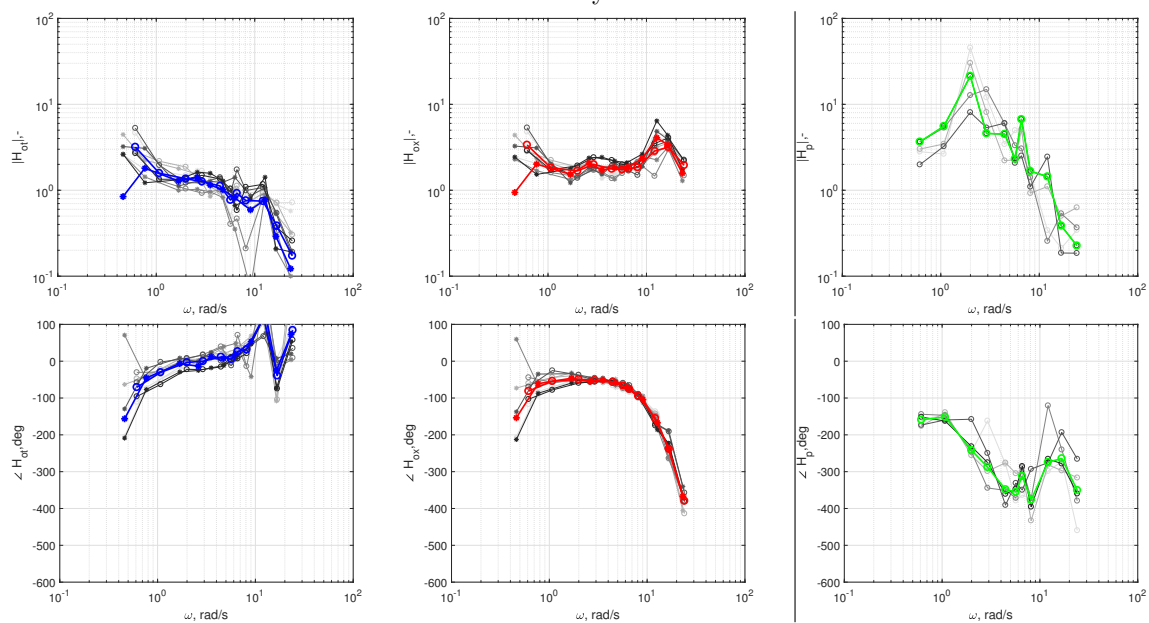


Single integrator dynamics

c: Subject 3

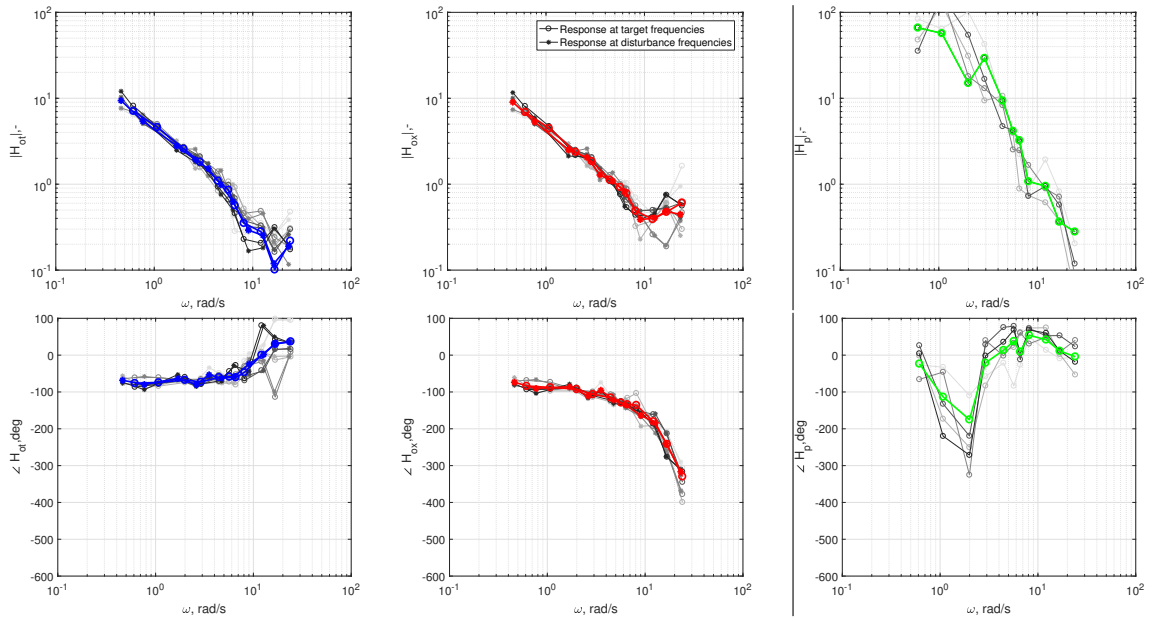


Gain dynamics

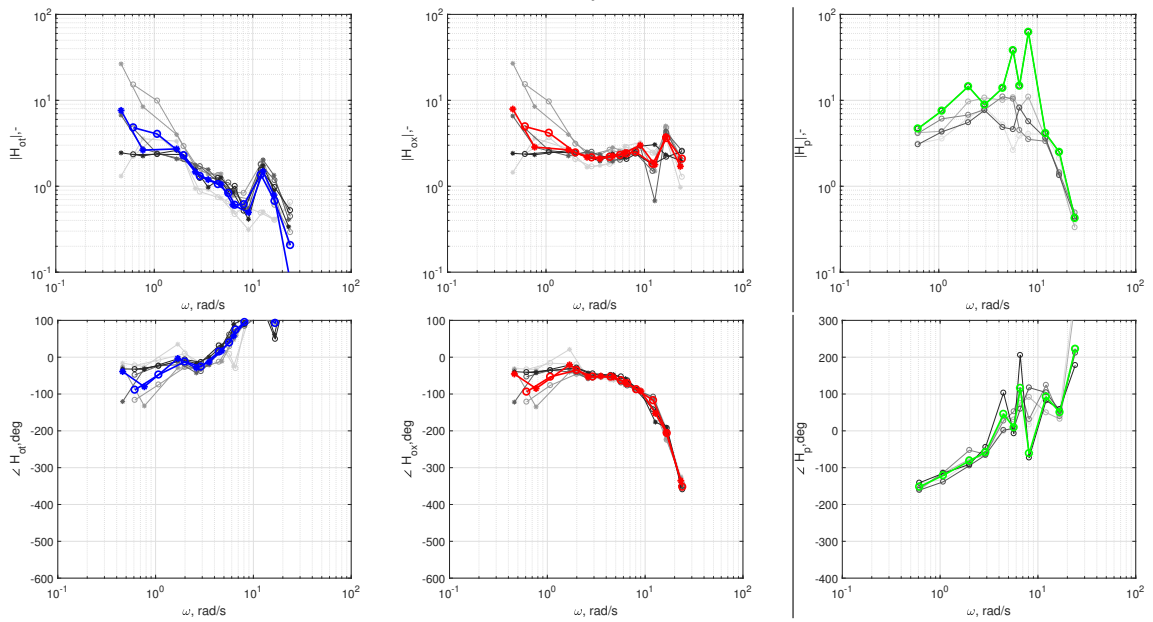


Single integrator dynamics

d: *Subject 4*

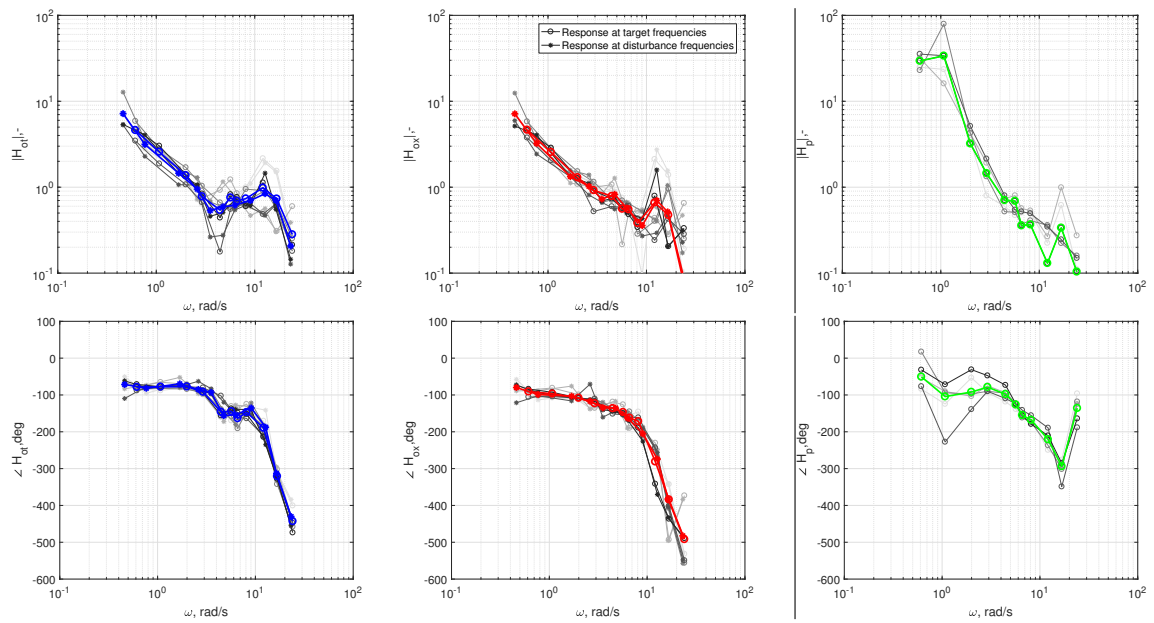


Gain dynamics

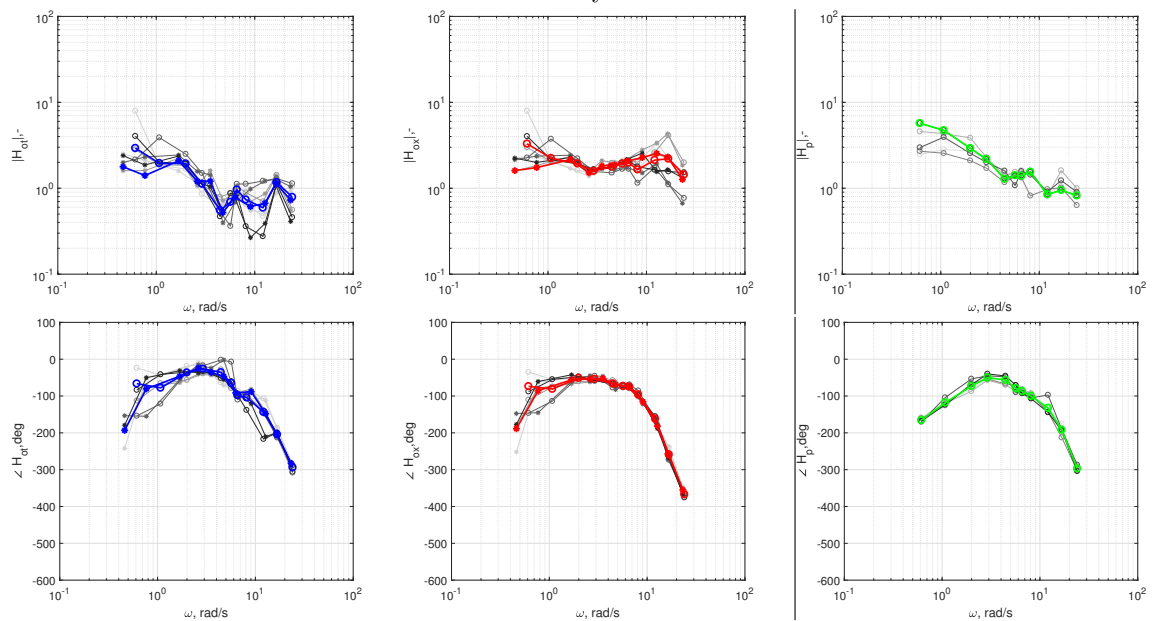


Single integrator dynamics

e: Subject 5

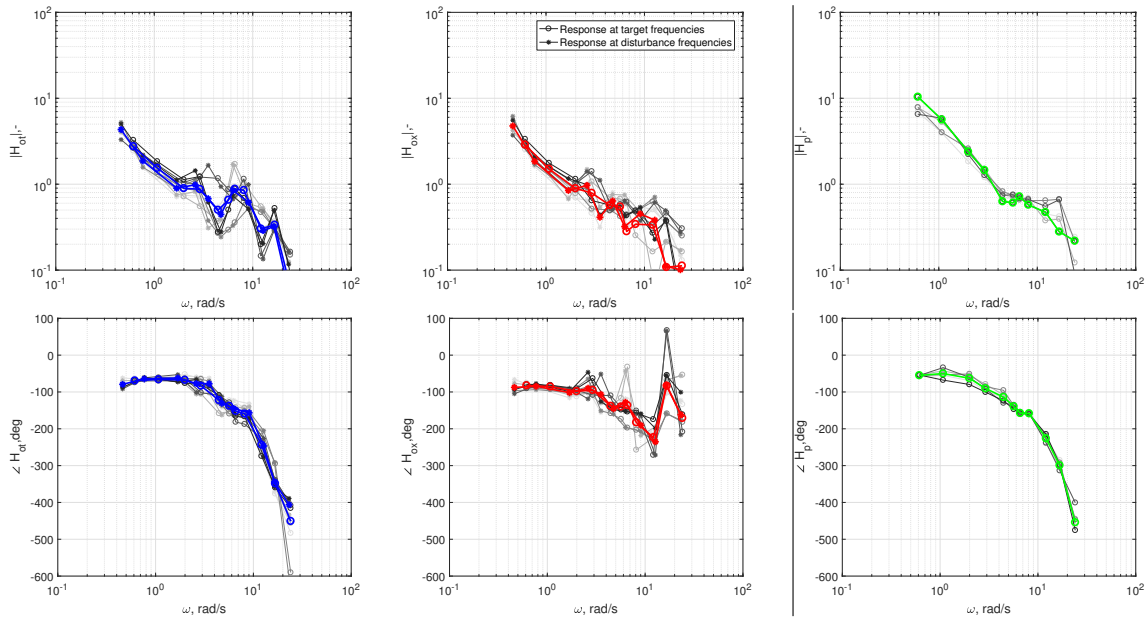


Gain dynamics

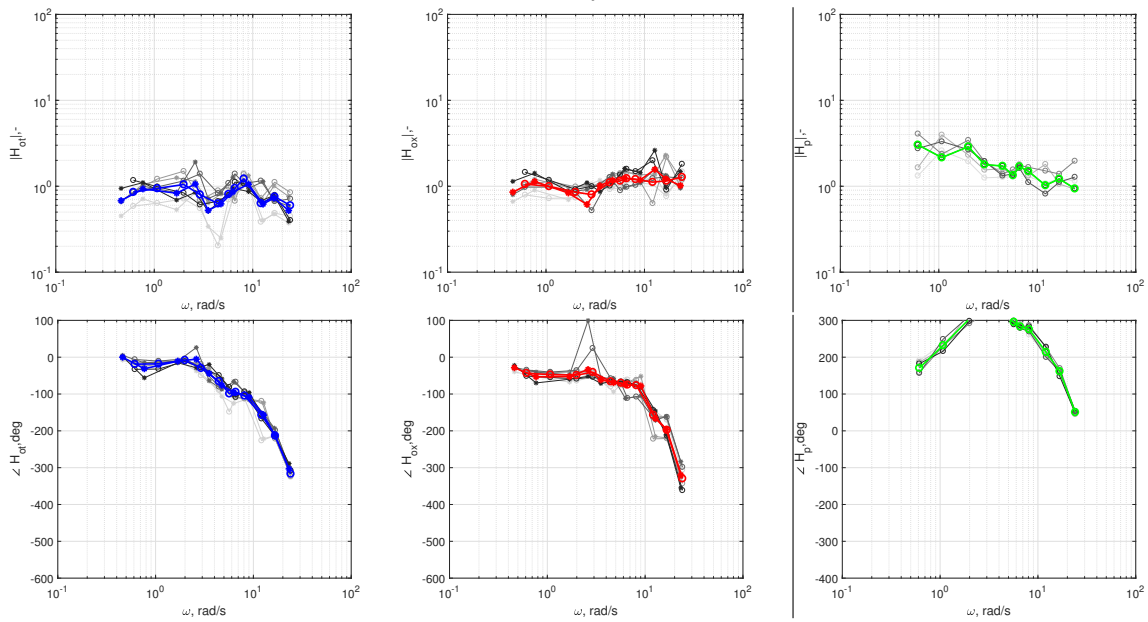


Single integrator dynamics

f: Subject 6

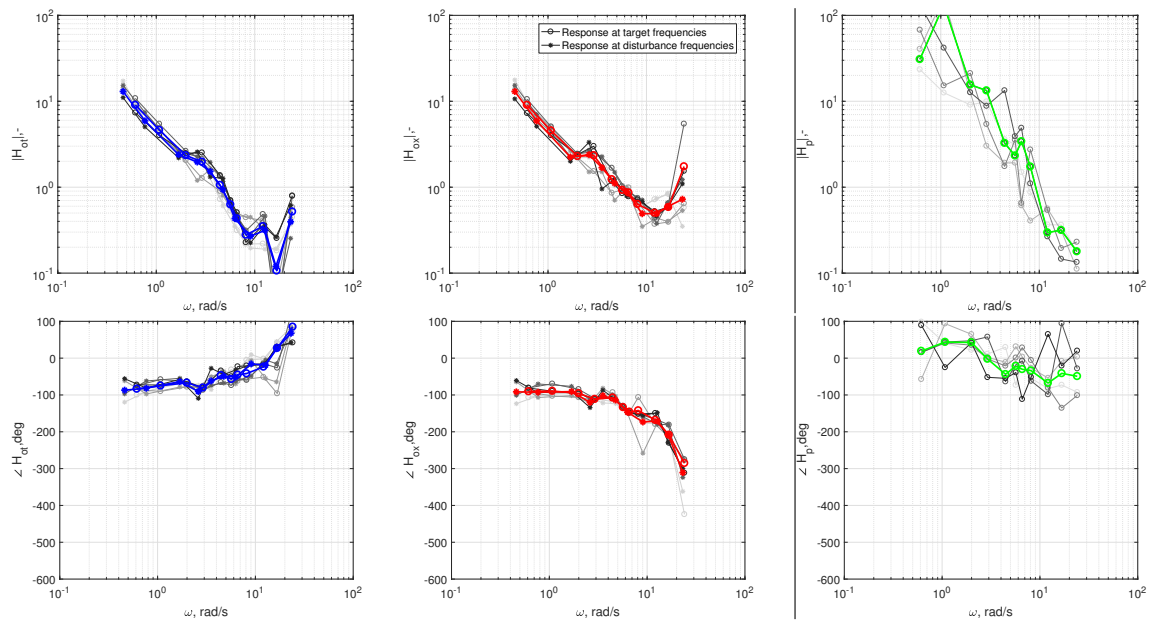


Gain dynamics

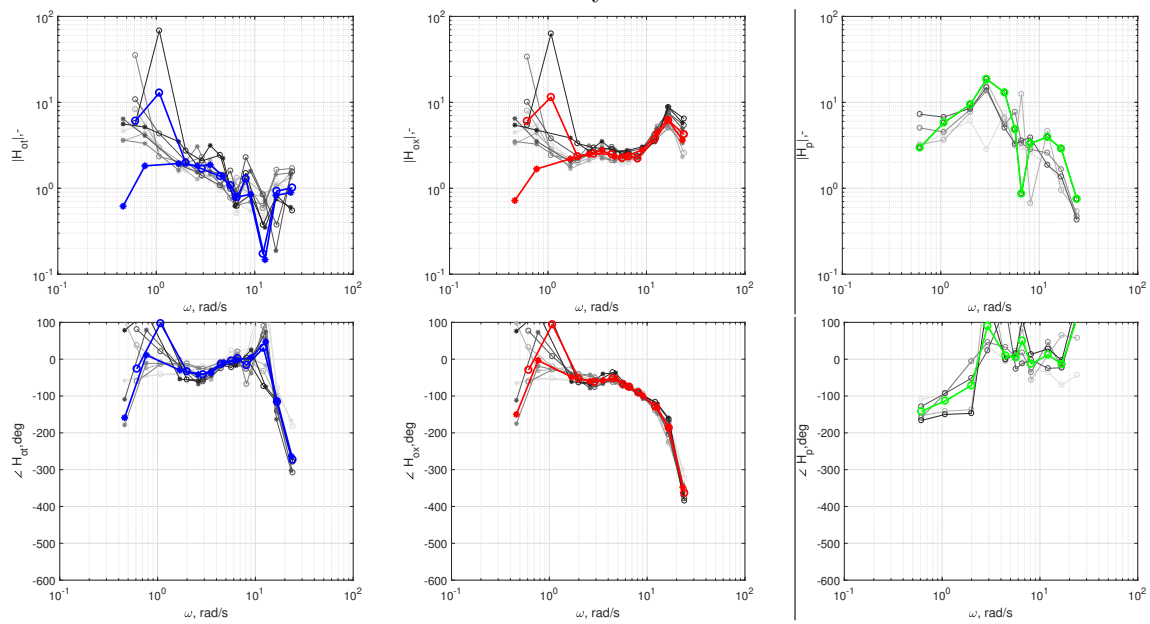


Single integrator dynamics

g: Subject 7



Gain dynamics



Single integrator dynamics

h: Subject 8

Appendix E

Individual variance contributions

This chapter gives the split variance of the error signal and control signal from the experiment of Chapter 7. Variances are shown per subject for each condition.

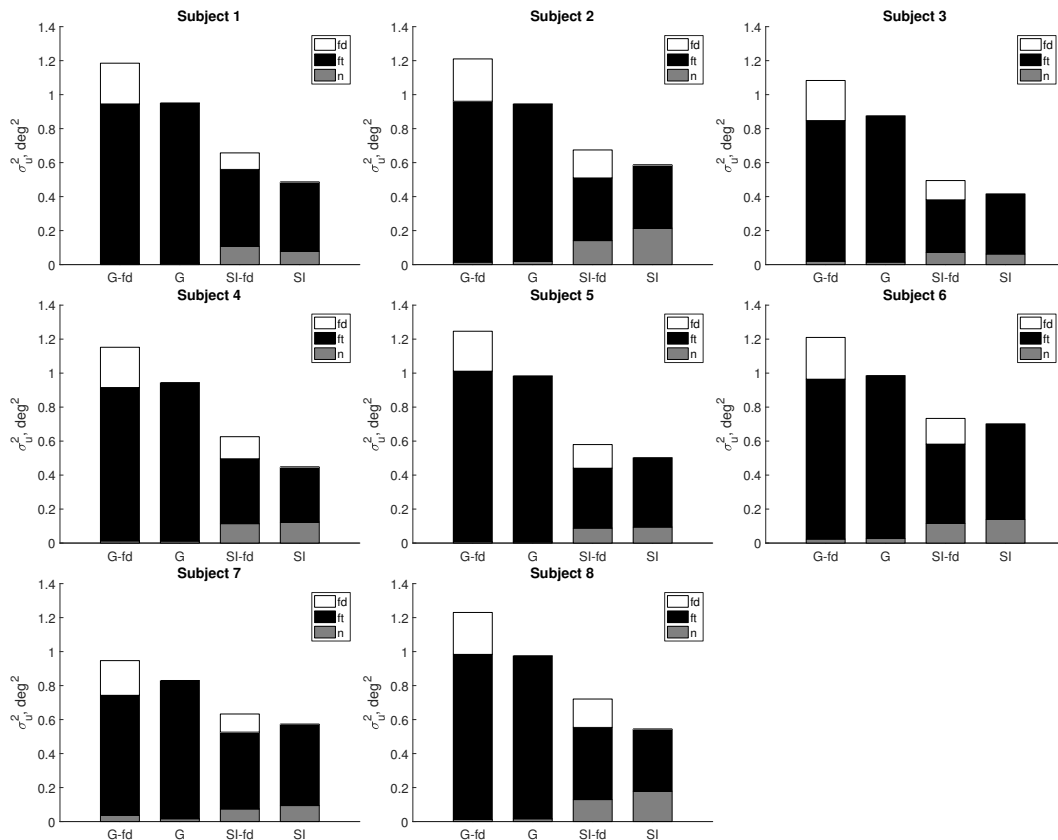


Figure E-1: Mean, splitted variance of control with contributions of disturbance (f_a), target (f_t) and remnant (n), for each subject

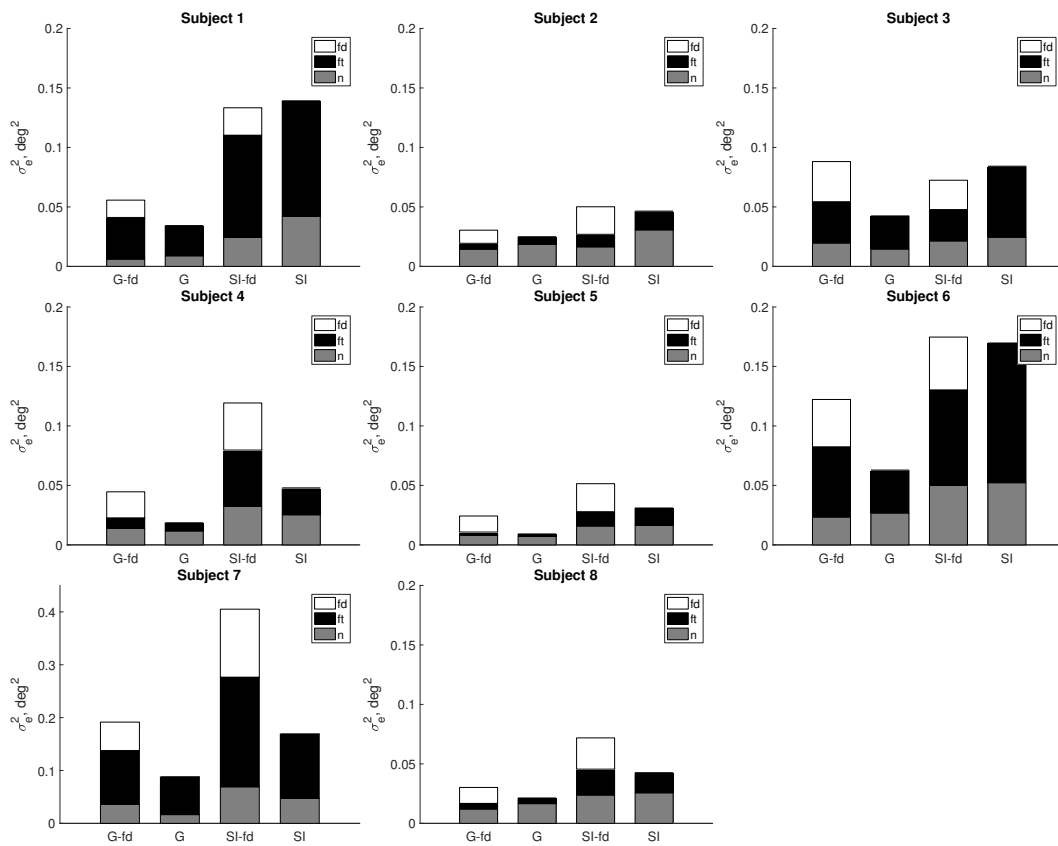


Figure E-2: Mean, splitted variance of error with contributions of disturbance (f_d), target (f_t) and remnant (n), for each subject

Appendix F

Left vs. right hand experiment operator describing functions

The following pages present the operator describing functions of the left- and right-handed subject that participated in the experiment from Chapter 9. The H_{ot} and H_{ox} responses and fitted model of both hands are depicted in the same figure. The circles (o) indicate the average response at the target frequencies, the stars (*) the average response at disturbance frequencies.

F-1 Lefthanded subjects

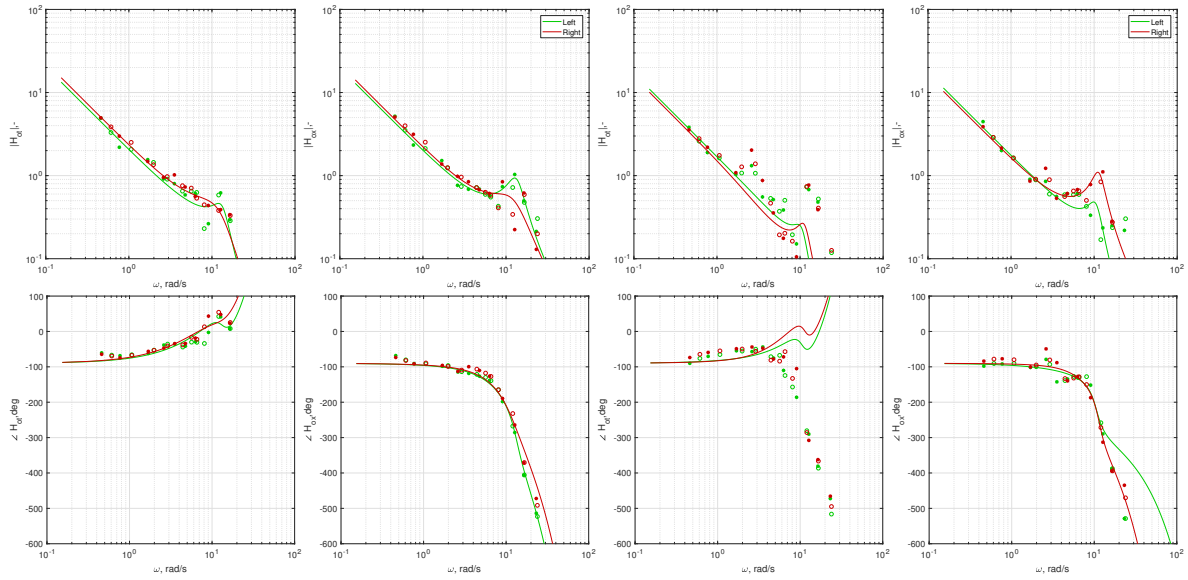


Figure F-1: Left-handed student 1

Figure F-2: Left-handed student 2

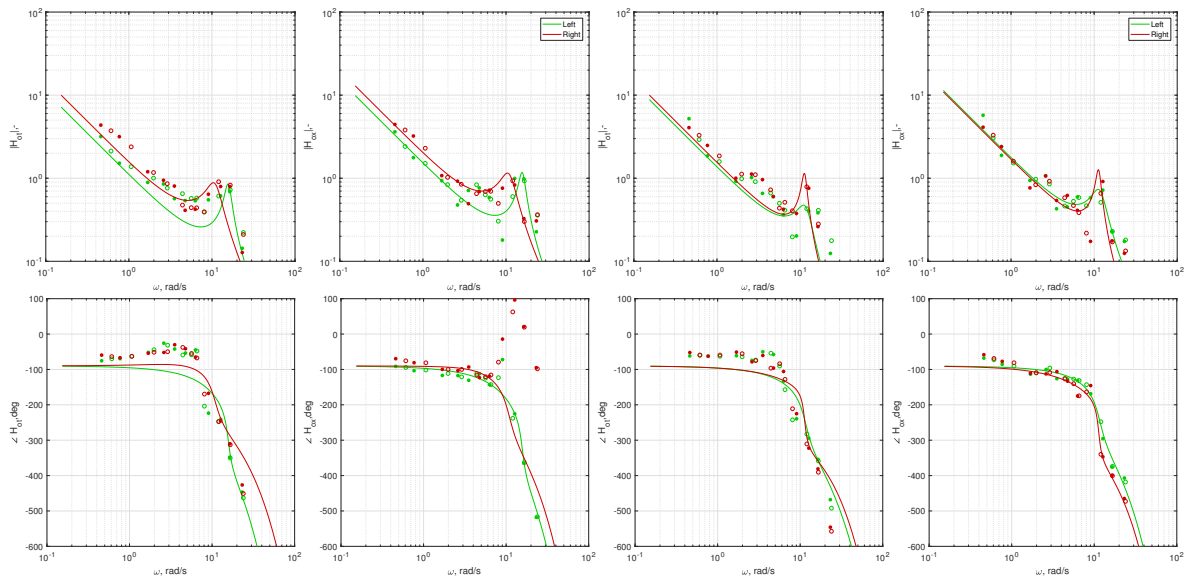


Figure F-3: Left-handed student 3

Figure F-4: Left-handed student 4

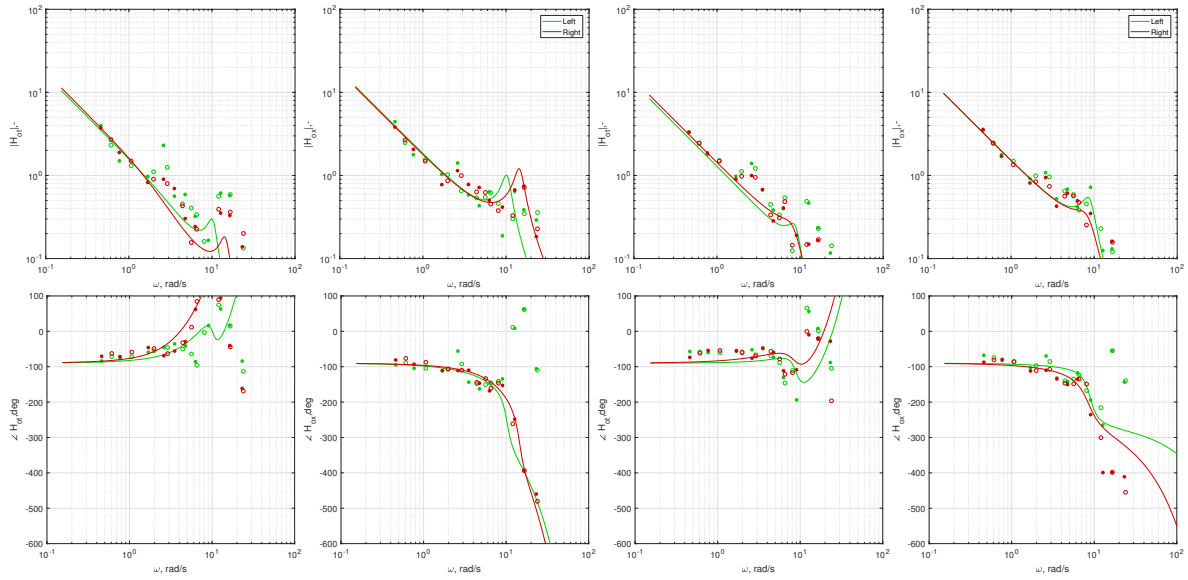


Figure F-5: Left-handed student 5

Figure F-6: Left-handed student 6

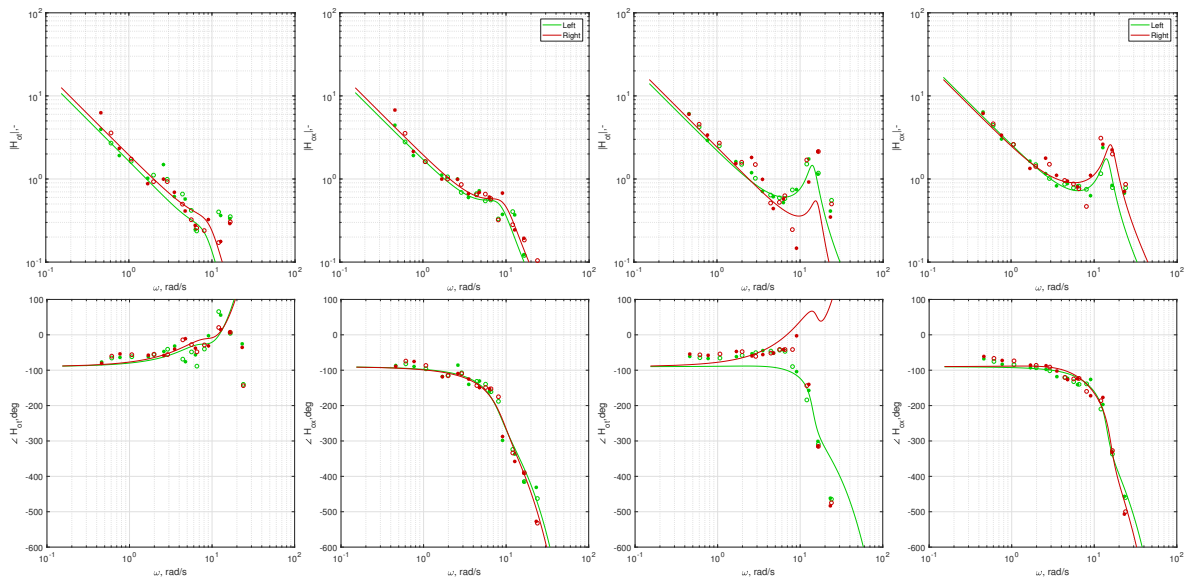


Figure F-7: Left-handed student 7

Figure F-8: Left-handed student 8

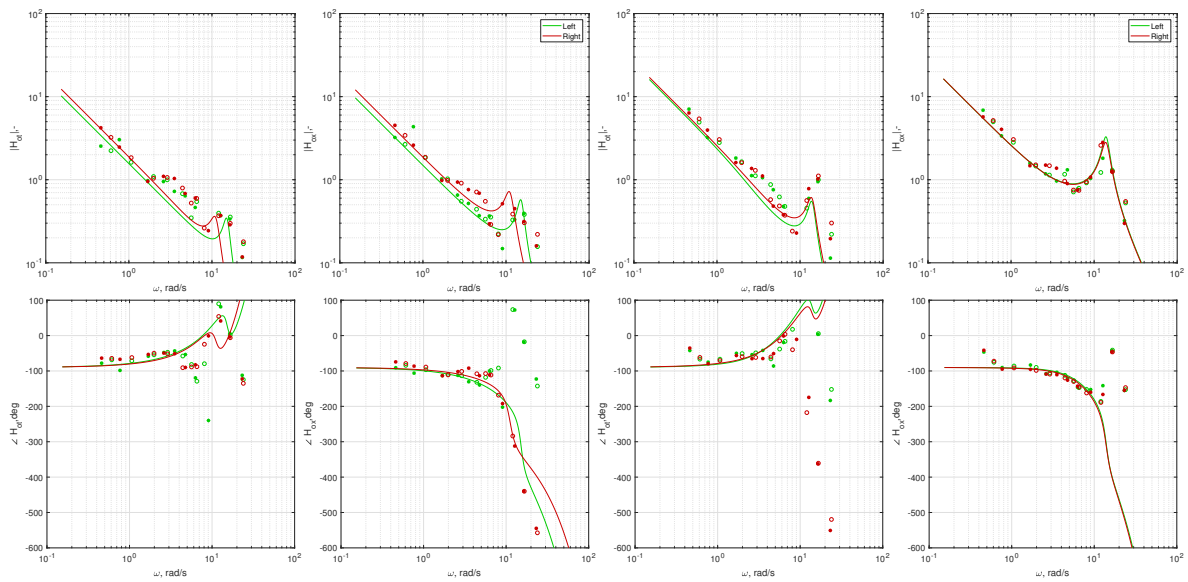


Figure F-9: Left-handed student 9

Figure F-10: Left-handed student 10

F-2 Righthanded subjects

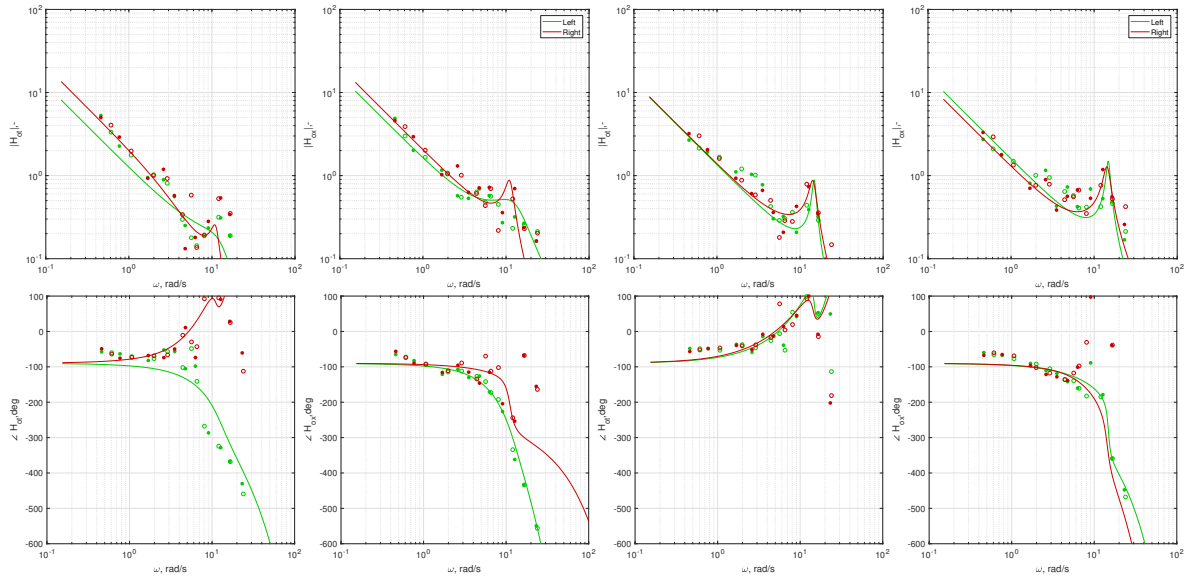


Figure F-11: Right-handed student 1

Figure F-12: Right-handed student 2

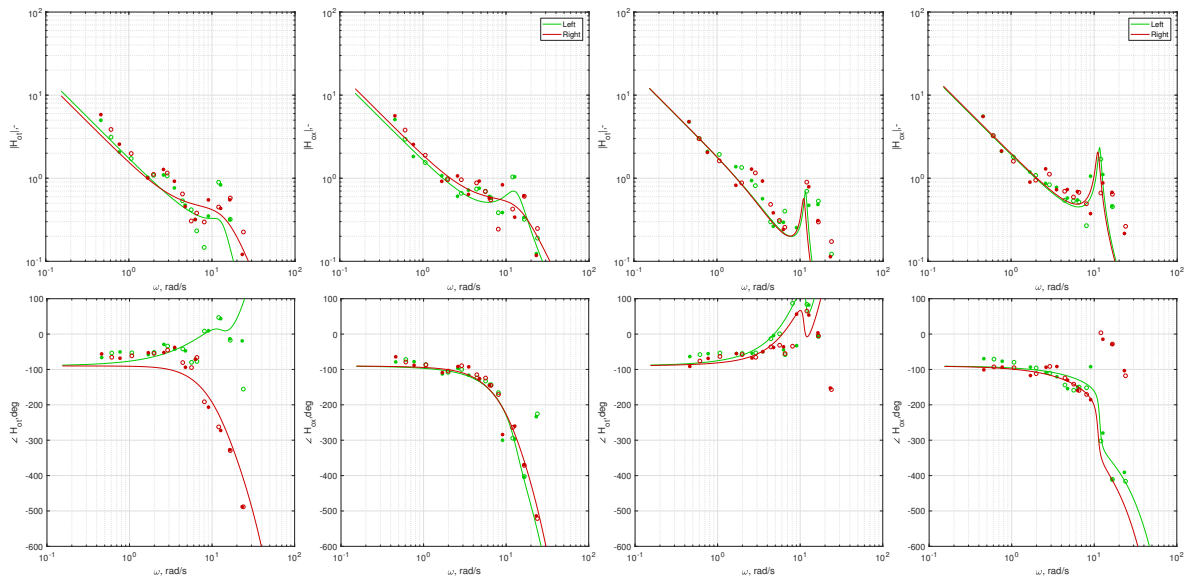


Figure F-13: Right-handed student 3

Figure F-14: Right-handed student 4

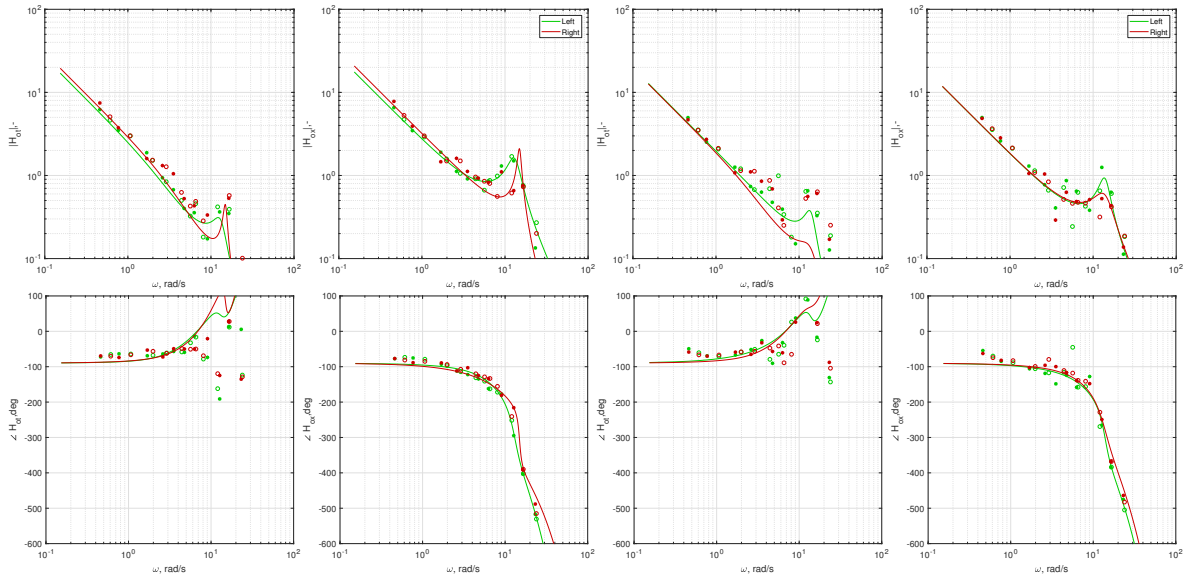


Figure F-15: Right-handed student 5

Figure F-16: Right-handed student 6

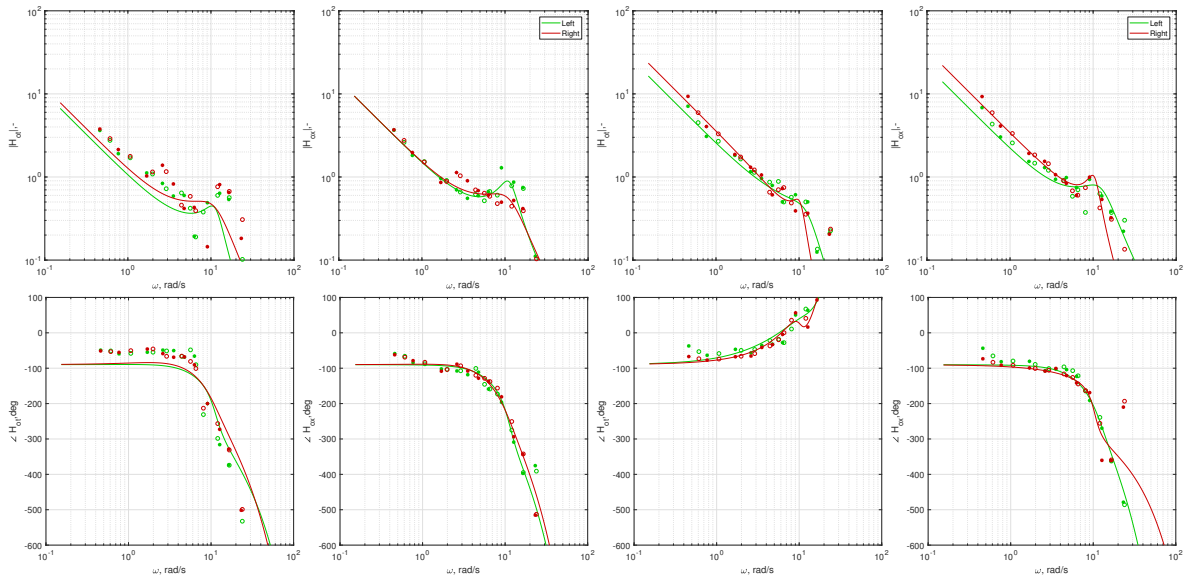


Figure F-17: Right-handed student 7

Figure F-18: Right-handed student 8

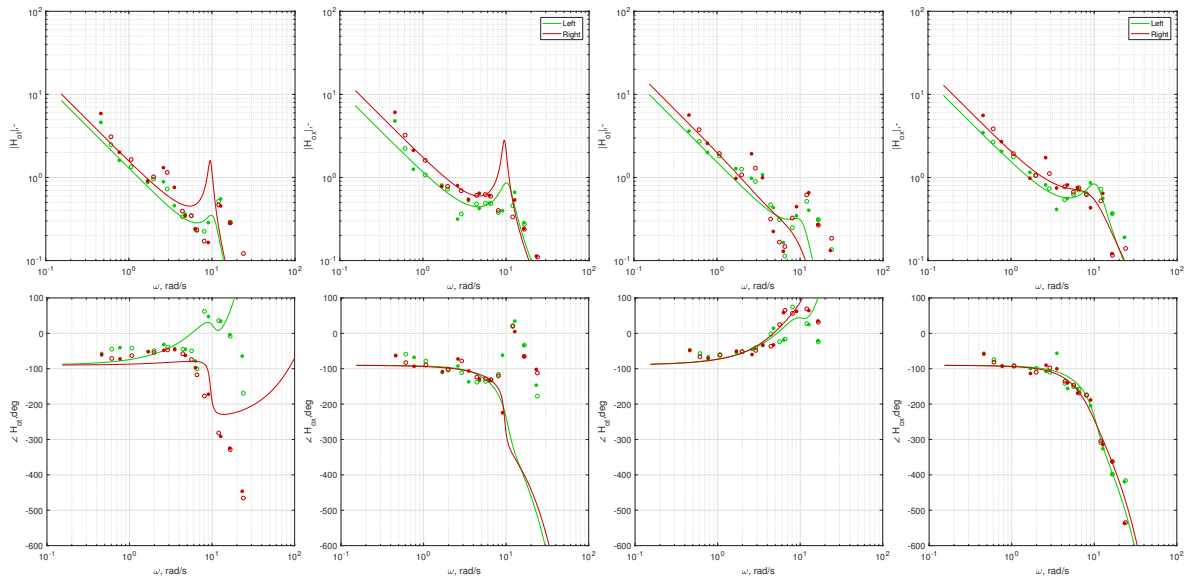


Figure F-19: Right-handed student 9

Figure F-20: Right-handed student 10

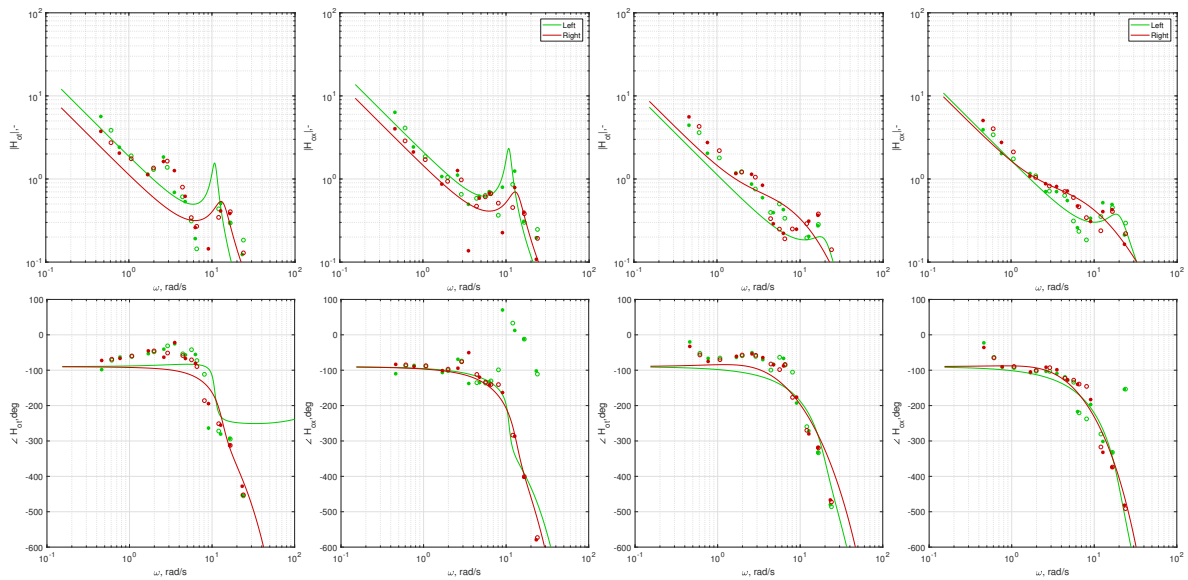


Figure F-21: Right-handed student 11

Figure F-22: Right-handed student 12

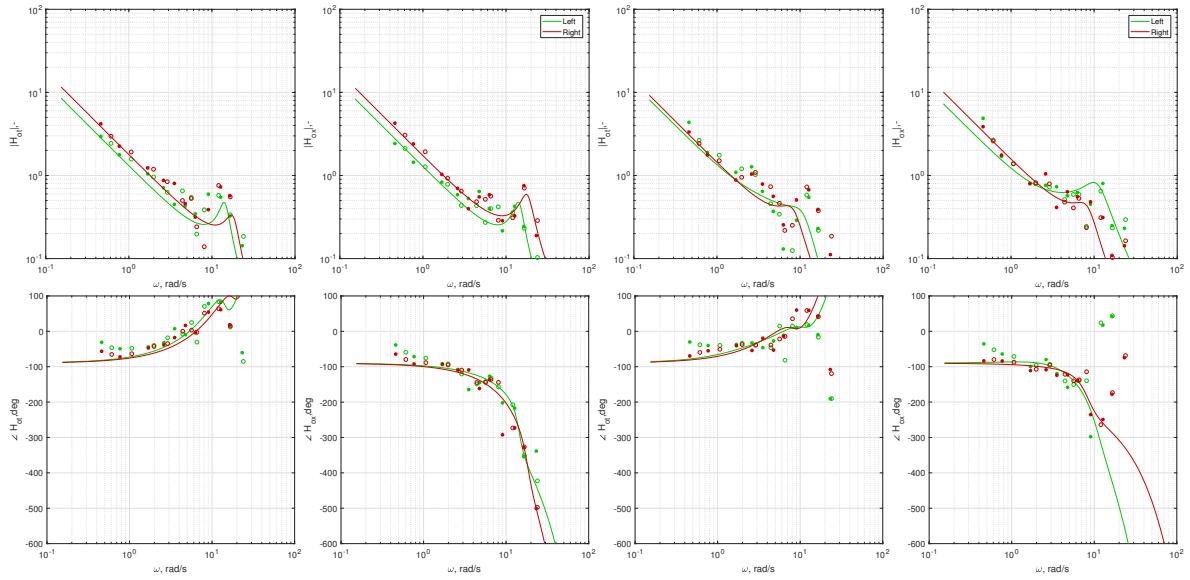


Figure F-23: Right-handed student 13

Figure F-24: Right-handed student 14

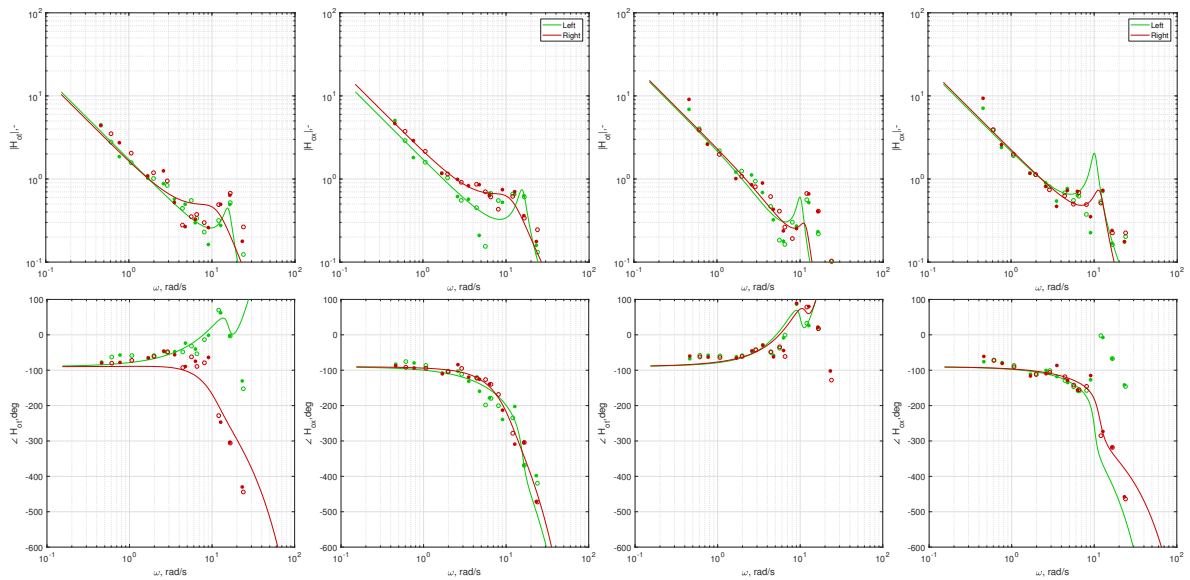


Figure F-25: Right-handed student 15

Figure F-26: Right-handed student 16

Part IV

Paper Appendices

Appendix G

Individual operator describing functions

This chapter presents the results of the subjects that participated in the experiment described in Part I. The operator response to H_{o_t} and H_{o_x} are depicted. The circles (o) indicate the response at the target frequencies, the stars (*) the response at disturbance frequencies. All included trials are shown on the plots. The first trial is depicted in light grey, the second is slightly darker, etc. The last trial is shown in black. The thick lines indicate the mean of all trials.

G-1 Patients affected

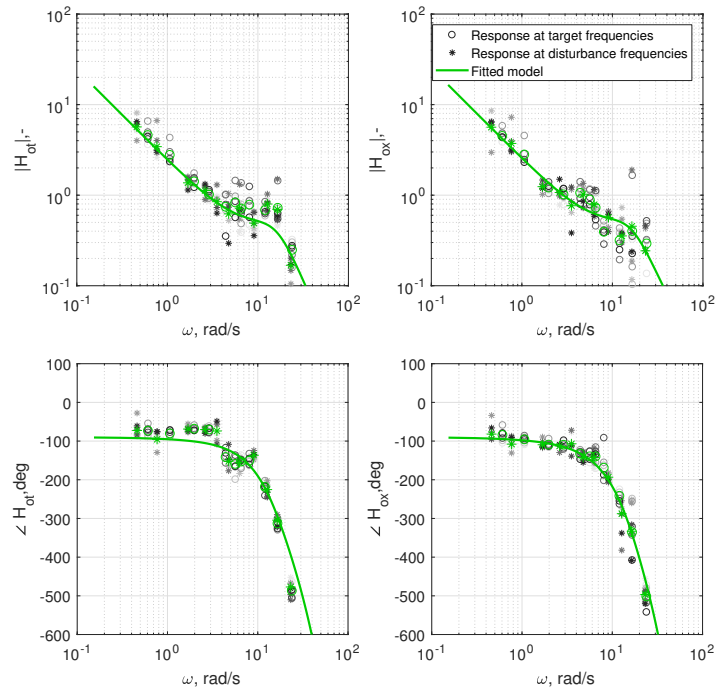


Figure G-1: Patient 1

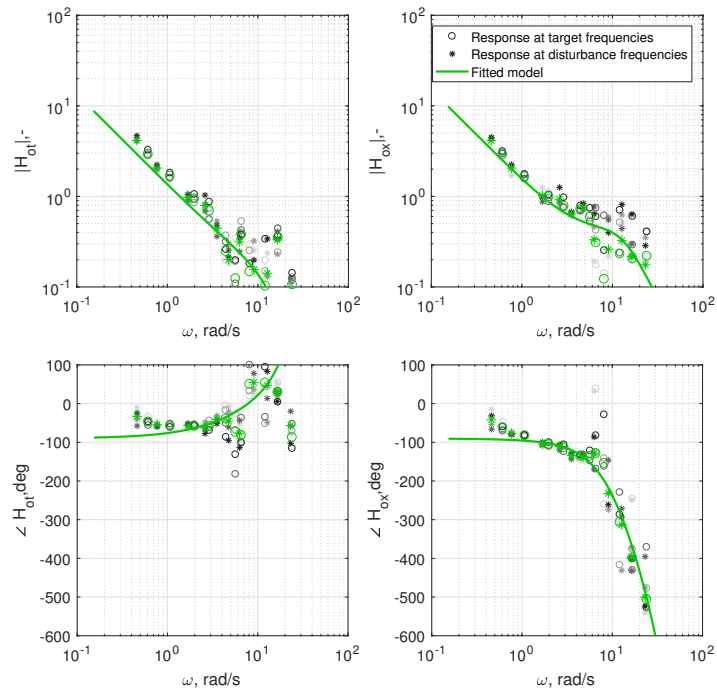


Figure G-2: Patient 2

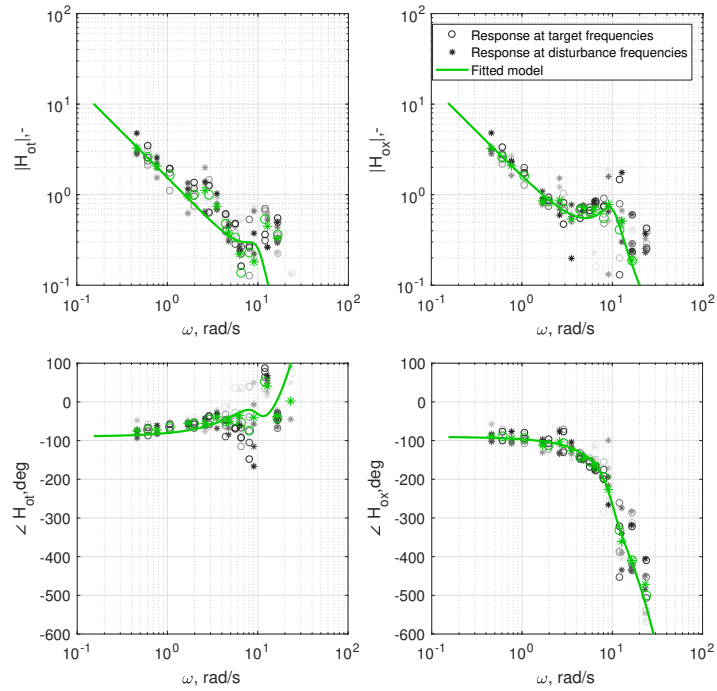


Figure G-3: Patient 3

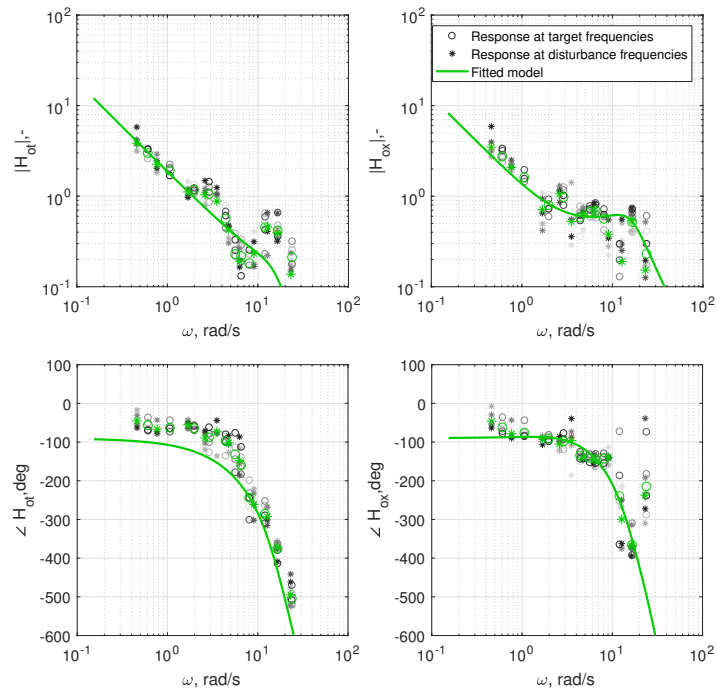


Figure G-4: Patient 4

G-2 Patients unaffected

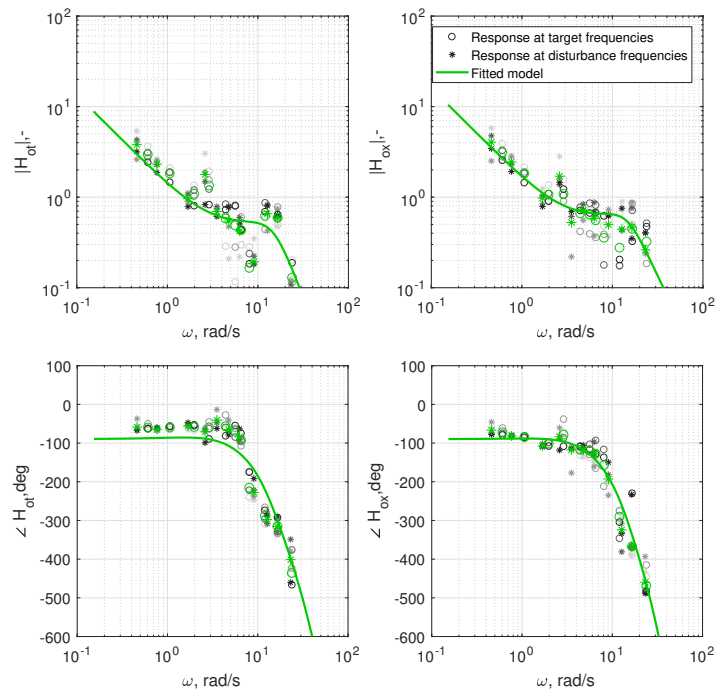


Figure G-5: Patient 2

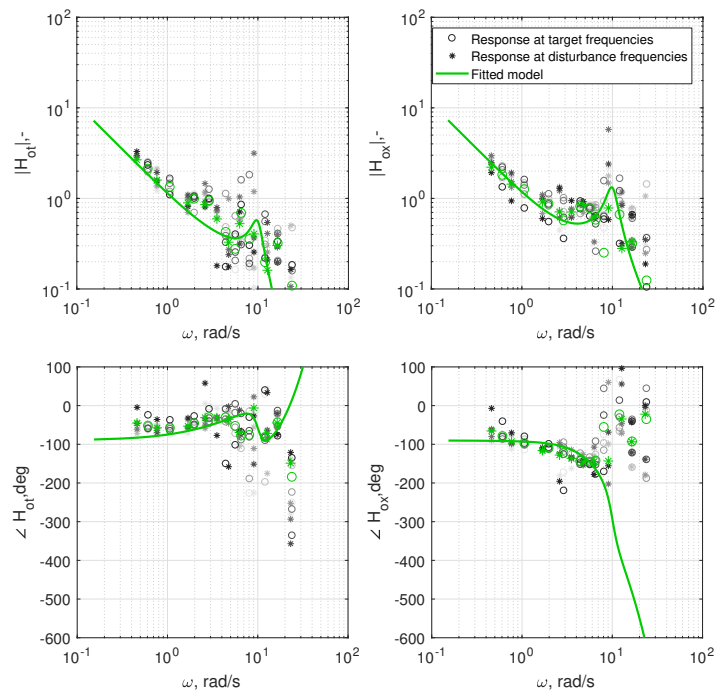


Figure G-6: Patient 3

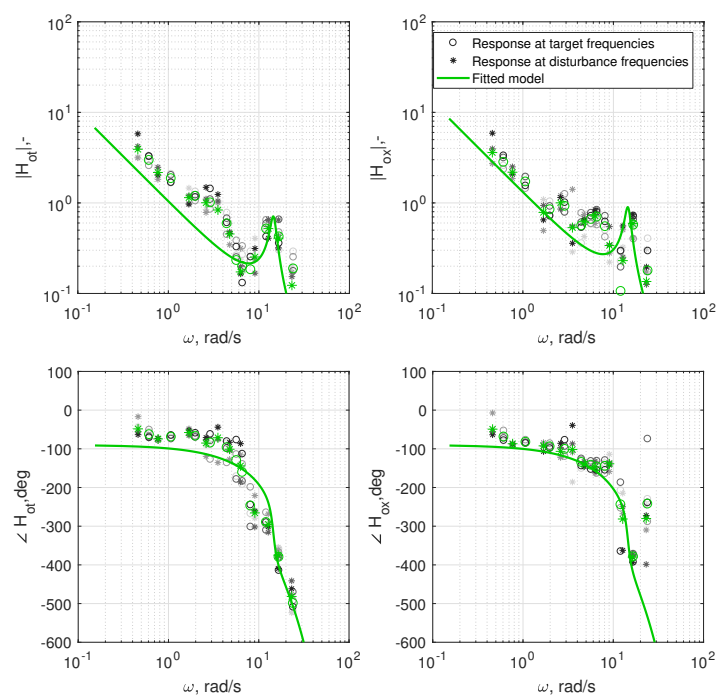


Figure G-7: Patient 4

G-3 Control subjects

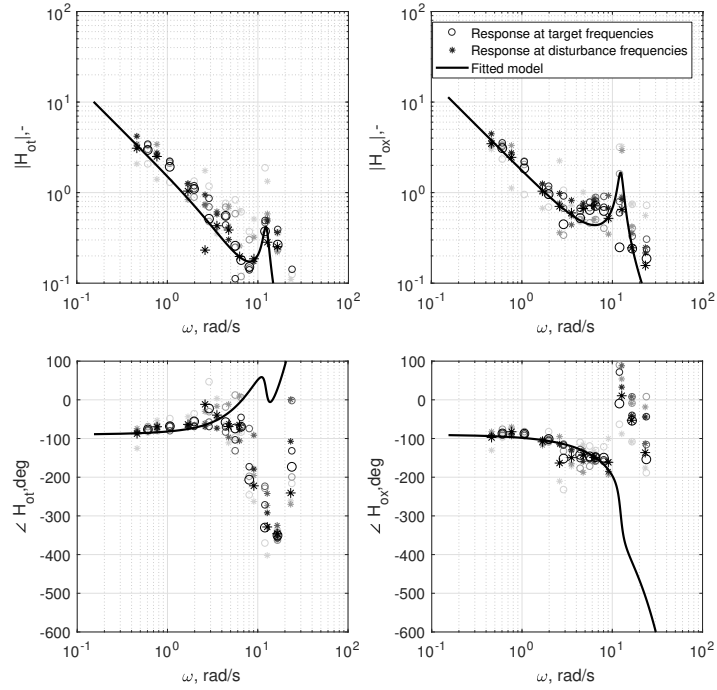


Figure G-8: Control subject 1

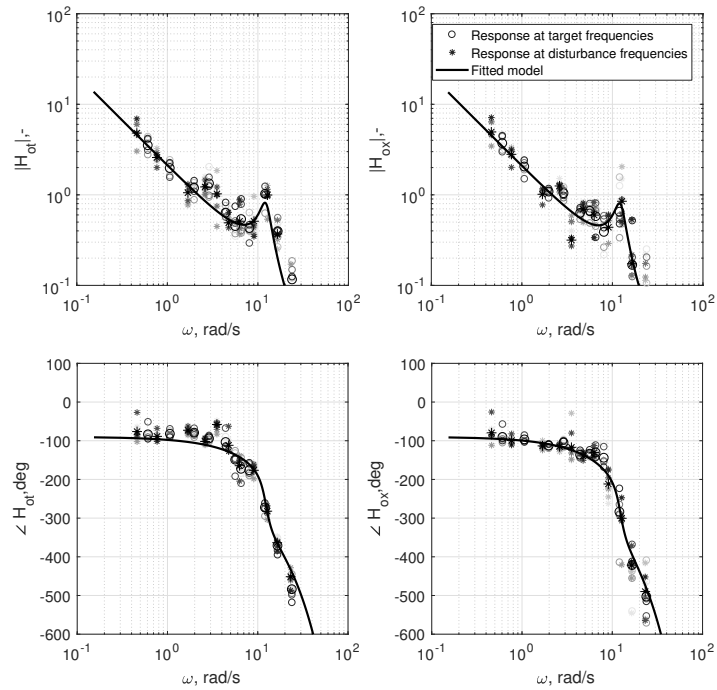


Figure G-9: Control subject 2

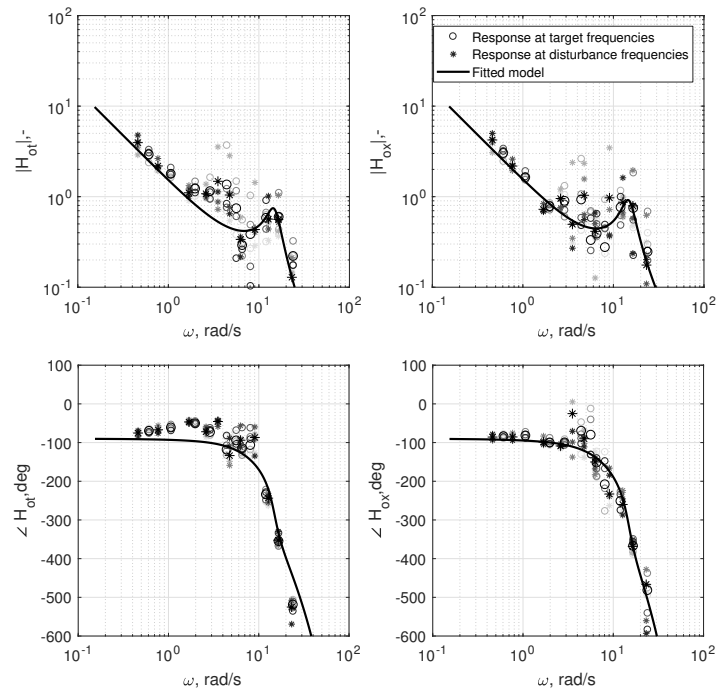


Figure G-10: Control subject 3

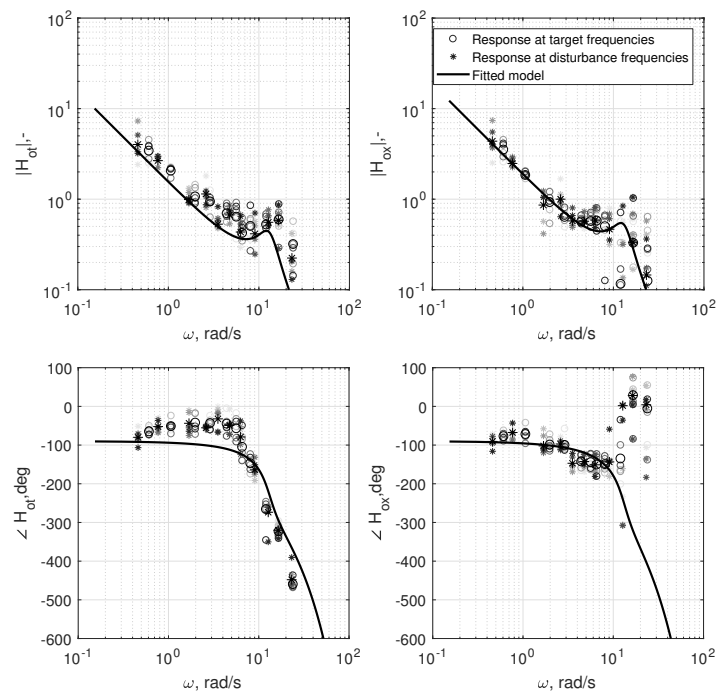


Figure G-11: Control subject 4

G-4 Young adults

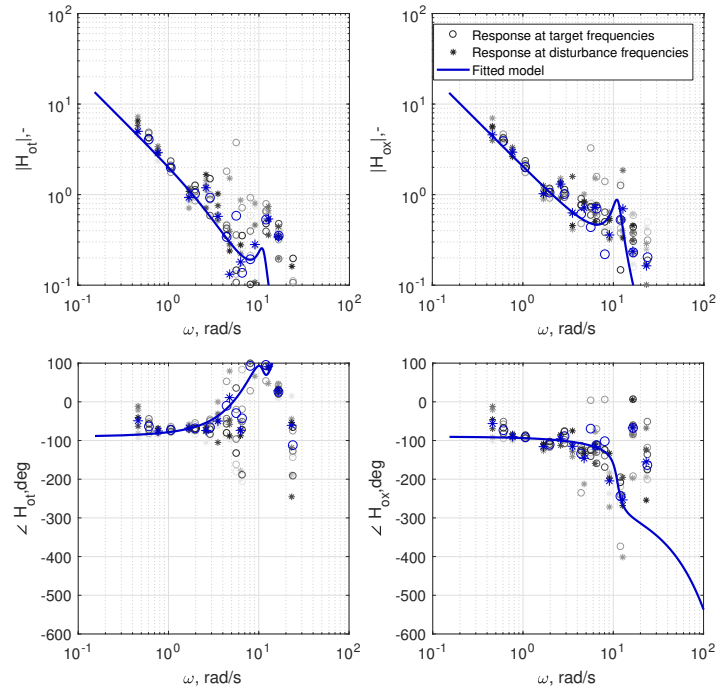


Figure G-12: Young adult 1

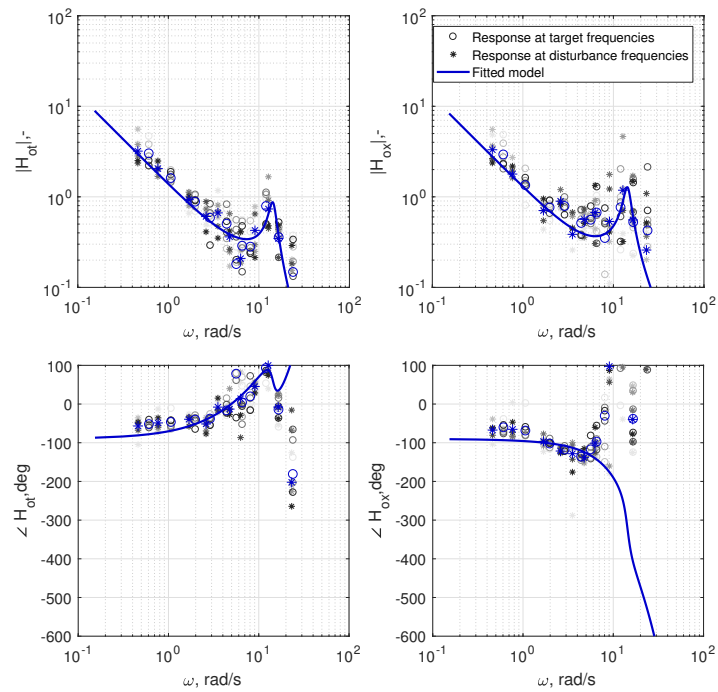


Figure G-13: Young adult 2

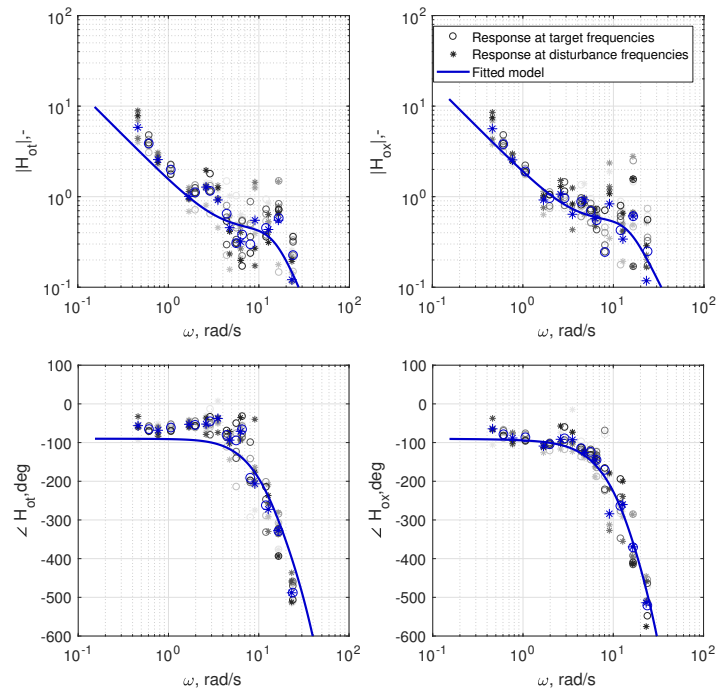


Figure G-14: Young adult 3

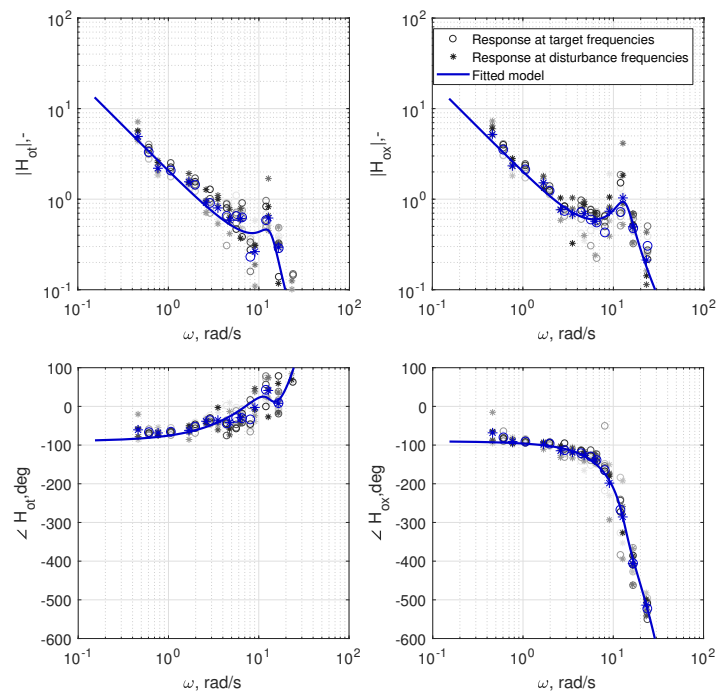


Figure G-15: Young adult 4

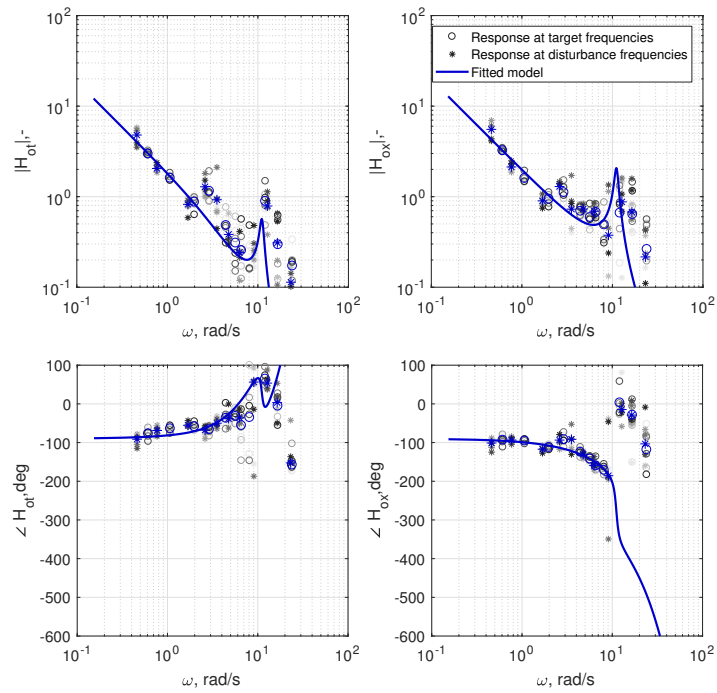


Figure G-16: Young adult 5

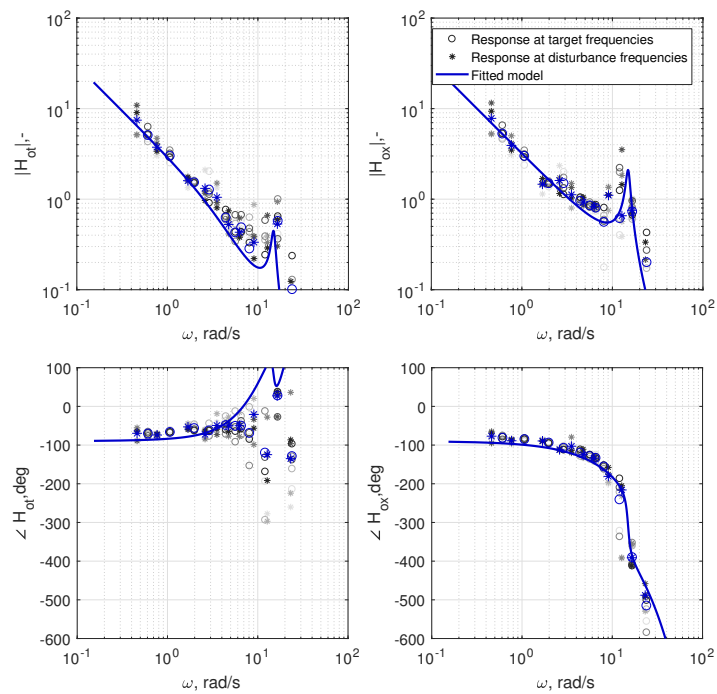


Figure G-17: Young adult 6

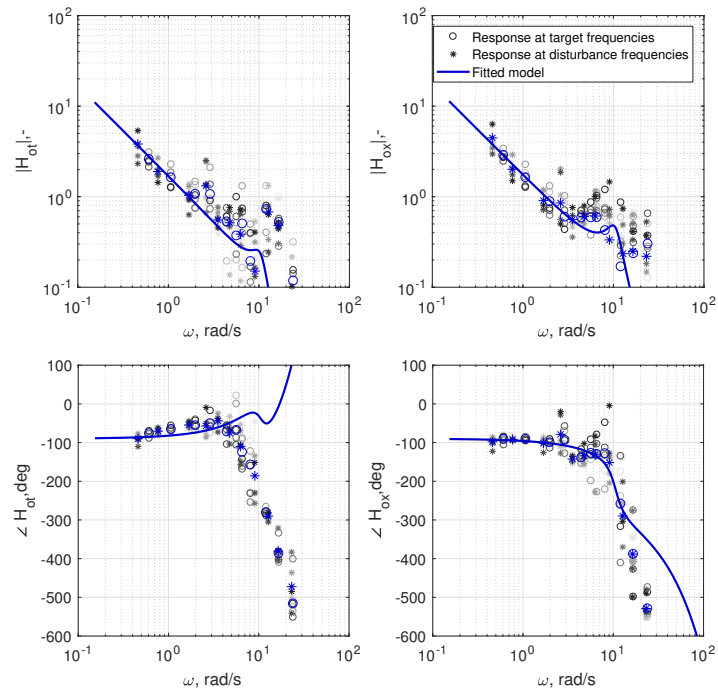


Figure G-18: Young adult 7

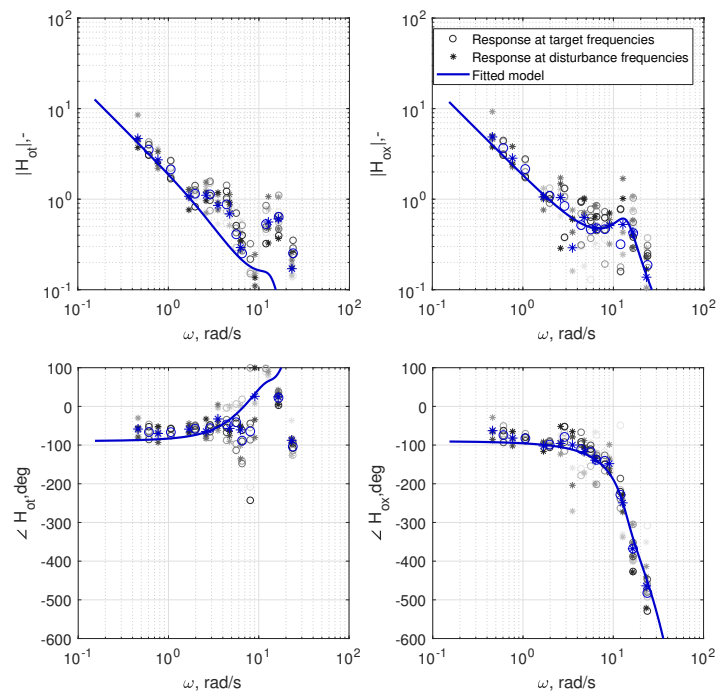


Figure G-19: Young adult 8

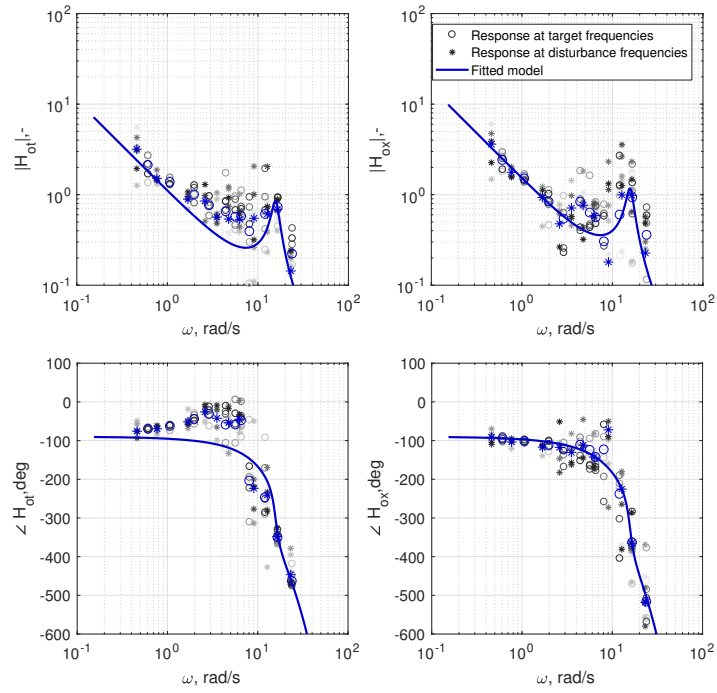


Figure G-20: Young adult 9

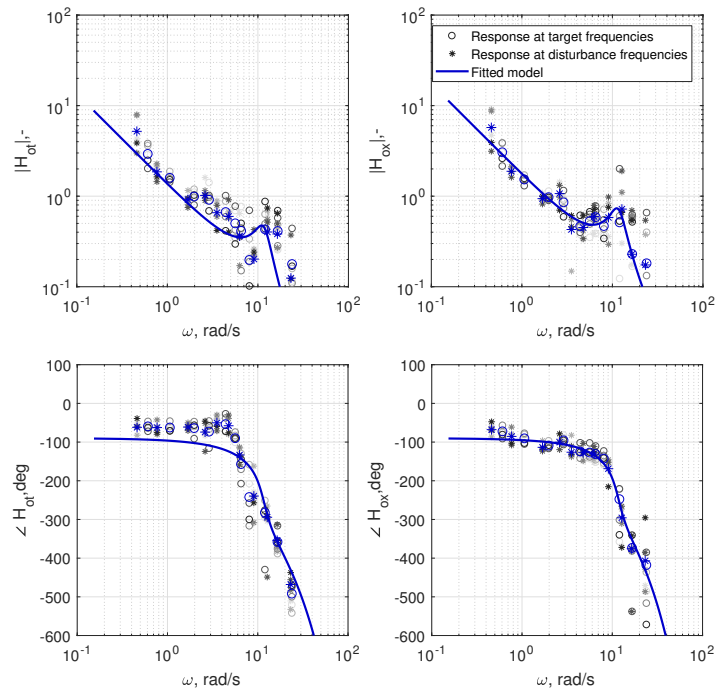


Figure G-21: Young adult 10

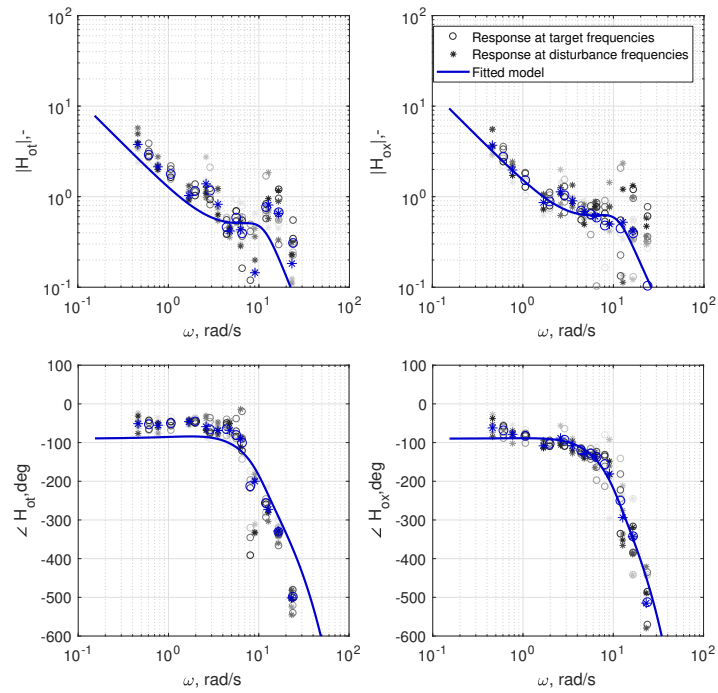


Figure G-22: Young adult 11

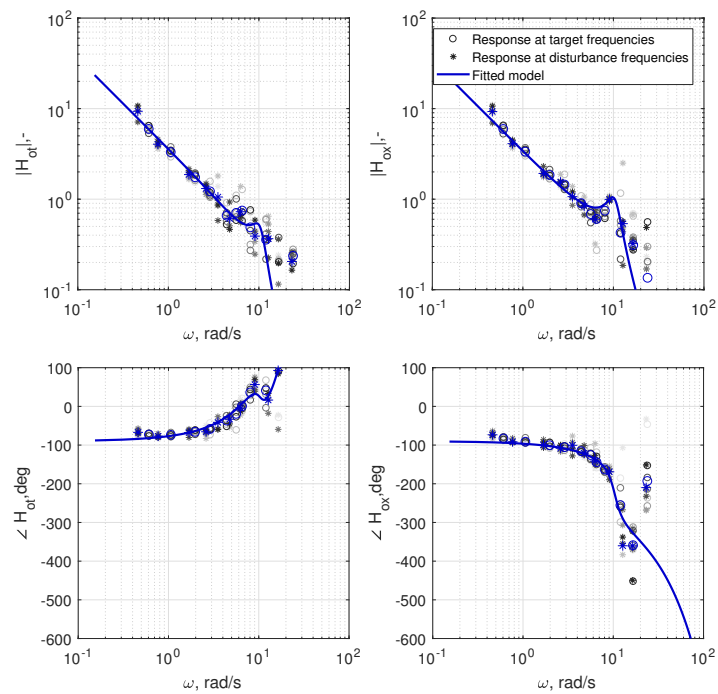


Figure G-23: Young adult 12

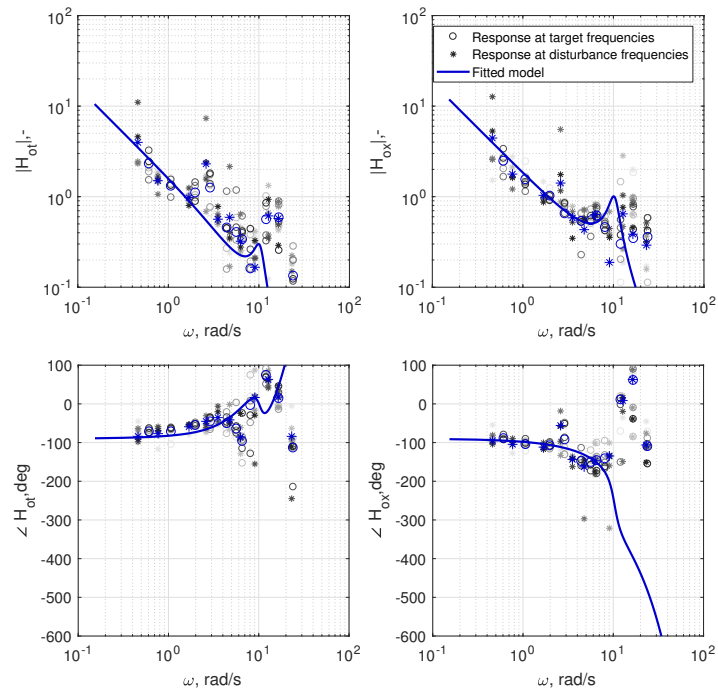


Figure G-24: Young adult 13

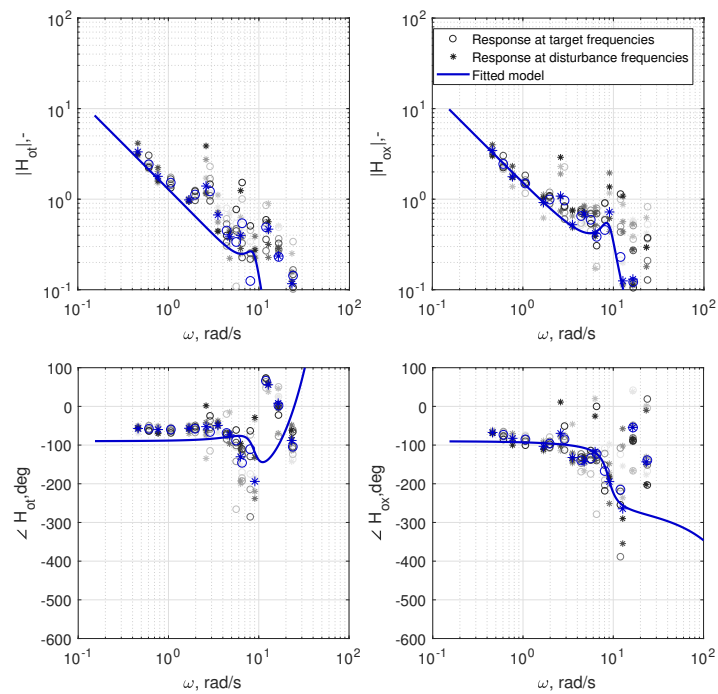


Figure G-25: Young adult 14

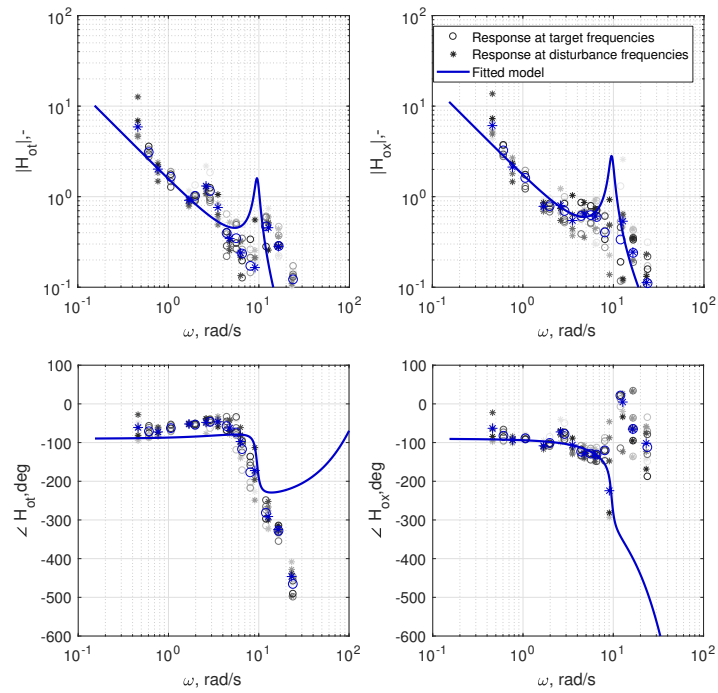


Figure G-26: Young adult 15

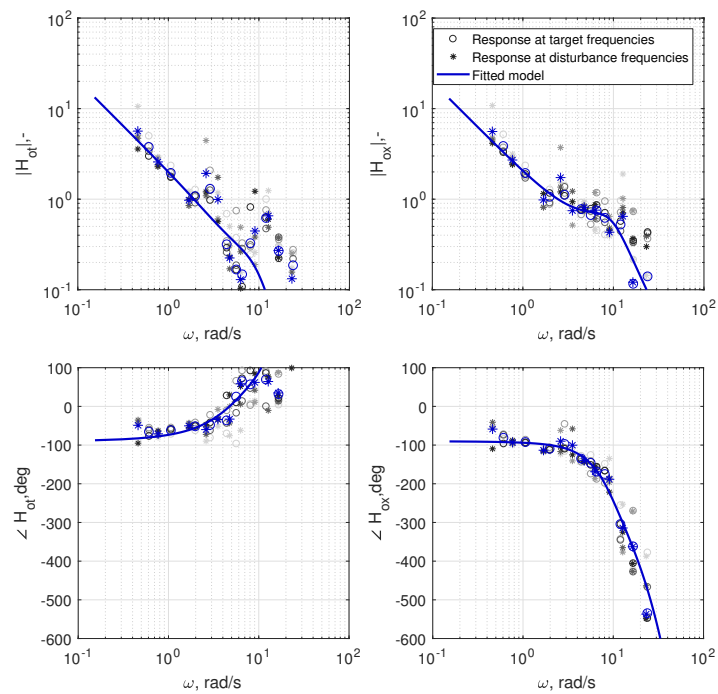


Figure G-27: Young adult 16

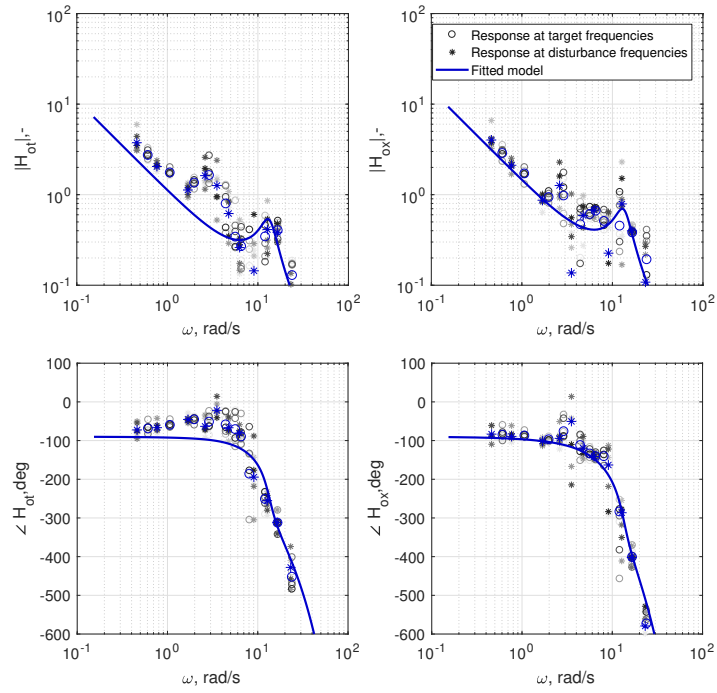


Figure G-28: Young adult 17

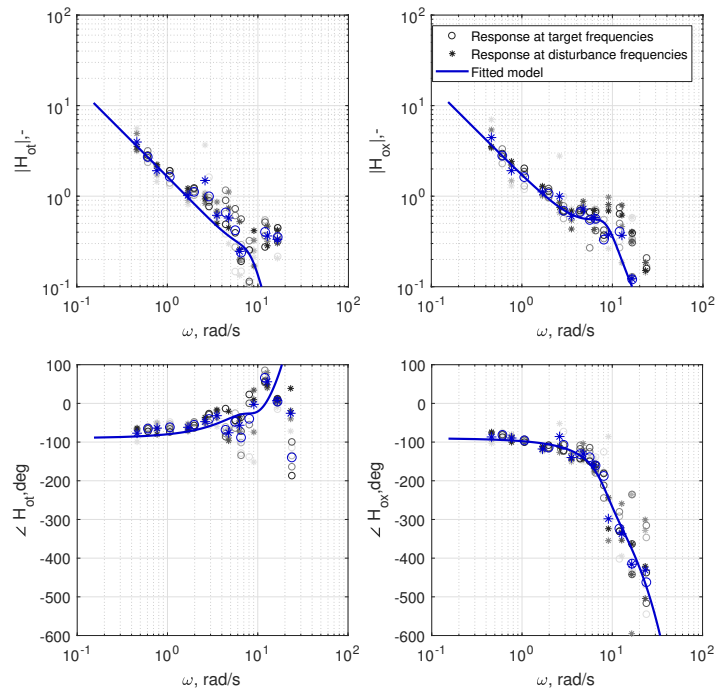


Figure G-29: Young adult 18

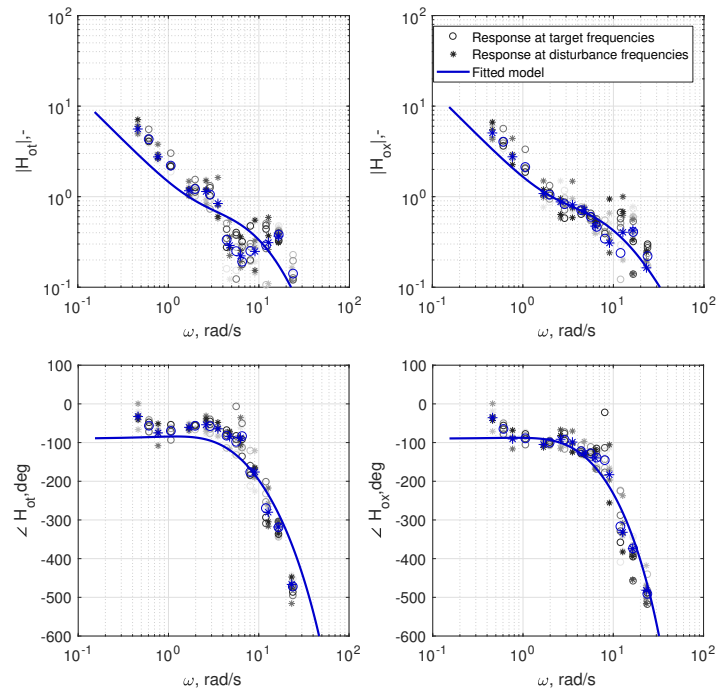


Figure G-30: Young adult 19

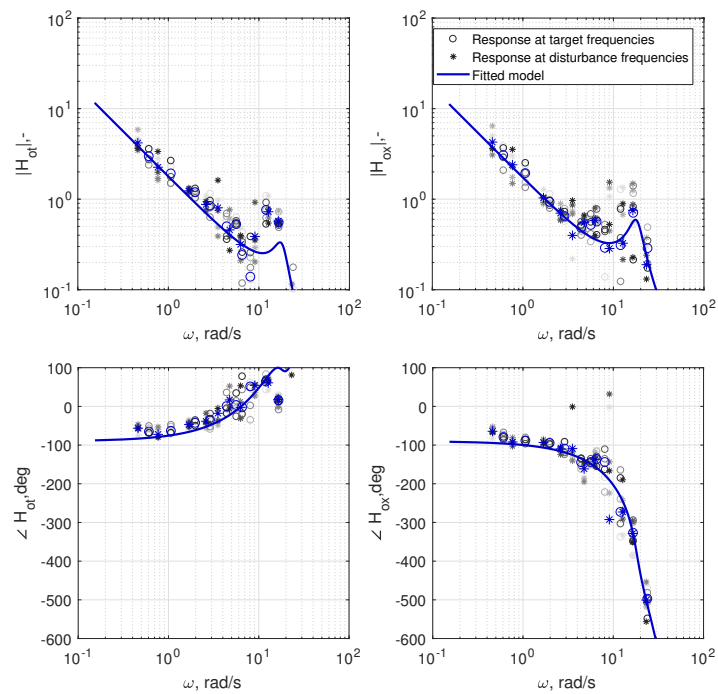


Figure G-31: Young adult 20

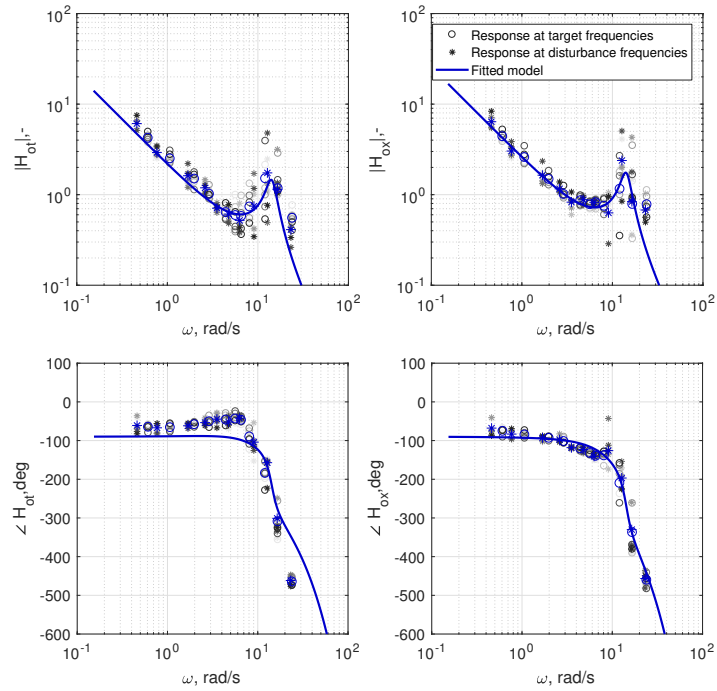


Figure G-32: Young adult 21

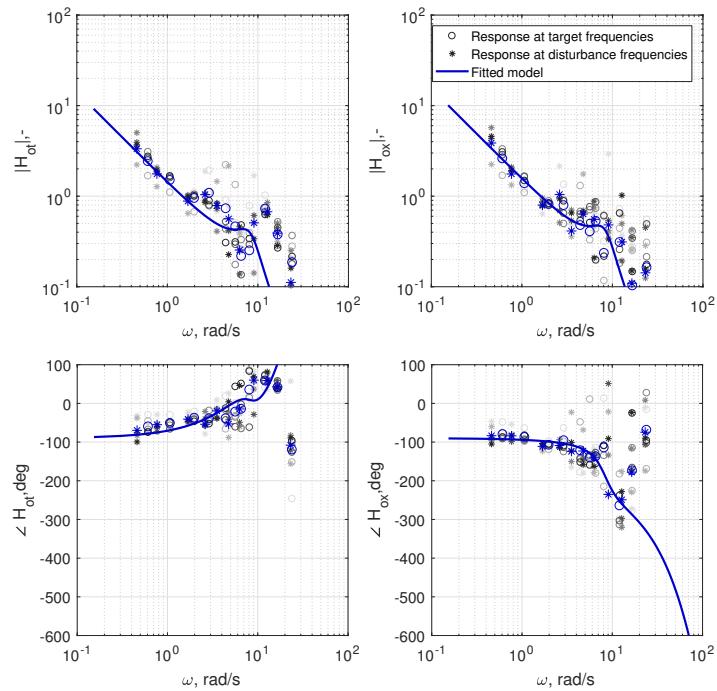


Figure G-33: Young adult 22

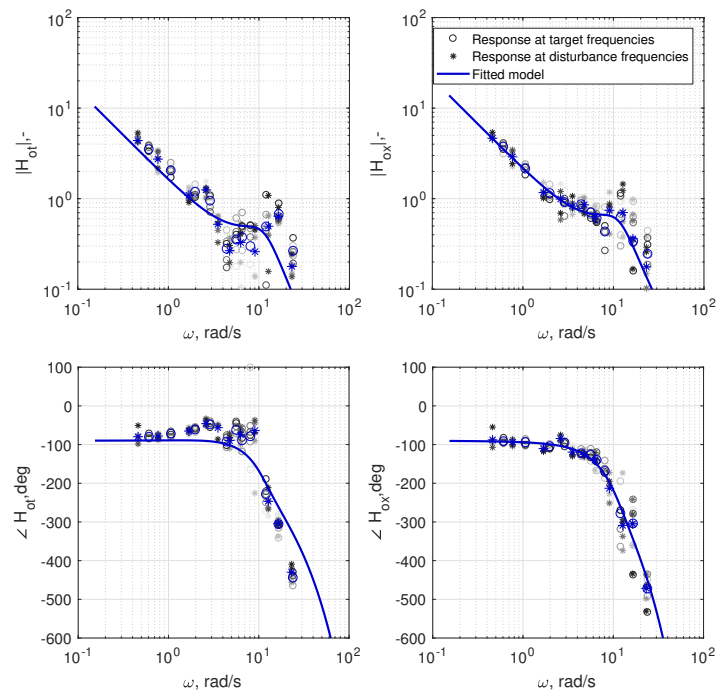


Figure G-34: Young adult 23

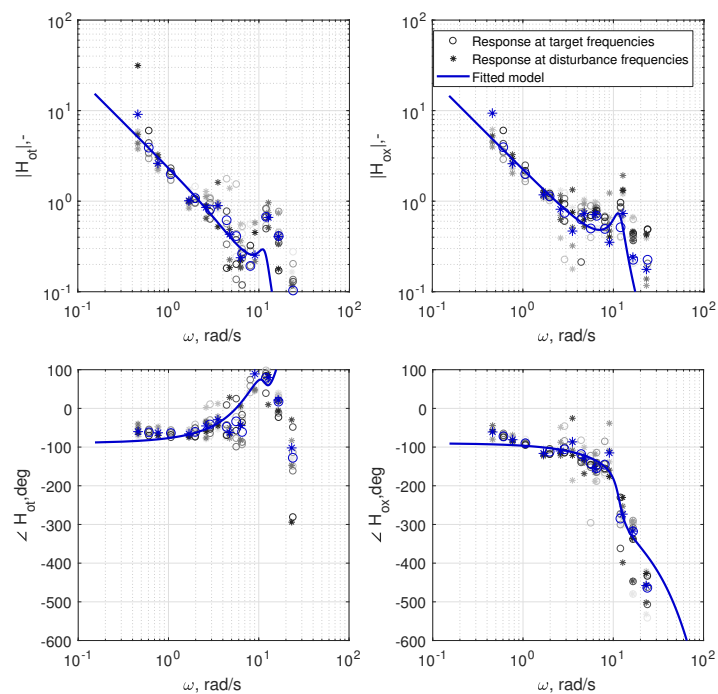


Figure G-35: Young adult 24

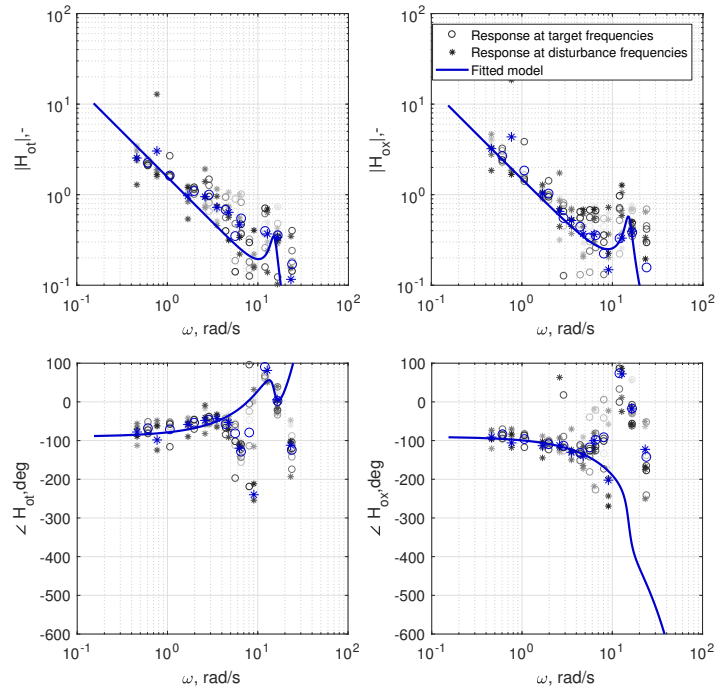


Figure G-36: Young adult 25

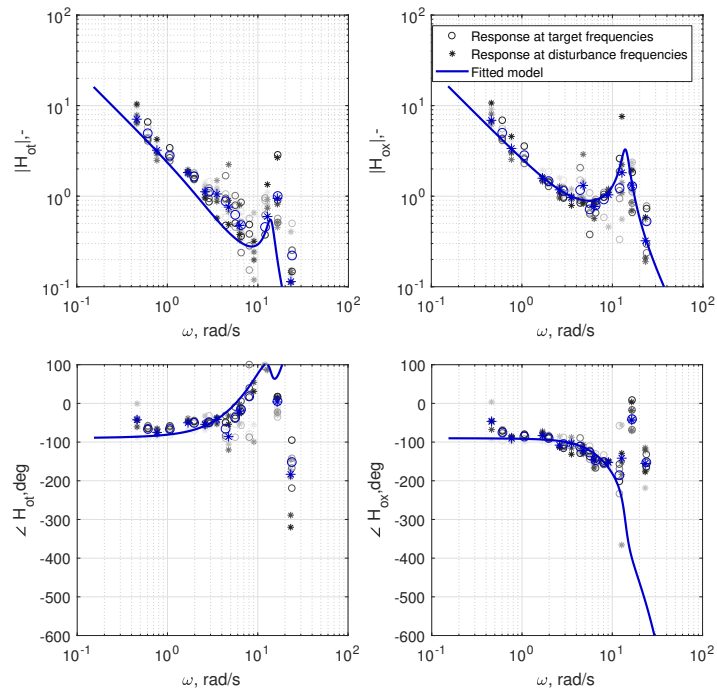


Figure G-37: Young adult 26

Appendix H

Experiment information and consent forms

Patiënteninformatie voor deelname aan het onderzoek:

**Kan het meten van oogbewegingen en handbewegingen leiden tot
meer inzicht over cognitieve problemen bij patiënten met een
cerebellaire beroerte?**

Geachte heer/mevrouw,

Wij vragen u vriendelijk om mee te doen aan een medisch-wetenschappelijk onderzoek (zie titel). U beslist zelf of u wilt meedoen. Voordat u de beslissing neemt, is het belangrijk om meer te weten over het onderzoek. Lees deze informatiebrief rustig door. Bespreek het met partner, vrienden of familie. Ook is er een onafhankelijke persoon, die veel weet van het onderzoek. Lees ook de Algemene brochure. Daar staat veel algemene informatie over medisch-wetenschappelijk onderzoek in. Hebt u na het lezen van de informatie nog vragen? Dan kunt u terecht bij de onderzoeker. Op bladzijden 7 vindt u zijn contactgegevens.

1. Wat is het doel van het onderzoek?

U heeft waarschijnlijk een aantal onderzoeken achter de rug, waarna uw arts u heeft verteld dat u een beroerte in de kleine hersenen heeft gehad. Bij deze ziekte kan het voorkomen dat u al enkele problemen ervaart in het dagelijks leven, maar dat de huidige diagnostiek hier (nog) geen aandacht aan besteedt. Er zijn aanwijzingen dat dit deel van de hersenen een rol spelen in het plannen en organiseren van zaken. Wij willen een methode ontwikkelen, waardoor het in de toekomst mogelijk is dat

subtiële klachten in een later stadium van de aandoening met meer zekerheid herkend kunnen worden.

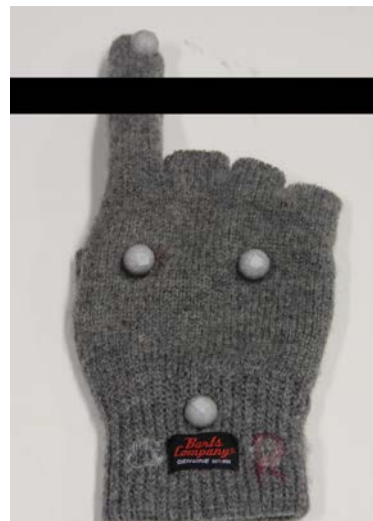
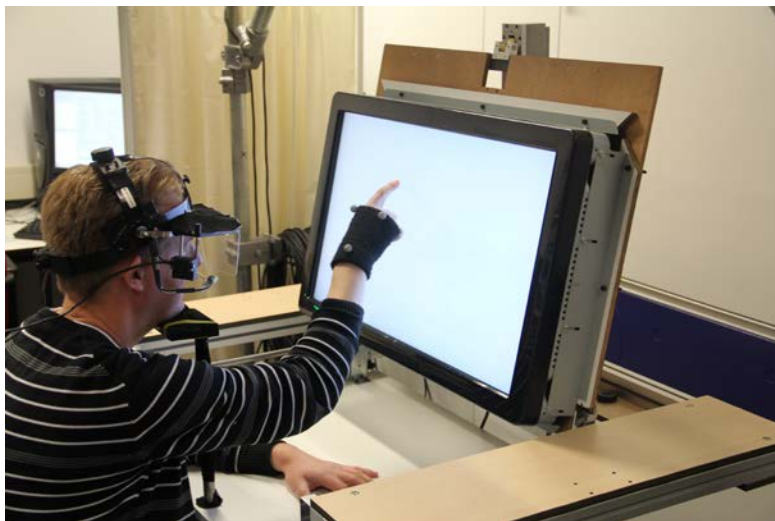
2. Hoe wordt het onderzoek uitgevoerd?

Het onderzoek vindt plaats op de afdeling neurowetenschappen van het Erasmus MC. Wij gaan uw beweeglijkheid, uw oogbewegingen en uw oog-hand coördinatie meten.

Uw beweeglijkheid zullen wij gaan meten met een standaard bewegingsonderzoek (UPDRS). Tijdens dit onderzoek zullen wij testen hoe soepel uw gewrichten zijn en hoe soepel u eenvoudige arm – en beenbewegingen kunt maken.

We meten oogbewegingen en oog-hand coördinatie juist omdat we weten dat de gebieden, die in de hersenen aangetast worden bij een beroerte in de kleine hersenen, deze bewegingen kunnen verstoren.

De oogbewegingen meten we met kleine camera's, welke u op uw hoofd draagt (zie afbeelding 1). Dit is niet zwaar en doet geen pijn. Tijdens het onderzoek plaatst u uw kin bovendien op een steun. Zo worden uw kin en hoofd ondersteund. De bewegingen van uw hand gaan we meten met markers die op een handschoen zijn aangebracht. Een camera kan dan precies registreren welke beweging uw hand maakt. U krijgt dan van ons opdrachten naar welke objecten u moet kijken en welke objecten u aan moet raken. Al met al zullen de testen samen een uur van uw tijd in beslag nemen.



1. De camera op het hoofd en het hoofd steunt op een kinsteun. De handschoen met markers

3. Wat wordt er van u verwacht?

Van u wordt verwacht dat u zo goed mogelijk uw best doet tijdens de testen en zo goed mogelijk de aanwijzingen van de onderzoeker opvolgt. Daarnaast wordt er van u verwacht dat u naar het Erasmus MC komt, wij kunnen niet bij u thuis meten.

Ook willen wij u vragen om uw partner, broer, zus, een vriend of een kennis te vragen om ook deel te nemen aan dit onderzoek. Wij zoeken namelijk ook nog gezonde ouderen van 50 jaar en ouder om als controlepersoon aan het onderzoek mee te doen. Het meebrengen van een controlepersoon voor het onderzoek is geheel vrijwillig.

4. Wat zijn mogelijke voor - en nadelen van deelname aan dit onderzoek?

Er zijn voor u geen directe voordelen van dit onderzoek te verwachten. U helpt wel mee om in de toekomst een betere diagnose te kunnen stellen. Meedoen aan het onderzoek brengt géén risico voor uw gezondheid met zich mee.

Een nadeel van het onderzoek is dat er van u een kleine tijdsinvestering wordt verwacht. Het onderzoek duurt ongeveer een uur per persoon. Om de belasting voor u zo minimaal mogelijk te houden streven wij ernaar om het onderzoek te combineren met een (poli)klinische afspraak die u al heeft bij het Erasmus MC.

5. Wat gebeurt er als u niet wenst deel te nemen aan dit onderzoek?

U beslist zelf of u meedoet aan het onderzoek. Deelname is vrijwillig. Als u besluit niet mee te doen, hoeft u verder niets te doen. U hoeft niets te tekenen. U hoeft ook niet te zeggen waarom u niet wilt meedoen. Als u patiënt bent, krijgt u gewoon de behandeling die u anders ook zou krijgen. Als u wel meedoet, kunt u zich altijd bedenken en toch stoppen. Ook tijdens het onderzoek.

Binnen 2 weken na het ontvangen van deze brief zullen wij telefonisch contact met u opnemen om te vragen of u mee wilt doen of dat u dit niet wilt, waarna wij uw gegevens uit ons bestand zullen halen.

6. Wat gebeurt er als het onderzoek is afgelopen?

Uw gegevens worden gecodeerd verwerkt en na het onderzoek zullen uw adresgegevens uit ons bestand gehaald worden.

7. Bent u verzekerd wanneer u aan het onderzoek meedoet?

De toetsende commissie heeft ontheffing verleend van de verplichting een verzekering af te sluiten voor de deelnemers aan dit onderzoek, omdat zij van mening is dat dit onderzoek weinig of geen risico met zich meebrengt.

8. Wat gebeurt er met uw gegevens?

In de algemene brochure is uitgelegd dat de onderzoeker gegevens over u verzamelt en deze vertrouwelijk behandelt. Dit betekent dat een aantal personen uw medische status en de gegevens van het onderzoek mogen inzien. Deze personen mogen de gegevens gebruiken voor dit onderzoek, maar zij mogen deze gegevens alleen bekend maken zonder daarbij uw naam of andere persoonlijke gegevens te vermelden. Uw identiteit blijft dus altijd geheim. De onderzoeker bewaart de gegevens met een code. Dit betekent dat op de studie- documenten in plaats van uw naam enkel een letter-cijfercode staat. Alleen de onderzoeker houdt een lijst bij waarop staat welke letter- cijfercode bij welke naam hoort.

Normaal gesproken heeft alleen uw behandelend arts en zijn/ haar team inzage in uw gegevens. Als u meedoet aan deze studie krijgen meer mensen inzage in uw medische gegevens en studiegegevens. De personen die inzage kunnen krijgen in uw gegevens zijn:

- de medewerkers van het onderzoeksteam,
- de leden van de toetsingscommissie die de studie heeft goedgekeurd,
- de bevoegde medewerkers van de Inspectie voor de Gezondheidszorg.

Na de studie worden de gecodeerde gegevens gedurende 15 jaar bewaard. Dit is nodig om alles goed te kunnen controleren. Bovendien willen wij graag uw gegevens gebruiken voor andere onderzoeken die worden uitgevoerd naar verschillende vormen van Parkinsonisme. Deze onderzoeken hebben dus eenzelfde doel als het onderzoek waarvoor u nu wordt gevraagd. Het is dus niet zo dat uw gegevens ook zullen worden gebruikt voor onderzoek naar een geheel andere aandoening of een heel ander probleem. Vanzelfsprekend blijft de vertrouwelijkheid die we hierboven hebben beschreven altijd gelden. Vindt u het goed als wij uw

gegevens bewaren en gebruiken? Als u dat niet wilt, respecteren wij dat natuurlijk. U kunt uw keuze op het toestemmingsformulier aangeven.

Mogelijk willen we u in de toekomst opnieuw benaderen voor vervolgonderzoek. Op het toestemmingsformulier kunt u aangeven of u dit goed vindt.

9. Zijn er extra kosten / is er een vergoeding wanneer u besluit aan dit onderzoek mee te doen?

Wanneer u besluit mee te doen aan dit onderzoek en wij slagen erin om het onderzoek te combineren met een (poli)klinische afspraak die u al heeft op het Erasmus MC heeft u geen recht op vergoeding. Wanneer u apart naar het Erasmus MC komt voor dit onderzoek heeft u recht op vergoeding van uw parkeerkosten.

10. Welke medisch-ethische toetsingscommissie heeft dit onderzoek goedgekeurd?

De Medisch Ethische Toetsings Commissie Erasmus MC heeft dit onderzoek goedgekeurd. Meer informatie over de goedkeuring vindt u in de algemene brochure.

11. Wilt u nog iets weten?

Indien u tijdens de studie vragen of klachten heeft, vragen wij u contact op te nemen met een van de onderstaande onderzoekers of uw behandelend arts. U kunt voor vragen of klachten tijdens kantooruren contact opnemen met de volgende personen:

Dr. Hans van der Steen

Hoofdonderzoeker

Vestibulaire en oculomotorische onderzoeksgroep

Afdeling Neurowetenschappen, Erasmus MC

(tel) 010-7043572

Dr. Ir. Johan Pel

Onderzoeker

Afdeling Neurowetenschappen, Erasmus MC

(tel) 010-7043385

Buiten kantooruren of bij noodgevallen (24 uur bereikbaar wanneer nodig) kunt u contact opnemen met de volgende personen:

Dr. Ir. Johan Pel

Onderzoeker

Afdeling Neurowetenschappen, Erasmus MC

(tel) 06-28674609

Indien u twijfelt over deelname kunt u een onafhankelijke arts raadplegen, die zelf niet bij het onderzoek betrokken is, maar die wel deskundig is op het gebied van dit onderzoek en uw ziekte. Ook als u voor of tijdens de studie vragen heeft die u liever niet aan de onderzoekers stelt, kunt u contact opnemen met de onafhankelijke arts.

De onafhankelijke arts is:

Dr. J.W.M. Krulder, geriater in het Vlietland ziekenhuis te Schiedam.
Telefonisch bereikbaar op 010-8935316.

Als u niet tevreden bent over het onderzoek of de behandeling kunt u terecht bij de onafhankelijke klachtencommissie van het Erasmus MC. De klachtencommissie is te bereiken op telefoonnummer 010-7033198.

Met vriendelijke groeten,

Het onderzoeksteam

12. Bijlagen:

- Algemene brochure medisch – wetenschappelijk onderzoek met mensen (ontvangt u apart bij deze informatiebrief).
- Toestemmingsformulier.
- Toestemmingsformulier video.

Toestemmingsformulier voor deelname aan het onderzoek:

**Kan het meten van oogbewegingen en handbewegingen leiden tot
meer inzicht over cognitieve problemen bij patienten met een
cerebellaire beroerte?**

Ik heb de informatiebrief voor de proefpersoon gelezen. Ik kon aanvullende vragen stellen. Mijn vragen zijn genoeg beantwoord. Ik had genoeg tijd om te beslissen of ik meedoe.

Ik weet dat meedoen helemaal vrijwillig is. Ik weet dat ik op ieder moment kan beslissen om toch niet mee te doen. Daarvoor hoef ik geen reden te geven.

Ik weet dat sommige mensen mijn gegevens kunnen zien. Die mensen staan vermeld in de Algemene brochure.

Ik geef toestemming om mijn gegevens te gebruiken, voor de doelen die in de informatiebrief staan.

Ik geef toestemming om mijn gegevens 15 jaar na afloop van dit onderzoek te bewaren.

Ik geef wel/geen* toestemming om mijn gegevens 15 jaar na afloop van dit onderzoek te bewaren, zodat deze in de toekomst misschien gebruikt kunnen worden voor onderzoek met eenzelfde onderzoeksdoel.

Ik geef wel/geen* toestemming om mij in de toekomst opnieuw te benaderen voor vervolgonderzoek.

Ik vind het goed om aan dit onderzoek mee te doen.

Naam proefpersoon:

Handtekening:

Datum: __ / __ / __

Ik verklaar hierbij dat ik deze proefpersoon volledig heb geïnformeerd over het genoemde onderzoek.

Als er tijdens het onderzoek informatie bekend wordt die de toestemming van de proefpersoon zou kunnen beïnvloeden, dan breng ik hem/haar daarvan tijdig op de hoogte.

Naam onderzoeker (of diens vertegenwoordiger):

Handtekening:

Datum: __ / __ / __

* Doorhalen wat niet van toepassing is.

Toestemmingsformulier videoopname tijdens bewegingsonderzoek:

**Kan het meten van oogbewegingen en handbewegingen leiden tot
meer inzicht over cognitieve problemen bij patienten met een
cerebellaire beroerte?**

Ik geef wel/geen* toestemming om videobeelden te maken van het bewegingsonderzoek (UPDRS) zoals dit staat beschreven in de informatiefolder.

Ik geef wel/geen* toestemming om de gegevens van deze videobeelden te verwerken voor de doeleinden van het onderzoek.

Ik geef wel/geen* toestemming om mijn gegevens van de videobeelden gedurende maximaal 15 jaar na afloop van het onderzoek te bewaren.

Naam proefpersoon:

Handtekening:

Datum: __ / __ / __

Naam onderzoeker (of diens vertegenwoordiger):

Handtekening:

Datum: __ / __ / __

* Doorhalen wat niet van toepassing is.

Bibliography

- [1] J. L. Vercher and G. M. Gauthier, “Cerebellar involvement in the coordination control of the oculo-manual tracking system: effects of cerebellar dentate nucleus lesion,” *Experimental brain research*, vol. 73, pp. 155–166, 1988.
- [2] P. Trouillas, T. Takayanagi, M. Hallett, R. Currier, S. Subramony, K. Wessel, A. Bryer, H. Diener, S. Massaquoi, C. Gomez, P. Coutinho, M. Ben Hamida, G. Campanella, L. Filla, A. Schut, D. Timann, J. Honnorat, N. Nighoghossian, and B. Manyam, “International Cooperative Ataxia Rating Scale for pharmacological assessment of the cerebellar syndrome,” *Journal of the Neurological Sciences*, vol. 145, no. 2, pp. 205–211, 1997.
- [3] D. M. Pool, R. J. de Vries, and J. J. M. Pel, “Quantifying Loss of Motor Skills in Parkinson’s Disease Using Human Controller Modeling.” 2017.
- [4] R. de Vries, “Using Human Operator Modeling for Quantifying Loss of Motor Skills due to Parkinson’s Disease,” Master’s thesis, Delft University of Technology, 2016.
- [5] R. Jones and I. Donaldson, “Tracking tasks and the study of predictive motor planning in Parkinson’s disease,” in *Engineering in Medicine and Biology Society*, no. 11, pp. 1055–1056, 1989.
- [6] K. Ito and M. Ito, “Tracking Behaviors of the Human Operator in Preview Control Systems,” *Electrical Engineering in Japan (Translated from Dedd Cakkai Ronbunshi)*, vol. 95, no. 1, pp. 120–127, 1975.
- [7] M. Tomizuka and D. E. Whitney, “The human operator in manual preview tracking (an experiment and its modeling via optimal control),” *Journal of Dynamic Systems, Measurement, and Control*, vol. 98, pp. 407–413, 1976.
- [8] R. A. Hess and A. Modjtahedzadeh, “A preview control model of driver steering behavior,” *Systems, Man and Cybernetics*, pp. 504–509, 1989.
- [9] K. van der El, D. M. Pool, H. J. Damveld, M. M. van Paassen, and M. Mulder, “An Empirical Human Controller Model for Preview Tracking Tasks,” *IEEE Transactions on Cybernetics*, pp. 1–13, 2015.

- [10] J. Knierim, "Neuroscience online."
- [11] E. R. Kandel, *Principles of Neural Science*. McGraw-Hill, 5th ed., 2013.
- [12] J. R. Leigh and D. S. Zee, *The neurology of eye movements*. New York: Oxford University Press, 3rd ed., 1999.
- [13] R. C. Miall, D. J. Weir, and J. F. Stein, "Visuo-motor tracking during reversible inactivation of the cerebellum.," *Experimental brain research*, vol. 65, pp. 455–464, 1987.
- [14] K. Ito, "Neurophysiological aspects of the cerebellar motor control system," *International journal of neurology*, vol. 7, no. 2, pp. 162–176, 1970.
- [15] M. Kawato, K. Furukawa, and R. Suzuki, "A hierarchical neural-network model for control and learning of voluntary movement," *Biological Cybernetics*, vol. 57, no. 3, pp. 169–185, 1987.
- [16] D. M. Wolpert and M. Kawato, "Multiple paired forward and inverse models for motor control," *Neural Networks*, vol. 11, no. 7-8, pp. 1317–1329, 1998.
- [17] M. Haruno, D. M. Wolpert, and M. Kawato, "Mosaic model for sensorimotor learning and control.," *Neural computation*, vol. 13, no. 10, pp. 2201–20, 2001.
- [18] C. M. Fredericks, *Disorders of the cerebellum and its connections*. 1996.
- [19] K. C. Engel, J. H. Anderson, C. M. Gomez, and J. F. Soechting, "Deficits in ocular and manual tracking due to episodic ataxia type 2," *Movement Disorders*, vol. 19, no. 7, pp. 778–787, 2004.
- [20] D. Purves and R. Cabeza, *Cognitive Neuroscience*. Sunderland: Sinauer Associates, INc., 2nd ed., 2013.
- [21] C. de Boer, J. van der Steen, F. Mattace-Raso, A. J. Boon, and J. J. M. Pel, "The Effect of Neurodegeneration on Visuomotor Behavior in Alzheimer's Disease and Parkinson's Disease.," *Motor control*, vol. 20, no. 1, pp. 1–20, 2016.
- [22] G. Beusmans and H. G. C. Van Noortwijk-Bonga, "NHG-Standaard Beroerte," 2013.
- [23] Z. Nasreddine, N. Phillips, V. Bédirian, S. Charbonneau, V. Whitehead, I. Collin, J. Cummings, and H. Chertkow, "The Montreal Cognitive Assessment, MoCA: a brief screening tool for mild cognitive impairment," *Journal of the American Geriatrics Society*, vol. 53, no. 4, pp. 695–699, 2005.
- [24] D. T. McRuer, D. Graham, E. S. Krendel, and W. J. Weisener, "Human Pilot Dynamics in Compensatory Systems, theory, models and experiments with controlled element and forcing function variations," tech. rep., Air Force Flight Dynamics Laboratory (OH), Wright-Patterson Air Force Base (OH), 1965.
- [25] D. T. McRuer and H. R. Jex, "A Review of Quasi-Linear Pilot Models," *Human Factors in Electronics, IEEE Transactions on*, vol. HFE-8, no. 3, pp. 231–249, 1967.

-
- [26] R. J. Wasicko, D. T. McRuer, and R. E. Magdaleno, "Human Pilot Dynamic Response in Single-loop Systems with Compensatory and Pursuit Displays," tech. rep., Air Force Flight Dynamics Laboratory, 1966.
- [27] L. D. Reid and N. H. Drewell, "A pilot model for tracking with preview," in *Proc. 8th Annu. Conf. Manual Control*, pp. 191–204, 1972.
- [28] M. M. van Paassen and M. Mulder, "Identification of human operator control behaviour in multiple-loop tracking tasks," in *Proc. 7th IFAC/IFIP/IFORS/IEA Symp. Anal. Design Eval. Man Mach. Syst.*, (Kyoto, Japan), pp. 515–520, 1998.
- [29] S. Verheij, D. Muilwijk, J. J. M. Pel, T. J. M. Van Der Cammen, F. U. S. Mattace-Raso, and J. Van Der Steen, "Visuomotor impairment in early-stage alzheimer's disease: Changes in relative timing of eye and hand movements," *Journal of Alzheimer's Disease*, vol. 30, no. 1, pp. 131–143, 2012.
- [30] D. Muilwijk, S. Verheij, J. J. M. Pel, A. J. Boon, and J. van der Steen, "Changes in Timing and kinematics of goal directed eye-hand movements in early-stage Parkinson's disease.," *Translational neurodegeneration*, vol. 2, no. 1, p. 1, 2013.
- [31] C. De Boer, J. Van der Steen, R. J. Schol, and J. J. M. Pel, "Repeatability of the timing of eye-hand coordinated movements across different cognitive tasks," *Journal of Neuroscience Methods*, vol. 218, no. 1, pp. 131–138, 2013.
- [32] K. Flowers, "Lack of prediction in the motor behaviour of parkinsonism," *Brain*, vol. 101, pp. 35–52, 1978.
- [33] J. D. Cooke, J. D. Brown, and V. B. Brooks, "Increased dependence on visual information for arm movement in patients with Parkinson's disease," *Extrapyramidal System and its Disorders*, vol. 24, no. 4, pp. 185–189, 1979.
- [34] H. Beppu, M. Suda, and R. Tanaka, "Analysis of Cerebellar Motor Disorders By Visually Guided Elbow Tracking Movement," *Brain*, vol. 107, pp. 787–809, 1984.
- [35] R. D. Jones and I. M. Donaldson, "Measurement of integrated sensory-motor function following brain damage by a computerized preview tracking task.," *International rehabilitation medicine*, vol. 3, no. 2, pp. 71–83, 1981.
- [36] B. L. Day, J. P. R. Dick, and C. D. Marsden, "Patients with Parkinson's disease can employ a predictive motor strategy.," *Journal of neurology, neurosurgery, and psychiatry*, vol. 47, no. 12, pp. 1299–1306, 1984.
- [37] R. D. Jones and I. M. Donaldson, "Measurement of sensory-motor integrated function in neurological disorders: three computerised tracking tasks.," *Medical & biological engineering & computing*, vol. 24, no. 5, pp. 536–540, 1986.
- [38] B. L. Morrice, W. J. Becker, J. A. Hoffer, and R. G. Lee, "Manual tracking performance in patients with cerebellar incoordination: effects of mechanical loading," *Can J Neurol Sci*, vol. 17, no. 3, pp. 275–285, 1990.

- [39] P. van Donkelaar and R. G. Lee, "Interactions between the eye and hand motor systems: disruptions due to cerebellar dysfunction.," *Journal of neurophysiology*, vol. 72, no. 4, pp. 1674–85, 1994.
- [40] P. Soliveri, R. G. Brown, M. Jahanshahi, T. Caraceni, and C. D. Marsden, "Learning manual pursuit tracking skills in patients with Parkinson's disease," *Brain*, vol. 120, no. 8, pp. 1325–1337, 1997.
- [41] L. A. Boyd and C. J. Winstein, "Cerebellar Stroke Impairs Temporal but not Spatial Accuracy during Implicit Motor Learning," *Neurorehabilitation and Neural Repair*, vol. 18, no. 3, pp. 134–143, 2004.
- [42] M. H. Heitger, T. J. Anderson, R. D. Jones, J. C. Dalrymple-Alford, C. M. Frampton, and M. W. Ardagh, "Eye movement and visuomotor arm movement deficits following mild closed head injury," *Brain*, vol. 127, no. 3, pp. 575–590, 2004.
- [43] M. M. K. Oishi, P. Talebifard, and M. J. McKeown, "Assessing manual pursuit tracking in parkinson's disease via linear dynamical systems," *Annals of Biomedical Engineering*, vol. 39, no. 8, pp. 2263–2273, 2011.
- [44] K. Hiramatsu and H. Uno, "Older drivers ' performance with variation of preview time in tracking task," *Technical Notes/JSAE Review*, vol. 17, pp. 65–77, 1996.
- [45] T. B. Sheridan, "Three Models of Preview Control," *IEEE Transactions on Human Factors in Electronics*, vol. 7, no. 2, pp. 91–102, 1966.
- [46] R. D. Jones, "Measurement and Analysis of Sensory-Motor Performance: Tracking Tasks," in *Human performance engineering*, pp. 31–1–27, 2014.
- [47] R. D. Jones, I. M. Donaldson, and N. B. Sharman, "Removal of the Visuospatial Component from Tracking Performance and its Application to Parkinson ' s Disease," vol. 43, no. 10, pp. 1001–1010, 1996.
- [48] R. W. Wilde and J. H. Westcott, "The characteristics of the human operator engaged in a tracking task," *Automatica*, vol. 1, pp. 5–19, 1962.
- [49] K. Flowers, "Some frequency response characteristics of Parkinsonism on pursuit tracking.," *Brain : a journal of neurology*, vol. 101, no. 1, pp. 19–34, 1978.
- [50] A. Hufschmidt and C. H. Lucking, "Abnormalities of tracking behavior in Parkinson's disease," *Movement Disorders*, vol. 10, no. 3, pp. 267–276, 1995.
- [51] A. Kivila, *Touchscreen interfaces for machine control and education*. PhD thesis, Georgia Institute of Technology, 2013.
- [52] A. Kivila, J. Potter, and W. Singhose, "Manual Tracking Using Touchscreen Interfaces," *Conference Proceedings - 10th Asian Control Conference (ASCC)*, 2015.
- [53] C. Lee, S. Bahn, G. W. Kim, and M. H. Yun, "Performance Comparison of Manual and Touch Interface using Video-based Behavior Analysis," *Journal of the Ergonomics Society of Korea*, vol. 29, no. 4, pp. 655–659, 2010.

-
- [54] P. M. T. Zaal, D. M. Pool, J. de Bruin, M. Mulder, and M. M. van Paassen, "Use of Pitch and Heave Motion Cues in a Pitch Control Task," *Journal of Guidance, Control, and Dynamics*, vol. 32, no. 2, pp. 366–377, 2009.
- [55] P. M. T. Zaal, D. M. Pool, Q. P. Chu, M. Mulder, M. M. van Paassen, and J. A. Mulder, "Modeling Human Multimodal Perception and Control Using Genetic Maximum Likelihood Estimation," *Journal of Guidance, Control, and Dynamics*, vol. 32, no. 4, pp. 1089–1099, 2009.
- [56] C. Vision, "Chronos Visio."
- [57] K. van der El, S. Barendswaard, D. M. Pool, and M. Mulder, "Effects of Preview Time on Human Control Behavior in Rate Tracking Tasks," in *13th IFAC/IFIP/IFORS/IEA Symposium on Analysis, Design, and Evaluation of Human-Machine Systems*, (Kyoto, Japan), 2016.
- [58] K. J. Connolly and D. V. M. Bishop, "The measurement of handedness: a cross-cultural comparison of samples from england and papua new-guinea," *Neuropsychologia*, vol. 30, no. 1, pp. 13–26, 1992.
- [59] P. K. Mutha¹, K. Y. Haaland, and R. L. Sainburg, "The effects of brain lateralization on motor control and adaption," *J Mot Behav*, vol. 44, no. 6, pp. 455–469, 2012.
- [60] S. Machado, O. Arias-Carriñán, A. V. O. Castillo, E. Lattari, A. C. Silva, and A. E. Nardi¹, "Hemispheric specialization and regulation of motor behavior on a perspective of cognitive neuroscience," *Salud Mental*, vol. 36, no. 6, pp. 471–478, 2013.
- [61] T. Aoki, G. Rivlis, and M. H. Schieber, "Handedness and index finger movements performed on a small touchscreen," *J Neurophysiol*, vol. 115, pp. 858–867, 2016.

